THE UNIVERSITY OF MICHIGAN

INDUSTRY PROGRAM OF THE COLLEGE OF ENGINEERING

LOCAL MASS TRANSFER FROM CYLINDERS TO A TRANSVERSELY FLOWING GAS

Philip J. Birbara

A dissertation submitted in partial fulfillment
of the requirements for the degree of
Doctor of Philosophy in the
University of Michigan
1961

April, 1961

IP-509

engn

UMR 0406

ACKNOWLEDGEMENTS

There are several people who deserve mention for their assistance in this dissertation. The members of my committee, Drs. DeRocco, Gordon, Sinnott, Tek, and Williams, each deserve thanks for their guidance throughout the course of this study, and for their helpful suggestions on the preparation of the manuscript.

I owe a special debt to Dr. Gordon. His generous donation of time and continual encouragement have contributed immeasurably to this study. He has been a ready and patient listener, an astute and constructive critic, and a fine friend. Working with Dr. Gordon, I have learned the pleasures and satisfactions which research provides. Through his guidance and example, he has had a profound influence.

The writer is indebted to Arthur Platz for assistance during the experimental and calculational phases.

The financial support of the ESSO Research and Engineering Trust Fund defrayed expenses and allowed me to devote my undivided energy to this study for 12 months.

I am indebted to the personnel of the Industry Program of the College of Engineering for their cooperation and assistance in the final preparation and reproduction of the manuscript.

Finally, to my parents for making this task possible, I dedicate this work.

TABLE OF CONTENTS

TABLE OF CONTENTS (CONT'D)

LIST OF TABLES

LIST OF FIGURES

LIST OF FIGURES (CONT'D)

LIST OF FIGURES (CONT'D)

ABSTRACT

Local mass transfer rates into air from 30° segments of a cylindrical surface were determined by measuring the sublimation loss of a cast organic solid. The cylindrical test piece could be rotated through 360° in increments of 30°.

Tests were made with naphthalene, p-dibromobenzene, propionamide, and anthracene; Reynolds numbers of 400-4000; surface temperatures from 25-150°C; diameters of 1" and 1.25"; and an estimated turbulence of less than 2%.

The mass transfer data were obtained with the same geometry, equipment, and flow conditions as the heat transfer data of Churchill[14] The local and average transfer results were correlated by $j_D = B(Re)^{-n}$ where B and n vary with angular position but are independent of flow rate and diameter. The standard deviations of the j_D's from the j_D correlating lines and Churchill's j_H correlations are 6.2% and 7.8% while the algebraic average deviations are -0.06% and 2.0% respectively. This confirms the heat and mass transfer analogy for the laminar and eddy flow regions of a cylinder.

At a Reynolds number of 2000, sublimation rates were determined over a temperature range of 125°C with the mass transfer j-factors decreasing less than 10% with increasing temperatures for all angles.

A Schmidt number exponent of 1/2 in the j-factor equation is more representative of the data than a value of 2/3.

The vapor pressures of the four organic solids, determined by an air saturation technique, were correlated by $\log p = B - C/T$.

PART I
MASS TRANSFER

I INTRODUCTION

1. Introduction

Many important problems concern the transfer of material from one phase to another. Mass transfer from a cylinder is of interest because a cylinder resembles many components; and next to the flat plate, it is the simplest two dimensional case.

Mass transfer studies have been concerned mainly with overall rates. Notable local mass transfer studies from cylinders to a transverse flow are those of Thoma,[106] Klein,[62] Powell and Griffiths,[84] and Winding and Cheney.[115]

Since the equations for mass transfer are of the same form as those for heat transfer, it would be expected and has been shown that mass transfer can be used as an experimental analogue for heat transfer. An aim of this research is to test and calibrate the analogy and to complement Churchill and Brier's[15] heat transfer determinations under similar conditions.

Most work on local mass transfer rates to gases has been at room temperature. Sublimation rates of four organics were measured over a temperature range of 125°C which is greater than any known work.

In this investigation, the local mass transfer rates from 30° segments of a cylindrical surface were determined by measuring the weight loss of cast organics. The angular positions of the test piece could be rotated through 360° with respect to the transverse air flow in increments of 30°. Tests were made with naphthalene, p-dibromobenzene, propionamide, and anthracene; a Reynolds number range from 400 - 4000; surface temperatures from 25 - 150°C; and an estimated turbulence of less than 2%.

2. Resume of Prior Work

a. Previous average heat and mass transfer studies

The literature on heat transfer to cylinders with a transverse flow of air gives many theoretical and empirical equations with correlating heat transfer coefficients. One of the earliest is that of Boussinesq[7] who proposed

$$hD/k = 1.015 \sqrt{Du\rho c_v/k} \tag{1}$$

This results from the Fourier heat conduction equation and assumptions of a film of uniform thickness, an incompressible and inviscid fluid, and constant fluid properties.

Russell[89] has developed a similar equation and obtained data verifying the diameter and velocity effects indicated in Equation (1).

In 1914, King[61] used Boussinesq's assumptions to derive

$$hD/k = 0.318 + 0.798\sqrt{Du\rho c_v/k} \tag{2}$$

Langmuir[68][69] contributed papers on both free and forced convection from cylinders ascribing the thermal resistance to an effective film. He correlated the forced convection data by a relation similar to Equation (1).

Davis[18] obtained the following equation including the viscosity

$$hD/k = \psi[(Du\rho/\mu), (c\mu/k)] \tag{3}$$

For constant Prandtl number this reduces to

$$hD/k = \psi(Du\rho/\mu) = \psi(Du\rho c_p/k) = \psi(Du\rho c_v/k) \tag{4}$$

Davis represented data for wires by Equation (4).

Rice[87] used Hughes data for 0.164 - 1.199 inch pipes to obtain

$$hD/k_f = 0.465 \sqrt{Du\rho_f/\mu_f} \tag{5}$$

Fischenden and Saunders[29] successfully correlated the heat transfer data of Carpenter, King, Hughes, Taylor, Gibson, Reiher, and the mass transfer data of Thoma and Lohrisch by plots of log Nu_f versus log Pe_f. Since Pe is the product of the Prandtl and Reynolds numbers, these correlations are expressed by Equation (3).

Ulsamer[107] correlated his data and those of Kennelly, King, Hughes, Reiher, and Vornehem by

$$Nu_m = B(Re)^n \tag{6}$$

where physical properties are the mean of those at the gas and surface temperatures. The data of Hilpert[46], correlated by Equation (6), covered the largest range of diameters, 0.0079 to 5.9 inches. When log Nu is plotted against log Re, the data fall on a series of straight lines with slight bends at log Re equal to 1.6, 3.6, and 4.6 coinciding with variations in flow patterns. With increasing Reynolds number, n increases and B decreases. According to Ulsamer, for Re between 50 and 10,000, the values of n and B are 0.5 and 0.536; for Hilpert's correlation, n = 0.466 and B = 0.615.

McAdams[80] correlated available data by Equation (6) evaluating the physical properties at the film temperature, the average of the bulk and surface temperatures.

For liquids flowing perpendicular to cylinders, Ulsamer[107] correlated his data by another form of Equation (3).

$$Nu = E(Re)^n(Pr)^m \tag{7}$$

He recommended

	n	m	E
Re = 0.1 to 50	0.385	0.31	0.91
Re = 50 to 10,000	0.50	0.31	0.60

A value of m = 1/3 is often used.

In 1933, Chilton and Colburn[12][13] presented the j-factor correlations which related heat and mass transfer and in some cases momentum transfer. The equations

$$hD/k = \psi(Re, Pr) \tag{8}$$

$$k_c D/D_V = \psi(Re, Sc) \tag{9}$$

become

$$j_H = (h/c_p G)\psi(Pr) = \psi(Re) \tag{10}$$

$$j_D = (k_g p_{bm}/G_m)\psi(Sc) = \psi(Re) \tag{11}$$

Assuming with Chilton and Colburn

$$j_H = (St)(Pr)^{2/3} \tag{12}$$

and dividing Equation (7) for m = 1/3 by $(Re)(Pr)^{1/3}$, there results

$$Nu/(Pr)^{1/3}(Re) = E(Re)^{n-1} = (St)(Pr)^{2/3} \tag{13}$$

$$j_H = E(Re)^{n-1} \tag{14}$$

Analogously

$$j_D = E(Re)^{n-1} \tag{15}$$

Chilton and Colburn plotted the data of Lohrisch for the absorption of water from air flowing across a fused caustic cylinder as j_D vs Re. The values of j_D from Lohrisch were 10 to 15% greater than accepted values for j_H.

An excellent summary of such mass transfer results appears Sherwood and Pigford[97]. The j_D-factors calculated from the data of Powell on water vaporization, Lohrisch's water and ammonia absorption, Vint's liquid evaporation, London's et al. water evaporation, and Winding and Cheney's naphthalene sublimation are in agreement with McAdams' j_H versus Re curve.

Linton and Sherwood[72] dissolved cast benzoic and cinnamic acid cylinders placed transverse to a turbulent water stream verifying the 2/3 exponent on the Schmidt group for values up to 3000.

Bedingfield and Drew[4] correlated their psychrometric data for solids by

$$j_H = h/c_p G(c_p\mu_f/k_f)^{0.56} = 0.281(D\,G/\mu_f)^{-0.4} \qquad (16)$$

$$j_D = k_g M_f/\beta G(\mu_f/M_f D_v)^{0.56} = 0.281(D\,G/\mu_f)^{-0.4} \qquad (17)$$

They recalculated psychrometric measurements of Arnold, Dropkin, and Mark and found them to agree with Equations (16) and (17). Bedingfield and Drew did not include the data of Vint, Lohrisch, Powell, and Clapp because of inadequacies in presentation of data or experimental techniques.

Giedt[36] measured the local heat transfer coefficients around a cylinder with a non-isothermal surface. The average Nusselt numbers agreed within 12% of Hilpert's for an isothermal surface, the greatest discrepencies occurring at the higher Reynolds numbers ($Re > 1.5 \times 10^{-5}$).

Churchill and Brier[15] investigated heat transfer from cylinders at very high temperature differences proposing

$$Nu_m = 0.60(Pr)^{1/3}\,(Re_b)^{1/2}(T_b/T_s)0.12 \qquad (18)$$

b. Previous local heat and mass transfer studies

Local heat or mass transfer results for a cylinder are usually given as plots of Nusselt numbers versus angular position for a given Reynolds number. Lohrisch[74] measured ammonia absorbtion over 40° segments; Drew and Ryan[23] steam condensation over 20° intervals; Powell and Griffiths[84] water vaporization over 40° segments; Churchill and Brier[15] heat transfer over 30° segments.

The local heat transfer data of Fage and Falkner[28], Small[98], Schmidt and Wenner[92], obtained over segments subtending 2° to 15°, were presented as point values. Krujilin and Schwab[67] Giedt[36], Robinson and Han[88] measured local heat transfer coefficients by thermocouples in the surface.

the surface. Local transfer coefficients for sublimation are presented by Klein[62] for ice by Winding and Cheney[115] for naphthalene.

Plots of log Nu versus log Re for given angular positions by Lohrisch, Klein, Krujilin and Schwab, and Churchill and Brier were linear with slopes varying with angular position.

Schmidt and Wenner, as well as Winding and Cheney, compare their data with those of Lohrisch, Drew and Ryan, Klein, Small, and Krujilin and Schwab at approximately Re = 40,000. Winding and Cheney, whose data agree with those of Small, have results about 50% greater than those of Schmidt and Wenner. The plots of all these local Nusselt numbers, for D = 1 to 12 inches, versus angular position agree in shape. Schmidt and Wenner indicate the results of Drew and Ryan, Klein, and Lohrisch to be less reliable than their own due to experimental techniques. They suggest the high Nusselt numbers of Krujilin to be less reliable due to surface roughness.

Giedt compared two runs (Re = 101,300 and 170,000) with those of Schmidt at the same Reynolds numbers finding considerable disagreement, particularly in the rear of the cylinder. He attributes this to higher turbulence for his non-isothermal surface.

Squire, as reported by Goldstein[39], theoretically derived

$$Nu_\theta = 1.14\ Pr^{0.4} \sqrt{Re_b}\ \sqrt{\sin\theta/\theta} \qquad (19)$$

near the stagnation point of the cylinder. For air, Pr = 0.74, at the stagnation point, this becomes

$$Nu_{\theta=0} = 1.01 \sqrt{Re_b} \qquad (20)$$

The agreement of Equation (20) with the experimental measurements of Schmidt and Wenner, Giedt, Churchill and Brier, and Eckert and Soehngen is exceptionally good.

Martinelli et al.[79] studied the data of Schmidt and Wenner proposing the empirical equation

$$Nu_\theta = 1.14\ Pr^{0.4} \sqrt{Re_b}\ [1 - (\theta/90)^3] \tag{21}$$

This applies when the angular position is no greater than 80° and the main stream turbulence is less than 1%. For air with a Prandtl number of 0.74, this reduces to

$$Nu_\theta/Nu_{\theta=0} = 1 - (\theta/90)^3 \quad 0° \leq \theta \leq 80° \tag{22}$$

Krujilin[66] theoretically derived

$$Nu_\theta = \psi(\theta)\ Pr^{1/3} \sqrt{Re_b} \tag{23}$$

The function $\psi(\theta)$ was determined by numerical integration for a number of angles extending from $0° < \theta < 90°$ and a Reynolds number range from 10,000 to 250,000.

Eckert[26] presents an equation based on the Squire derivation near the stagnation point of a cylinder. For the stagnation point region, a thermal boundary layer exists while the velocity outside the boundary, u_s, increases linearly. Solution of the differential equations for the heat transfer coefficients to an isothermal cylindrical surface placed transversely to the fluid gives,

$$h = Bk \sqrt{u_s/\mu} = Bk \sqrt{F/\mu} \tag{24}$$

where $F = u_s/x$

Expressed in dimensionless form

$$Nu_x = hx/k = B \sqrt{u_s x/\mu} \tag{25}$$

For potential flow around the cylinder,

$$u_s = 2u_b \sin (2x/D) \tag{26}$$

Then for potential flow at the stagnation point,

$$u_s = 4u_b(x/D) \tag{27}$$

Substituting Equation (27) into Equation (25), there results

$$Nu_{\theta=0} = hD/k = 2B \sqrt{Re_b} \tag{28}$$

B is a function of the Prandtl number, tabulated by Eckert[20]. For air, Equation (28) reduces to Equation (21). Eckert's calculations for the laminar boundary layer in the region $0° \leq \theta \leq 90°$ agree with the heat transfer data of Schmidt and Wenner.

c. Average experimental techniques

Average heat transfer coefficients were measured by King[61] and Kennelly et al.[58] who observed the heat loss from electric wires swinging around their long axis. The heat loss from electric wires, rods, and tubes with a transverse air flow were measured by Rice[87], Taylor[103], Griffiths and Awberry[42], Goukham[41], Hilpert[46], Benke[5], Billman et al.[6], Comings et al.[17], and van der Zijnen[108].

Hughes[51], Carpenter[10], Hilpert[46], and Comings et al.[17] measured the condensation of steam in tubes obtaining average heat transfer coefficients. Gibson[35] circulated hot water through a tube measuring its temperature drop. Reiher[86] and Vornehem[110] determined the heat transferred from hot air to cold water flowing through tubes.

London et al.[76] used the transient behavior of a thermal capacitor to determine convective transfer from cylinders to gases. The results agreed with the literature for steady state procedures.

Thoma[106] and Lohrisch[74] investigated mass transfer from an ammonia-air flow to tubes of various sizes wrapped with blotting paper saturated with phosphoric acid. Lohrisch[74] determined the transfer of water from air by the weight increase of sodium hydroxide rods.

Mark[78], Arnold[1], and Dropkin[24] obtained psychrometric data for a variety of liquids from a cylindrical cloth surface measuring the liquid lost. Powell[84] used cloth covered cylinders of several diameters in his wet-bulb studies. Comings et al.[17] and Maisel and Sherwood[77] determined heat and mass transfer coefficients for cylinders. The latter studied the effects of turbulence.

Winding and Cheney[115] measured the sublimation of naphthalene tubes placed transverse to a turbulent air stream. Bedingfield and Drew[4] obtained psychrometric data with volatile cylindrical solids as wet-bulbs. Linton and Sherwood[72] present data on the solution of cast benzoic and cinnamic acid cylinders in turbulent water flow where the Schmidt number varied from 1000 to 3000.

Dobry and Finn[21] obtained mass transfer rates at low Re by observing the diffusion-limited electric current discharging at a cylindrical microelectrode.

d. Local experimental techniques

As reported by Stanton[100], Jakeman measured the relative heat loss from an electrically heated metal strip attached to a cylindrical ebonite rod. He observed the heat loss from the back of the cylinder to be about one-half that from the front. Similarly, Kirpitshev as reported by Krujilin and Schwab[67] made the same observation. Reiher[86]

measured the surface temperature distribution around a water cooled pipe placed transversely to a hot air stream.

Lohrisch[74] wrapped 12 longitudinal strips of blotting paper saturated with phosphoric acid along glass tubes of various sizes. An air-ammonia stream flowed transversely to the cylindrical surface and the amount of ammonia absorbed was determined by titration. As the ammonia was introduced into the air a short distance from the cylinder, there is doubt as to the homogeneity of the gaseous stream. Photos were taken of ammonium chloride clouds formed when the cylindrical surface was saturated with hydrochloric acid.

Fage and Falkner[28] presented data of local heat transfer and skin friction coefficients from the electrical input to a nickel strip subtending 2°.

Drew and Ryan[23] reported variations in condensation rates and local heat transfer coefficients to air in 20° sectors of a vertical steam pipe. These results were similar to those of Lohrisch for ammonia absorbtion.

Klein[62] studied the change in shape of ice tubes in a transverse stream of warm air. The average heat and mass transfer coefficients were obtained from the weight loss while change in dimensions gave local coefficients.

Krujilin and Schwab[67] inserted a 0.1 mm thermocouple in a surface groove on a stream tube measuring the angular heat transfer variation in transverse air flow. They also measured the surface temperature of an iron cylinder by 32 peripheral thermocouples.

Small[97] used a thermopile in a steam heated cylinder to measure local heat transfer coefficients.

Powell and Griffiths[84] measured the vaporization of water to an air stream in 40° sectors. Water circulated over the wick covered surface. The evaporation was measured by the quantity evaporated in each sector and indirectly from the power required to maintain a uniform surface temperature by electric heaters in each sector. Highest rates were observed at the stagnation point, somewhat lower rates at 180°, and a sharp minima at approximately 100°.

Schmidt and Wenner[92] developed a method for local heat transfer measurements. Except for a narrow longitudinal thermally isolated sector of a steam heated tube, the cylindrical surface was maintained at the same constant temperature as the remainder of the surface by small electric heating coils. The heating element sector could be turned to any angle with respect to the air flow direction. Measurements of heat transfer and pressure distributions for 10° intervals are presented.

Winding and Cheney[115] and Klein[62] measured transfer coefficients from the change in dimensions of subliming solids.

Giedt[36] investigated the variation of the heat transfer coefficients around a cylinder with a non-isothermal surface. An electrically heated nichrome ribbon 1" by 0.002" in cross section was wrapped helically around a 4" O.D. lucite cylinder. Local heat transfer coefficients resulted from peripheral temperature variations and the electrical input. A correlation between these results and the skin-friction distributions as indicated by the pressure variations was noted. Giedt, Krujilin[67], and Robinson and Han[88] observed no significant difference in the heat transfer coefficients when the surface temperature distribution was not uniform.

Churchill and Brier[15] measured local heat transfer coefficients at gas temperatures varying from 580°F to 1800°F and Reynolds numbers from 300 to 2300. The outer surface was maintained at approximately 100°F by circulating water through a hollow inconel cylinder. The radial temperature profile through a 30° sector of the tube wall was measured permitting the calculation of the heat transfer coefficient.

Robinson and Han[88] determined local heat transfer coefficients for cylinders in ducts of various widths. A 1.5" O.D. cylindrical tube with 19 thermocouples evenly spaced over one-half of the periphery was electrically heated. The radial temperature differentials and the thermal conductivity were used to calculate the heat flux distribution. The relative heat transfer distributions for a cylinder in a 6" wide duct are similar to those reported for free stream conditions.

Eckert and Soehngen[27] used an interferometer to determine the temperature field around solid copper cylinders obtaining local heat transfer coefficients for $23 \leq Re \leq 597$.

Seban (93) measured local transfer coefficients from bakelite cylinders with nichrome ribbons wrapped on their surfaces for heating by electric dissipation.

3. Flow Characteristic Studies

Drag coefficients for gases past cylinders have been measured by Wieslberger[112], Fage and Falkner[28], Delany and Sorenson[20], and Giedt[37]. Similar to flow in pipes, they observed that the shear stress at low Reynolds numbers (< 1) varies as the first power of the velocity. The flow is completely laminar and only viscous forces contribute to the drag. As the Reynolds number increases beyond 1, separation of flow from the cylindrical surface results. This has been studied by a number of

techniques (Thoma, Green, Fage and Falkner, Giedt, etc.). The point of separation is approximately 70° for the laminar and 110° for the turbulent boundary layers. Beyond the separation point eddies dissipate the kinetic energy.

At small velocities the drag of the cylinder is mostly frictional resistance while at Re $\geq$ 1000 mostly form resistance. At the lower Reynolds numbers, the heat and mass transfer coefficients on the impact side are much greater than in the back side. As the Reynolds number increases, both coefficients increase becoming equal at Re $\approx 5 \times 10^5$.

4. Effects of Air Turbulence on Transfer Rates

In 1925, Reiher[86] placed a grid upstream from a heated cylinder obtaining up to 50% increases in the heat transfer coefficients. Goukham et al.[41] located two 1.2 cm diameter cylinders 3.5 cm apart upstream from a 3.5 cm cylinder obtaining increases of 23 to 30%.

Loitsiansky and Schwab[75] observed 30 to 35% increases in the heat transfer coefficients to a 7 cm diameter sphere as the turbulence increased from 0.4 to 2.8% for $4 \times 10^4 \leq Re \leq 1.2 \times 10^5$. McAdams[80] states that the heat transfer coefficient in a tube bank is approximately 27% greater than that for a single cylinder under equivalent conditions. Fage and Falkner[28] indicated that the relationships between heat and mass transfer and surface friction are not altered by turbulence.

Comings et al.[17] studied the effect of turbulence on both the heat and mass transfer. Evaporation of water in air was measured for $400 < Re < 20{,}000$ and turbulence from 1 to 20%. The coefficients increased similarly with increasing turbulence. The rate of increase is greatest at a turbulence of 2 to 4%. At Re = 5,800, the transfer coefficients vary little for turbulences of 7 to 25%. Increasing turbulence

at a constant Reynolds number, caused a maximum increase of 25% in the heat transfer coefficient. This was more pronounced at the higher Reynolds numbers.

Giedt[37] measured the effect of turbulence on local heat transfer and skin friction coefficients for $70,800 \leq Re \leq 219,000$. Transfer coefficients increased 10-20% as the turbulence increased from 1 to 4%. For the 1% turbulence, the ratio of the average front half to the rear half heat transfer coefficient is 0.85 while for 4% turbulence it is 1.1.

Using the evaporation from a cylinder, Maisel and Sherwood[77] were the first to observe the effects of intensity of scale on the transfer coefficient. They found little variation in the mass transfer coefficients with changes in scale levels. At Re = 1000 no change in coefficients was observed below an intensity level of 12%; while at Re = 5000, no effect was apparent below 4%. Like Comings et al., they observed an increase in turbulence to be more effective at higher Reynolds numbers.

Van der Zijnen[108] measured the heat transfer coefficients from wires and cylinders in both smooth and turbulent air flow. For $60 \leq Re \leq 25,800$, the turbulence varied from 2 to 13% and the ratio of the turbulence scale to the cylindrical diameter varied from 0.31 to 240. The data were correlated by three independent groups: Reynolds number, intensity of turbulence, and (scale/diameter).

Kestin and Maeder[59] showed that slight increases in screen produced turbulence resulted in substantial increases in the heat transfer coefficient.

Seban[93] recently presented results on the effect of turbulence on local transfer coefficients from cylinders. For $0.5x10^5 < Re < 3.0x10^5$, the increased turbulence resulted in increased heat transfer coefficients in the laminar boundary layer, an earlier transition to turbulence, and possible alteration in the character of the separated flow. No functional relationship was established specifying the increase in the heat transfer coefficient relative to the turbulence intensity.

5. Effects of Surface Roughness

Most experimenters attempt to work with "smooth" surfaces. In view of the Chilton-Colburn analogy, roughness should increase the pressure drop, heat, and mass transfer at the same ratio. McAdams[80] reports on the experiments of Cope who studied the effect of roughness in cooling water tubes. In the turbulent region, the pressure drop was varied to six times that of a smooth tube and the relative heat transfer was increased only 20 to 100%.

Grimson[43] measured heat transfer to tube bundles with a transverse air flow. He noted an increase up to 20% in heat transfer and flow resistance with increasing roughness.

6. Effects of Surface Temperature Distribution

Krujilin[66] measured local heat transfer rates from thick walled tubes providing a pronounced surface temperature variation. Defining a temperature ratio $(T_{90°}-T_{0°}/T_{mean})$, (the difference of temperature between the stagnation point and the 90° positions divided by the mean cylindrical temperature), Krujilin observed no significant difference in local heat transfer coefficients for a cast-iron cylinder with a 3.3% temperature ratio and a porcelain cylinder with a 19% ratio.

Billman et al.[6] determined the variation in surface temperature by small thermocouples in the surface of a brass cylinder. For $562 \leq Re \leq 4440$ and average cylindrical temperatures between 125 and 315°F, a linear relationship exists between the heat transfer rate and the average surface temperature indicating that the surface temperature variations do not modify the flow.

Giedt[36] measured the temperature and electrical input to a thin nichrome heating ribbon wound helically around a cylinder. A four-fold increase in the power caused the temperature gradients to increase from 4 to 8 times along the ribbon surface. No variation in local heat transfer coefficients was apparent for the different surface temperature distributions.

Robinson and Han[88] investigated heat transfer from non-isothermal surfaces of banks of tubes to a forced transverse air flow. The distribution for a single cylinder was similar to that of Giedt.

The effect of surface temperature distribution considered above were based on experiments with small surface to bulk temperature differences. Churchill and Brier[15] measured heat transfer coefficients at high temperature differences and found that the mean coefficient varied as $(T_b/T_s)^{0.12}$ with fluid properties evaluated at the bulk temperature.

Douglas and Churchill[22] successfully correlated the data of many investigators with high and low temperature differences by Equation (4) with fluid properties evaluated at the film temperature.

7. Effects of Temperature on Mass Transfer Coefficients

Kowalke, Hougen, and Watson[64] made a series of runs to determine the temperature effect on the ammonia transfer coefficient for the absorption of ammonia into water in packed towers at constant mass flow rates. For 70-110°F, it was found that increasing the temperature diminished ($K_g a$) by approximately 0.3% for each 1°C rise.

For the absorption of ammonia in a 1" diameter packed tower from 70-95°F, Dwyer and Dodge[25] observed $K_g a$ decreases 1.2% for each 1°C increase. By variation of the water from 10 - 35°C, Molstad et al.[82] found the coefficients to decrease by 0.9% for each 1°C increase for the same system. Haslam, Hershey, and Kean[44] found that k_g varied inversely as $T^{1.4}$ for the absorption of NH_3 into water on a flat surface.

If the gas film is controlling, K_g should be practically independent of temperature according to correlations of the Gilliland-Sherwood equation for packed towers.

Explanations are lacking for the pronounced decrease of the transfer coefficient with temperature. Molstad et al. determined that for ammonia absorption the liquid film resistance is only 10-15% of the total, so that a large change of $K_l a$ with temperature should have little effect on $K_g a$.

Wilhelm[113] reports that Fischer observed that increasing the temperature decreased k_g for the sublimation of benzoic acid tubes to air in tubes at high Reynolds numbers ($1 \times 10^5 \leq Re \leq 4 \times 10^5$) at 25-45°C. The magnitude of the effect closely parallels that of Kowalke et al.

II APPARATUS

The apparatus, Figures 1 and 2, includes an air control flow system with a pressure reducer and rotameter; a resistance furnace for heating the gas; an adiabatic "tube section" for measuring the gas temperature; and the test piece section which includes a heat shield surrounding the test piece.

Air at 100 psi is dried in one of the two parallel silica gel beds. The unused bed may be replaced, or dried without interruption of the the air to the test cylinder. The air is then measured and regulated by three parallel metering units. Each contains a cutoff valve, pressure controller, bimetallic-element thermometer, a rotameter, and a needle valve. It then flows through a packed tube surrounded by an electrical resistance furnace and then through another packed tube (adiabatic section) for measurement of the gas temperature before going to the test piece.

The velocity profile, the scale and turbulence levels are maintained by two screens outside the adiabatic tube.

The Inconel test cylinder, above the top screen, is shown in Figures 2 and 3. It sits on a pair of brackets permitting rotation in 30° increments. The cylinder has a removable boat for holding the material to be sublimed and parallel grooves for thermocouples adjacent to the boat. The test piece is surrounded by a cylindrical heated shield with removable conical top for easy access to the test piece. To minimize radiation losses, the inner surface of the surrounding furnace is maintained at nearly the same temperature as the test object.

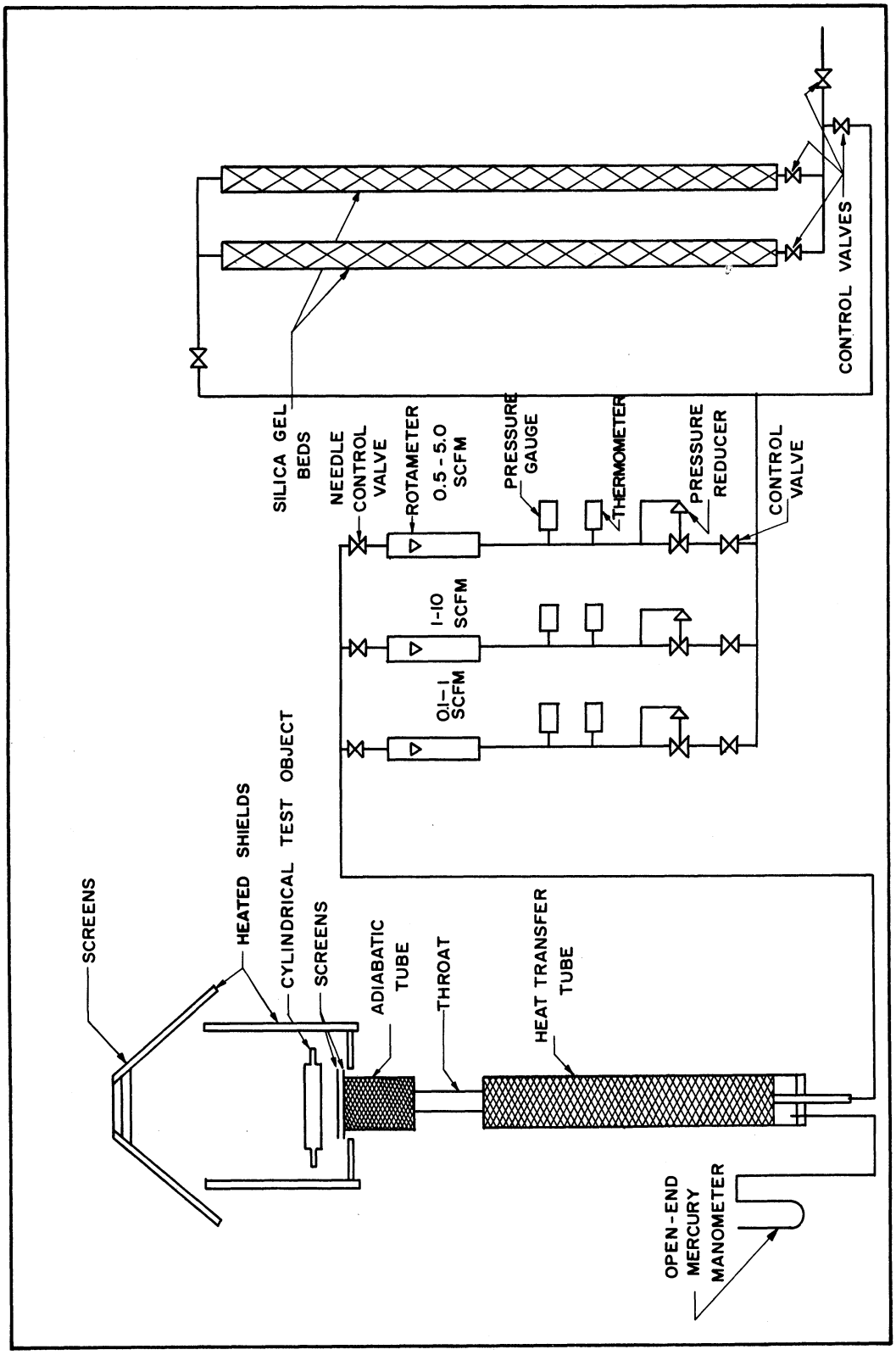

Figure 1. Schematic Diagram of Mass-Transfer Flow Equipment.

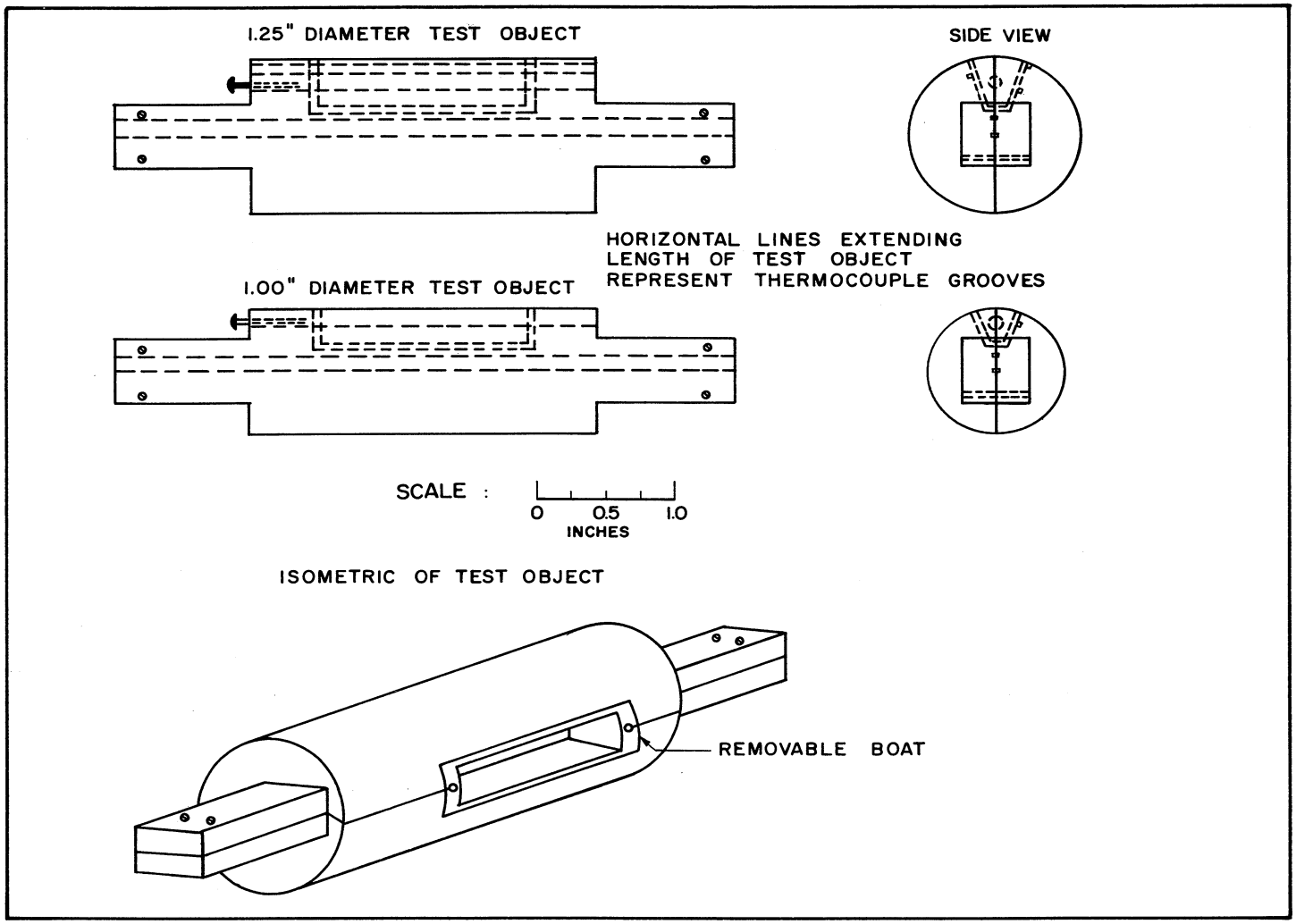

Figure 2. Diagrams of Test Object Details.

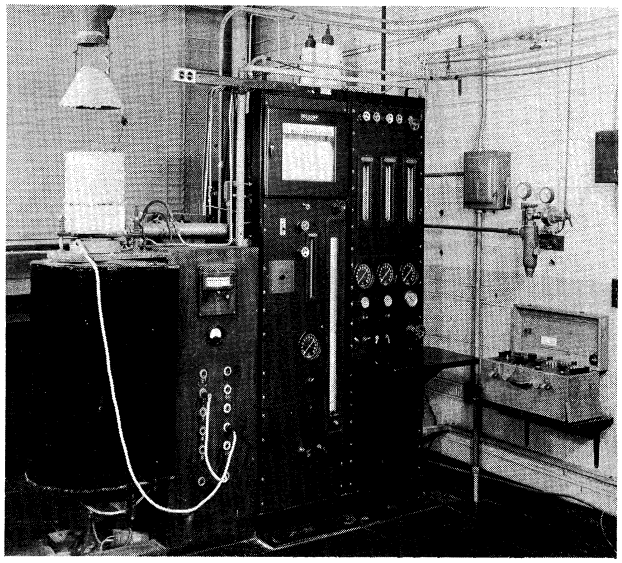

(a) View of Flow and Heating Units

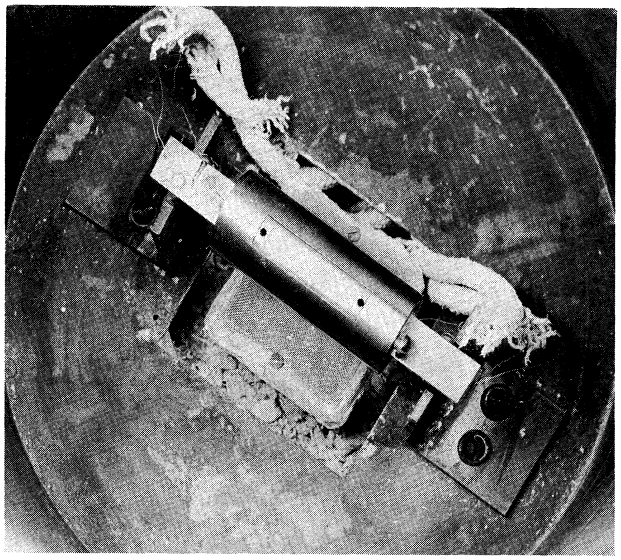

(b) Test Object in Run Position

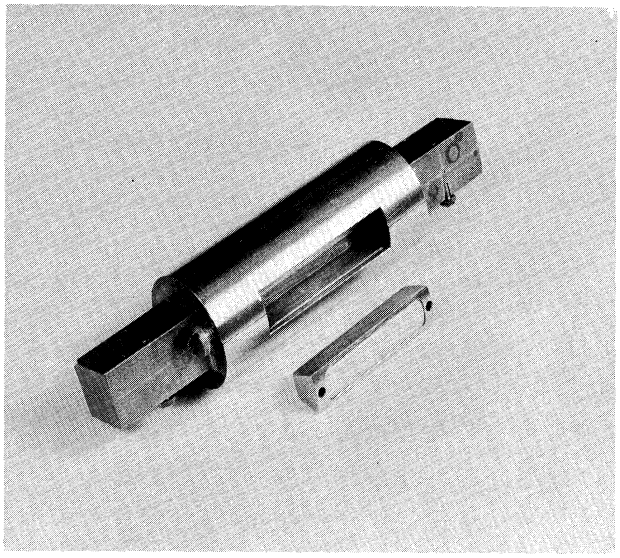

(c) Test Object with Boat

Figure 3. Photographs of Equipment.

III EXPERIMENTAL PROCEDURE

Optimum location of the test piece above the platinum screen was determined by Churchill[14] who employed a probing hot-wire anemometer at approximately 1-1/2" above the top screen. The hot-wire anemometer showed a uniform temperature, velocity, and turbulence zone in a cone with a base the size of the top screen and extending a distance from about 1/8" to approximately 8" above the top screen. Preliminary runs showed that slight variations in lateral, longitudinal, and elevational locations from Churchill's optimum plane 1-1/2" above the top screen resulted in insignificant mass transfer differences.

1. Preparations for a Run

Occasionally the test cylinder was polished to minimize thermal radiation. Negligible staining of the Inconel surface was observed.

The solid material to be sublimed is melted in a beaker and poured into the clean boat. A smooth surface is accomplished by "shaving" and "curing". A slight excess of material is cast and then removed by shaving with a scalpel to give a smooth cylindrical surface. In curing, any uneven surface is preferentially sublimed in hot air, leaving a smooth surface.

The interior surface temperature of both the cylindrical and conical shields were regulated independently by Variacs and measured by a probing thermocouple. They were maintained within 5°C of the Inconel test piece.

2. Experimental Procedure During Run Periods

The procedure was to: a) pre-weigh the boat plus contents; b) insert the boat in the test piece, and make the run; c) remove, cool, and weigh the boat.

A difference technique measured the mass transfer rate at the higher temperatures. This compensated for sublimation while approaching thermal equilibrium both after insertion and cooling prior to the final weighing. The difference of the two exposure times and weight losses, with other variables constant, furnished the steady-state mass transfer rate. Before the boat is placed in test position, aluminum foil is wrapped around it to reduce the material lost while approaching steady state temperatures, after which it is removed. At the end of the sublimation period, the hot boat is wrapped in foil, cooled in a desiccator foil removed, and weighed. The time the foil is around the cylinder and the time allowed for cooling are identical for both runs of a pair.

Temperatures were read by six thermocouples in about 15 seconds. A sample data sheet is shown in Figure 4. When there was a significant variation in temperature or flow rate, the run was stopped and discarded. Some twenty runs were discarded due to unsteady state conditions.

In all runs, the air pressure preceding the rotameter was fixed at 45 psia and the gas flow past the cylinder held at a series of Reynolds numbers of 400, 1000, 2000, and 4000. The test piece was rotated through 360° in 30° increments. Preliminary results indicated symmetrical mass transfer around the cylinder. Then most measurements were made at angular positions from 0° to 180° in 30° increments.

Summaries of results are given in Table IV. The numbers ascribed to the runs are assigned consecutively within the table and have no chronological connection.

DATA SHEET FOR MASS TRANSFER STUDIES

DATE - May 28 '59

MATERIAL - p-DIBROMOBENZENE

RUN No. 206

TIME (min)		0	15	30	45			
FURNACE								
Volts	0	→	→	→	→			
Amps	0	→	→	→	→			
ΔP (mm Hg)		→	→	→	→			
GAS ROTAMETERS								
Gas	AIR							
Press. (psig)	30	→	→	→	→			
Temp. (^{o}F)	76	→	→	→	→			
Rdg. (scfm)	8.10	→	→	→	→			
GAS TEMPERATURE								
Pot.TC-6 (mv)		1.063	1.064	1.065	1.070			
(^{o}C)		26.3	26.3	26.4	26.5			
Rec.	CONST.	→	→	→	→			
SURROUNDING TEMP.	25° approx.							
TEST OBJECT								
Angle (deg)	60°							
Elev. (in)	1"							
TC-1 (mv)		1.060	1.063	1.065	1.065			
(^{o}C)		26.2	26.3	26.4	26.4			
TC-2 (mv)		1.063	1.065	1.065	1.065			
(^{o}C)		26.3	26.4	26.4	26.4			
TC-3 (mv)		1.063	1.065	1.062	1.065			
(^{o}C)		26.3	26.4	26.3	26.4			
TC-4 (mv)		1.063	1.065	1.062	1.065			
(^{o}C)		26.3	26.4	26.3	26.4			
TC-5 (mv)		1.063	1.065	1.062	1.067			
(^{o}C)		26.3	26.4	26.3	26.4			

INCONEL BOAT

Initial wt. (gr)	153562
Final wt. (gr)	153459
Wt. loss (gr)	0.0103

COMMENTS cylindrical diameter = 1.25" ; "preliminary run" not necessary

Figure 4. Data Sheet for Mass-Transfer Studies.

IV EXPERIMENTAL RESULTS

1. Data Processing

Dimensionless analysis is widely used in correlating heat, mass, and momentum transfer data. The utility of dimensionless analysis is its ability to provide a relationship when the knowledge about the mechanism is incomplete.

Mass transfer to fluids flowing past cylinders has been found to be influenced by the mass velocity G, cylindrical diameter D, fluid viscosity μ, diffusivity D_V, and fluid density ρ, or

$$k_c = \psi(G, D, \mu, D_V, \rho) \tag{29}$$

From dimensional analysis, this becomes

$$k_c D/D_V = \psi\,[(DG/\mu)(\mu/\rho\, D_V)] = \psi\,[(Re)(Sc)] \tag{30}$$

Analogously for heat transfer, $$hD/k = \psi\,[(Re)(Pr)] \tag{31}$$

Equations (30) and (31) may be rearranged to the j-factors for heat and mass transfer.

$$j_D = k_g\, p_{bm}\, M_m/G\, \psi(Sc) \tag{32}$$

$$j_H = h/c_p G\, \psi(Pr) \tag{33}$$

The mass transfer coefficient k_g is calculated by

$$k_g = \Delta W/\, tA(p_s - p_b) \tag{34}$$

Compared to p_s, p_b is negligible. In view of the relatively low vapor pressure of the organic solids, the inert film pressure is taken as the total pressure.

The surface temperature of the subliming organic is taken to be the gas temperature less a small correction for the wet bulb depression.

For steady-state, the heat received by the organic is equal to the latent heat of sublimation at the surface temperature, or

$$\lambda_s k_g (p_s - p_b) = h(T_a - T_s) \tag{35}$$

Since p_b is negligible compared to p_s, Equation (35) can be rearranged to yield the surface temperature,

$$T_s = T_a - p_s \lambda_s k_g / h \tag{36}$$

In the present study, the heat loss by radiation and conduction is negligible compared to that transferred by convection. Radiation and conduction losses are minimized by maintaining the surrounding heated shield and the test object at nearly the same temperature as the subliming organic.

In Equation (36), (k_g/h) is calculated from the j-factors. Assuming the equality of j_H and j_D,

$$k_g/h = (Pr/Sc)^{0.5} \, (1/c_p \, M_m \, p_{bm}) \tag{37}$$

A value of 0.5 for the exponent of the Schmidt number is compatible with the data for $1.79 < Sc < 3.05$, discussed in Section V-1.

The vapor pressures of naphthalene, p-dibromobenzene, propionamide, and anthracene were measured by a gas saturation technique described in Part II. Heats of sublimation were calculated by the Clausius-Clapeyron equation.

Diffusivities were calculated by the method proposed by Hirshfelder, Bird, and Spotz[47]. For pairs of non-polar gases,

$$D_v = [(1.492 \times 10^{-3}) T^{3/2} \, Pr_{AB} \phi] \, (\sqrt{1/M_A + 1/M_B}) \tag{38}$$

Diffusivity data for some of the organics in air are not available for the temperatures used in this study. For consistency, all diffusivities were calculated by Equation (38).

The gas viscosity was that of air. The physical properties for the Schmidt and Reynolds numbers were calculated at a film temperature, the average of the surface and mainstream temperatures. Negligible differences would have resulted if the surface or mainstream values were used.

2. Correlation of Data

Appendix 2 contains the data and results. Local j-factors, for a given Reynolds number, are given in Figures 5 through 6. Plots of log j_D versus log Re with parameter of angular positions, 0° to 180°, are shown in Figures 7b - 7e. These are summarized in Figure 7a. Figure 8 gives the exponent on the Reynolds number for the equation, $j_D=B(Re)^n$, as a function of angular position.

Values of Churchill's heat transfer results are included. Most heat and mass transfer j-factors agree within 15%.

Ratios of j_H/j_D for all angular positions are given in Table 1. Table II contains the equations of the j_D correlating lines determined from Figures 7b - d. The standard deviations of the j_D's for all positions are 6.2% from the j_D correlating lines and 7.8% from Churchill's j_H correlations.

Table I

Ratios of Local j_H's to j_D's

Angle	j_H/j_D, (1)	j_H/j_D Limits, (2)	Standard Deviations (3)	(4)
0	1.01	0.90 - 1.18	6.2%	6.3%
30	1.04	0.91 - 1.12	5.1	6.3
60	1.01	0.89 - 1.15	5.9	5.9
90	0.94	0.86 - 1.06	5.8	7.8
120	0.98	0.89 - 1.18	6.9	7.5
150	0.92	0.84 - 1.02	5.1	10.8
180	0.97	0.87 - 1.10	7.3	9.0

(1) $\left(\dfrac{j_H, \text{ correlation line from Churchill and Brier}}{j_D, \text{ correlation line shown in Figs. 7b-d}} \right)$ Ratio averaged from Re=400-4000

(2) $\left(\dfrac{j_H, \text{ correlation line}}{j_D, \text{ from data points}} \right)$

(3) Deviations of j_D's from j_D correlation lines

(4) Deviations of j_D's from j_H correlation lines

The runs, at a Reynolds number of 2000, were made with a wider range of variables than those at the other values. Included were cylindrical diameters of 1" and 1.25"; four organic solids; and surface temperatures ranging from 25-150°C. At Reynolds numbers of 400, 1000, and 4000, the temperature was close to 25°C and only naphthalene and p-dibromobenzene were sublimed over the temperature range 25-65°C; anthracene, over 105-150°C. The upper temperature limit for each solid is set by high sublimation rates altering the surface area in the runs.

The average cylindrical mass transfer rates are obtained by integration of the local data and summarized in Figure 9. They are given by

$$j_D = 0.64 \, (Re)^{-0.5} \tag{39}$$

Churchill's, $j_H = 0.63(Re)^{-0.50}$ and McAdams' correlations are included for comparison.

The exponent, 0.5, for the Schmidt and Prandtl numbers used in the j-factor relations is determined from Figures 10a and 10b. Values of h are obtained from Churchill's results. Theory[4] requires the lines of these plots to pass through point P (0.69, 4.16). Thus when Sc = 0.69, the term (Pr/Sc) = 1 for air. For this condition, Equation (37) can be written

$$k_g M_m p_{bm}/h = 1/c_p = 4.16 \qquad (40)$$

Figures 12a and 12b show a slight decrease of the j_D -factor with increasing temperature at Re = 2000.

Most data points in Figures 6a-d and 7b-d are slightly displaced so that all the data may be clearly presented thereby preventing an objectional overlapping of points. In Figures 6a-d, these points are moved from the angular positions of 30°, 60°, 90°, 120°, 150° and 180° and in Figures 7b-d from the Reynolds numbers of 400, 1000, 2000, and 4000. The j_D- factors in these plots are the actual calculated values.

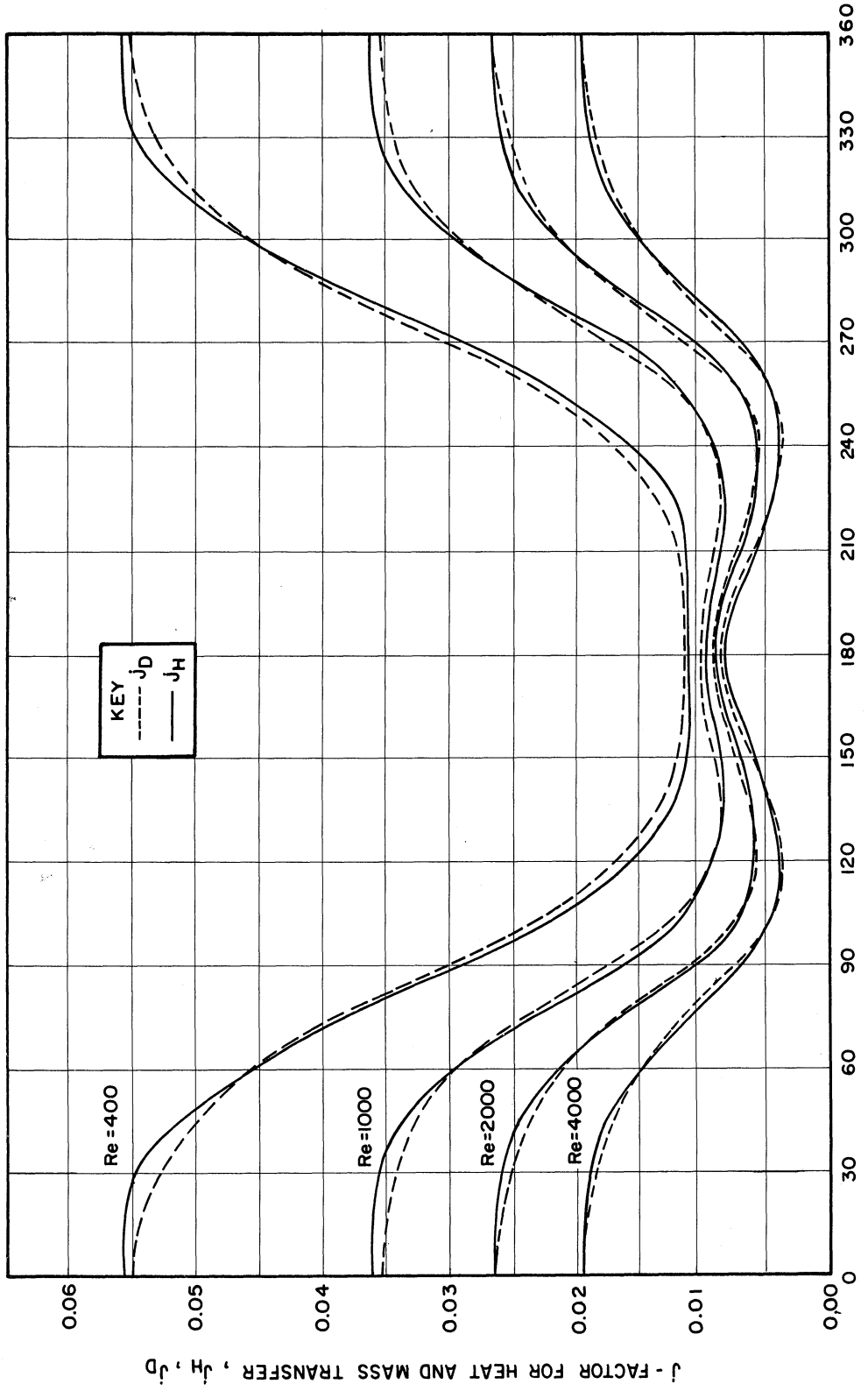

Figure 5. Angular Variation of Mass-Transfer j-Factors at Constant Reynolds Number.

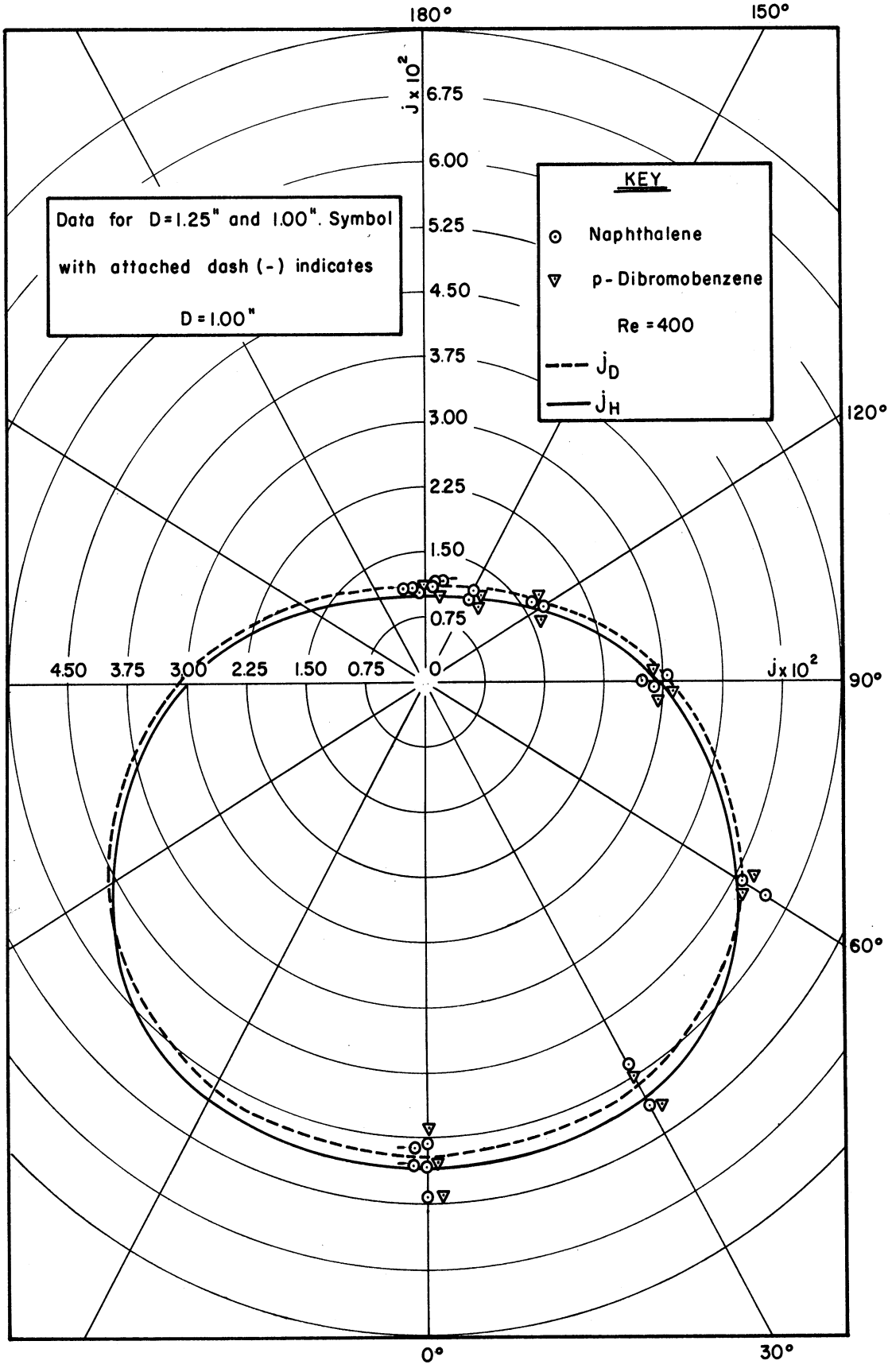

Figure 6a. Polar Diagrams for Heat and Mass-Transfer j-Factor Distributions at Re = 400. Data for θ = 0°, 30°, 60°, 90°, 120°, 150°, and 180°.

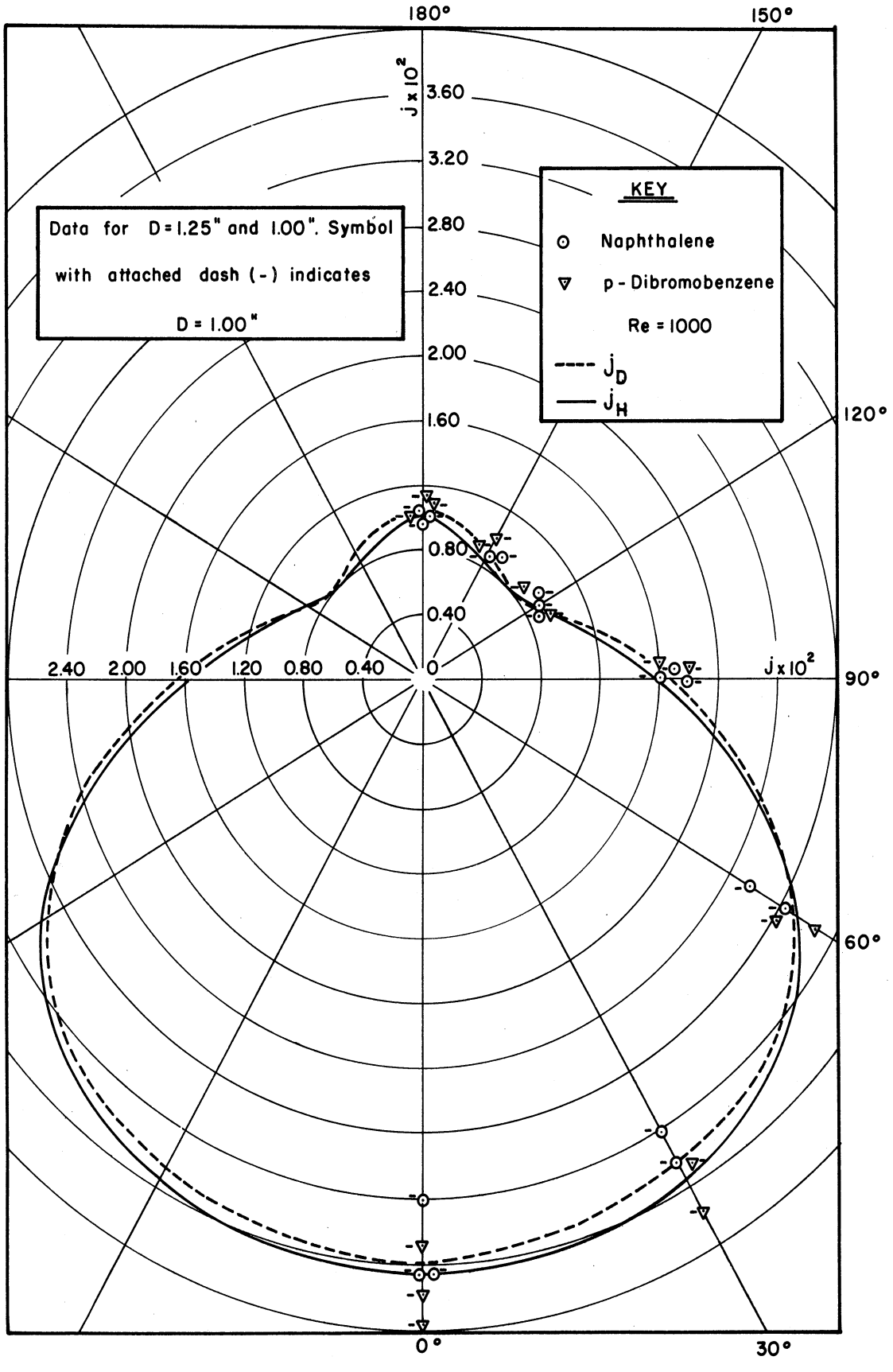

Figure 6b. Polar Diagrams for Heat and Mass-Transfer j-Factor Distributions at Re = 1000. Data for θ = 0°, 30°, 60°, 90°, 120°, 150°, and 180°.

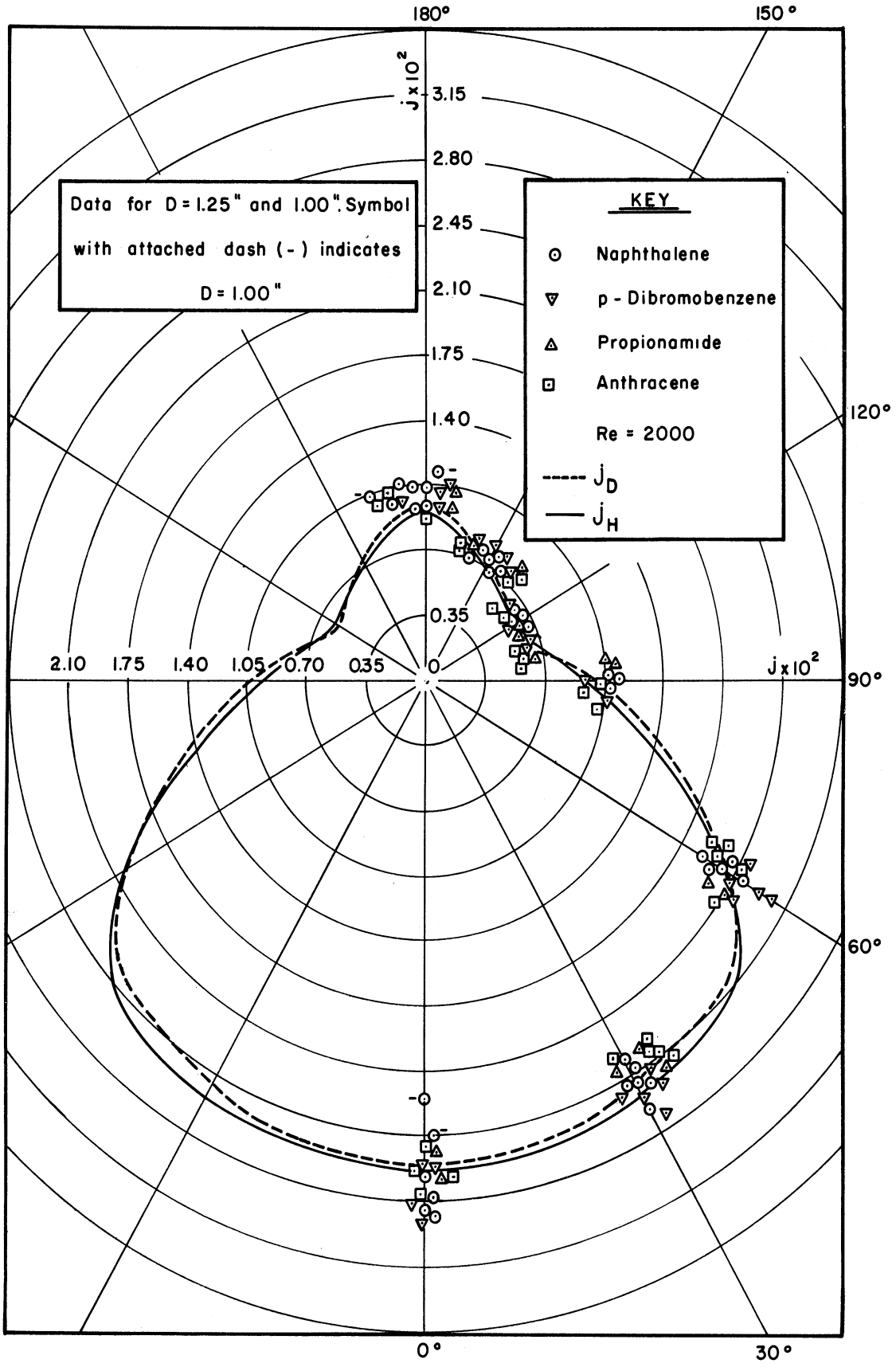

Figure 6c. Polar Diagrams for Heat and Mass-Transfer j-Factor Distributions at Re = 2000. Data for θ = 0°, 30°, 60°, 90°, 120°, 150°, and 180°.

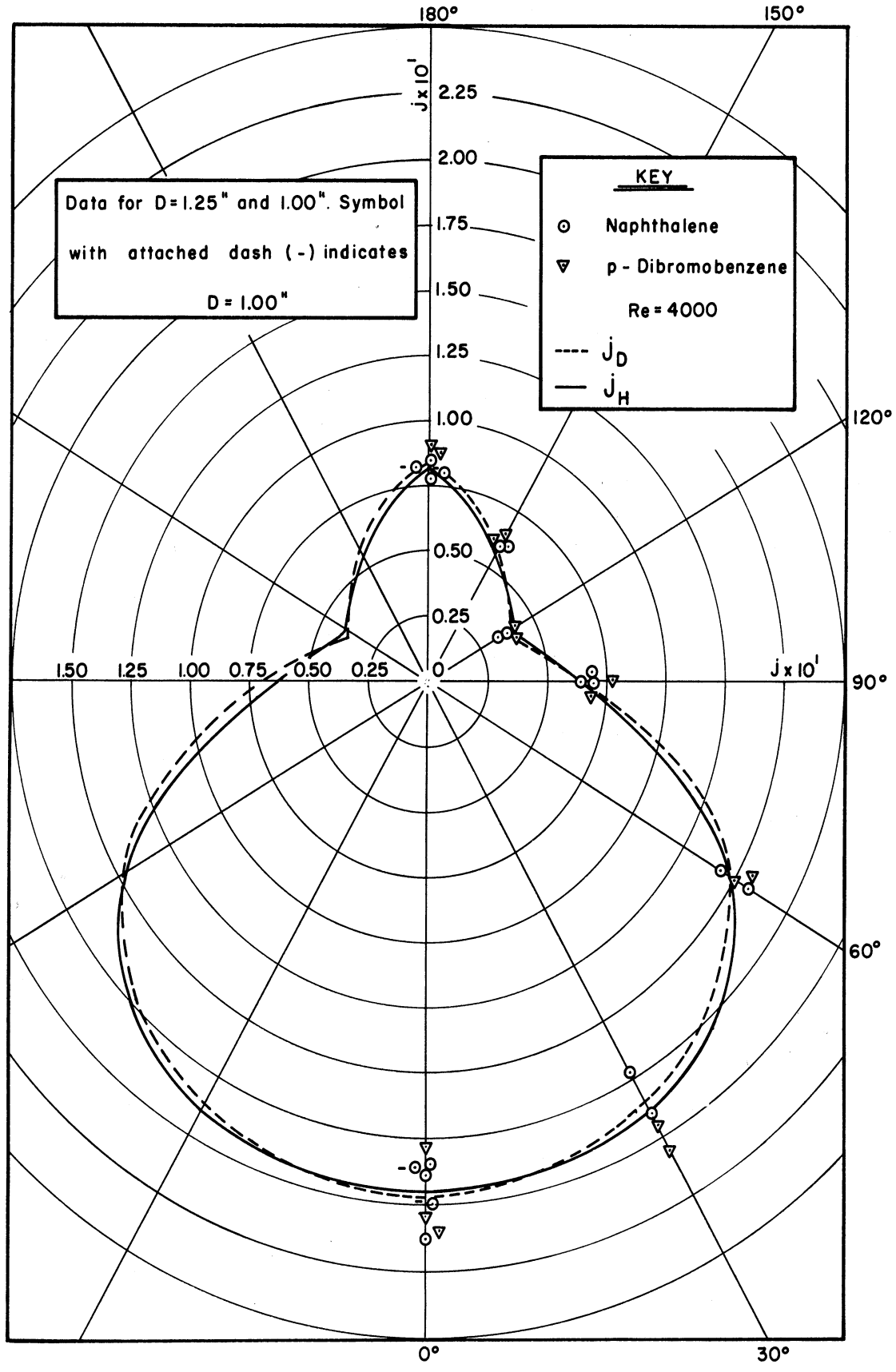

Figure 6d. Polar Diagrams for Heat and Mass-Transfer j-Factor Distributions at Re = 4000. Data for θ = 0°, 30°, 60°, 90°, 120°, 150°, and 180°.

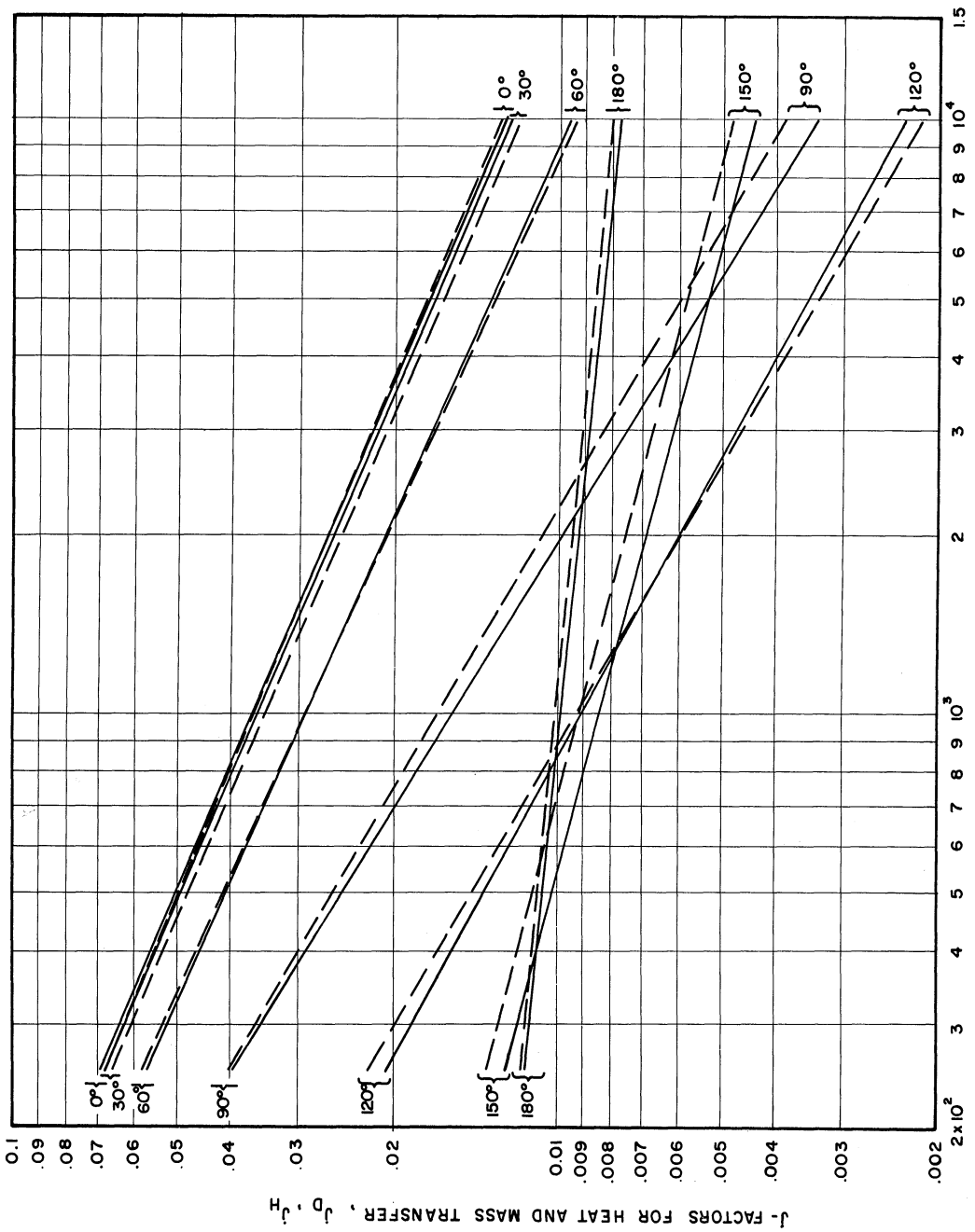

Figure 7a. Correlation of Local Mass-Transfer Data at Various Angles, Summary of Correlations.

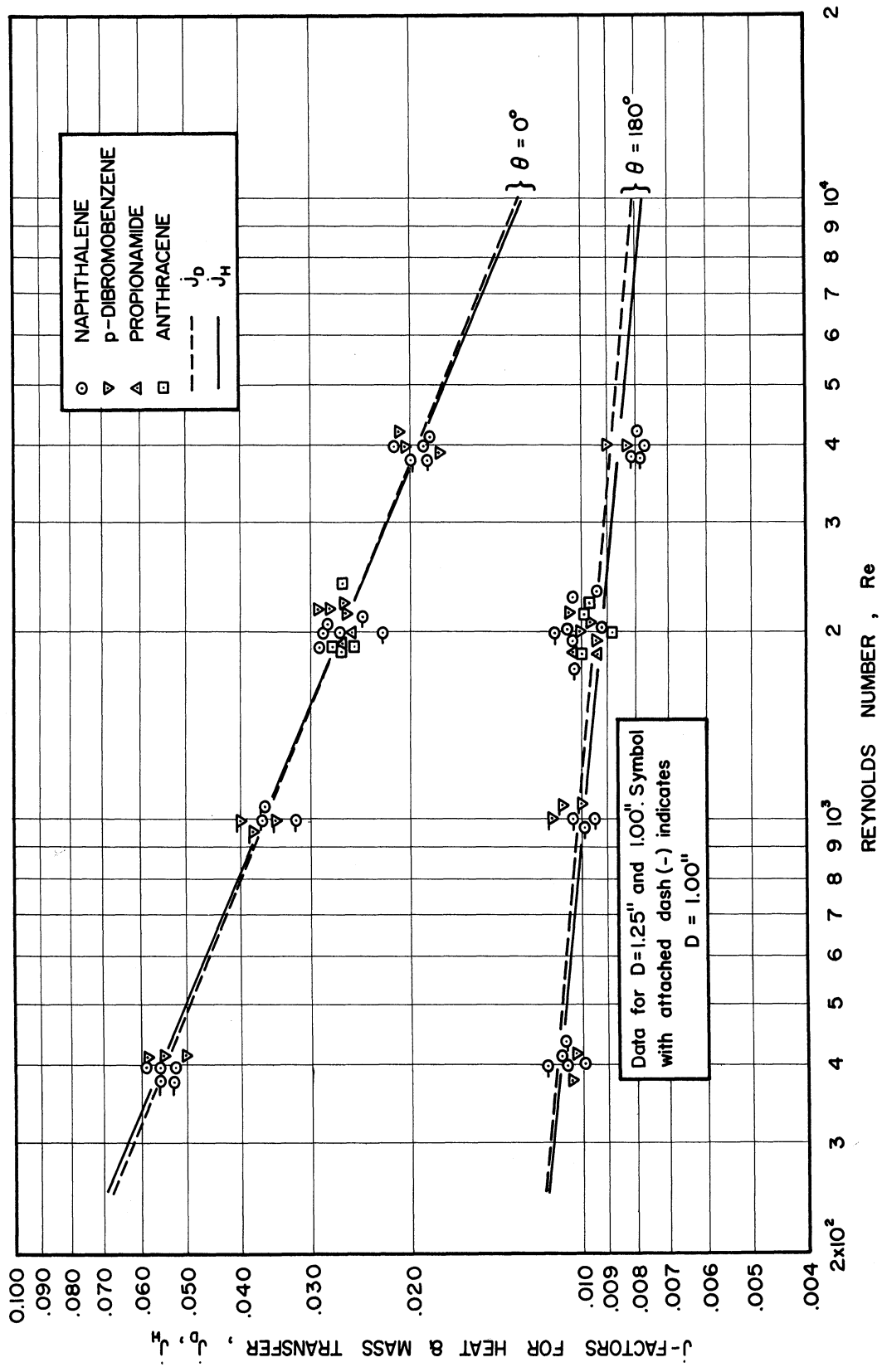

Figure 7b. Correlation of Local Mass-Transfer Data for θ = 0°, 180°. Data for Re = 400, 1000, 2000, and 4000.

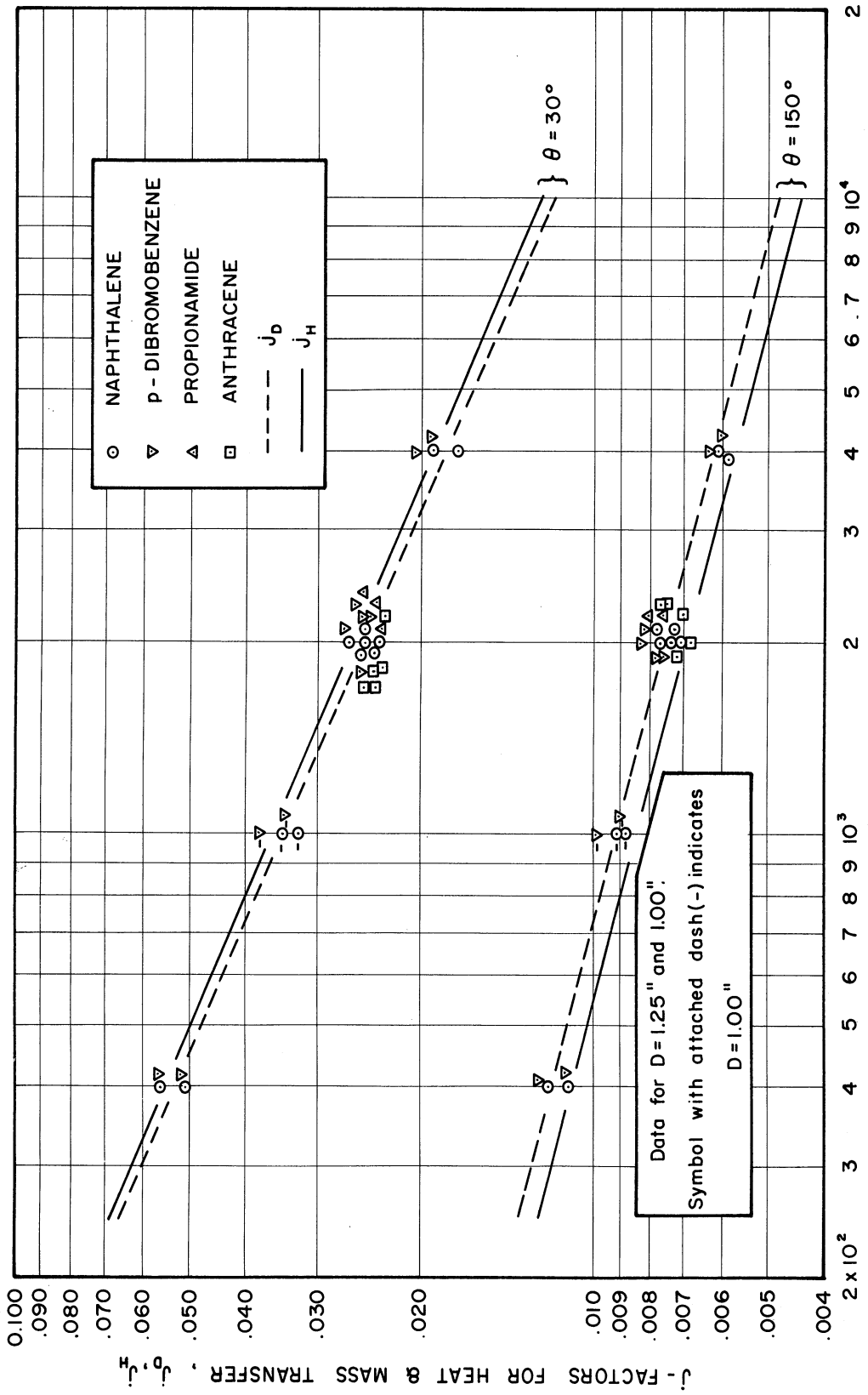

Figure 7c. Correlation of Local Mass-Transfer Data for θ = 30°, 150°. Data for Re = 400, 1000, 2000, and 4000.

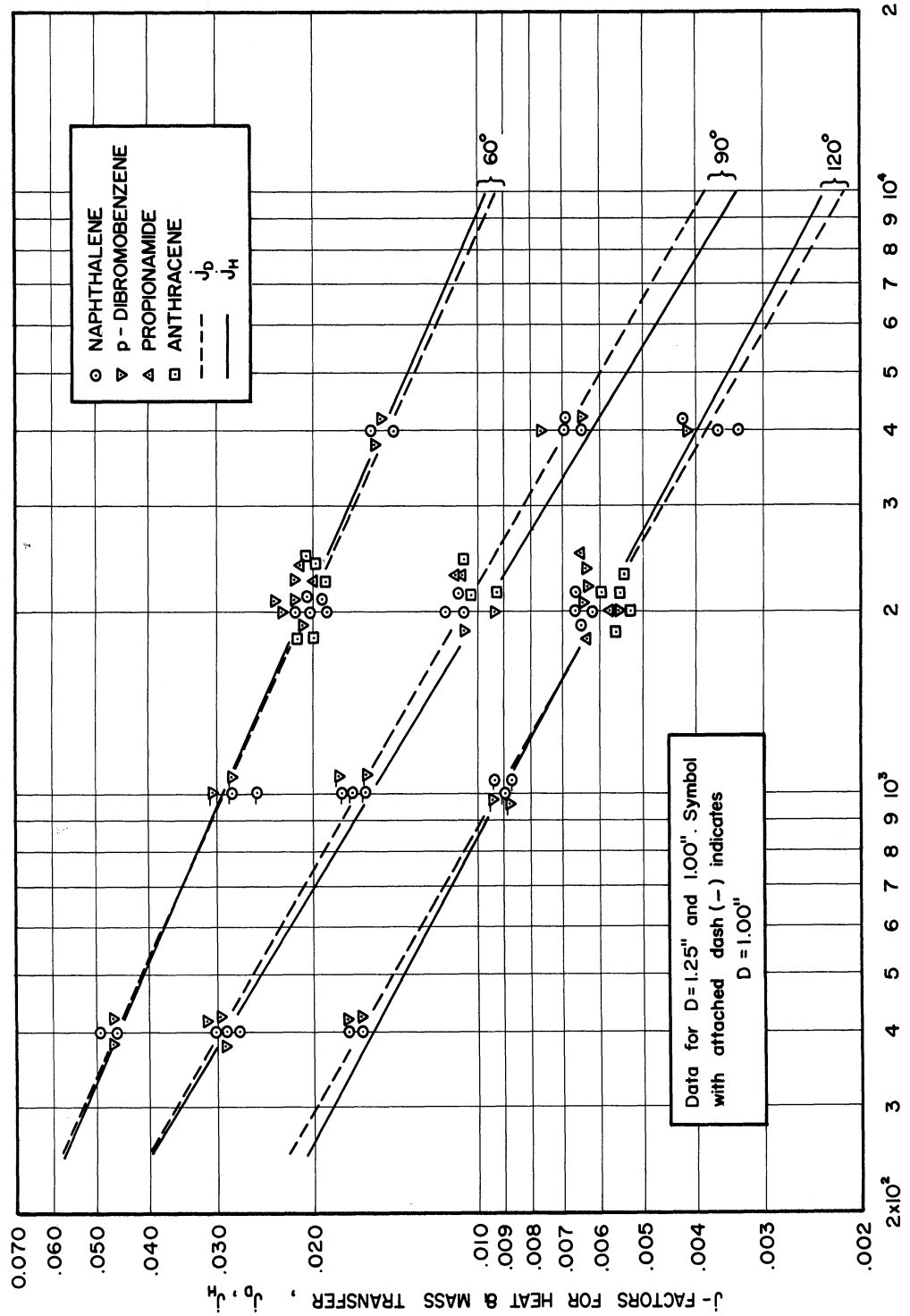

Figure 7d. Correlation of Local Mass-Transfer Data for θ = 60°, 90°, 120°. Data for Re = 400, 1000, 2000, and 4000.

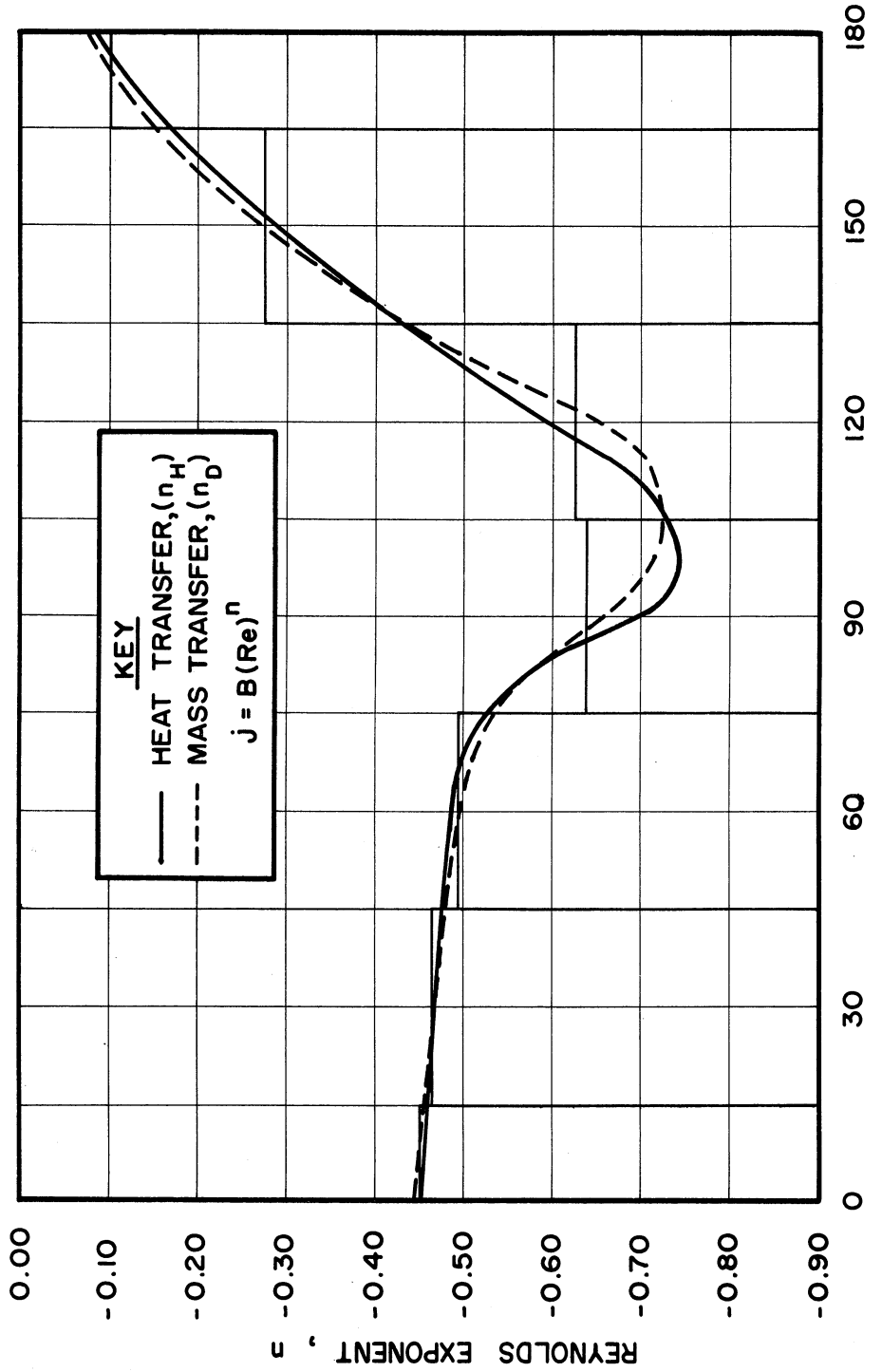

Figure 8. Angular Variation of the Reynolds Number Exponent, (n).

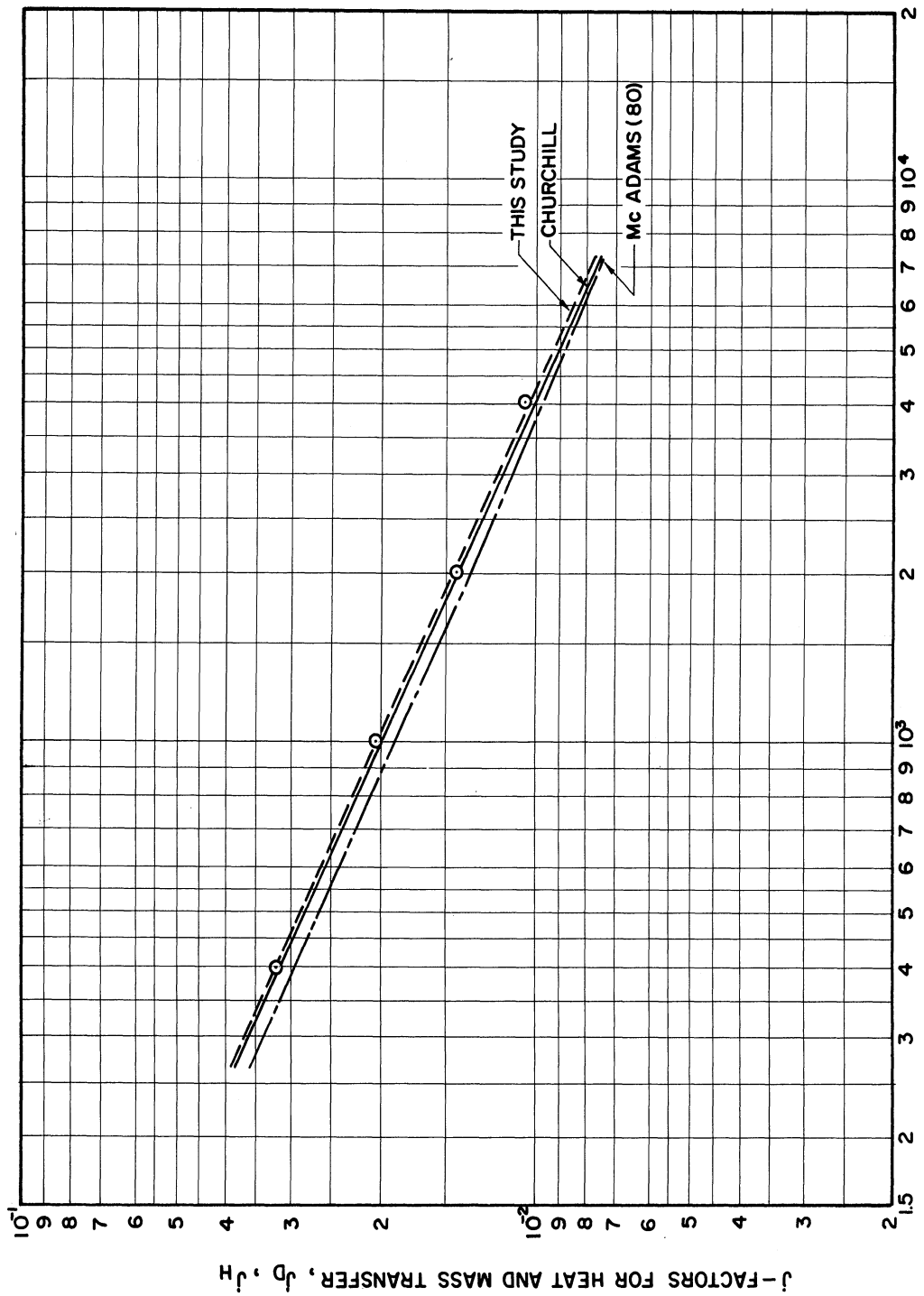

Figure 9. Correlation of Average Mass-Transfer Data.

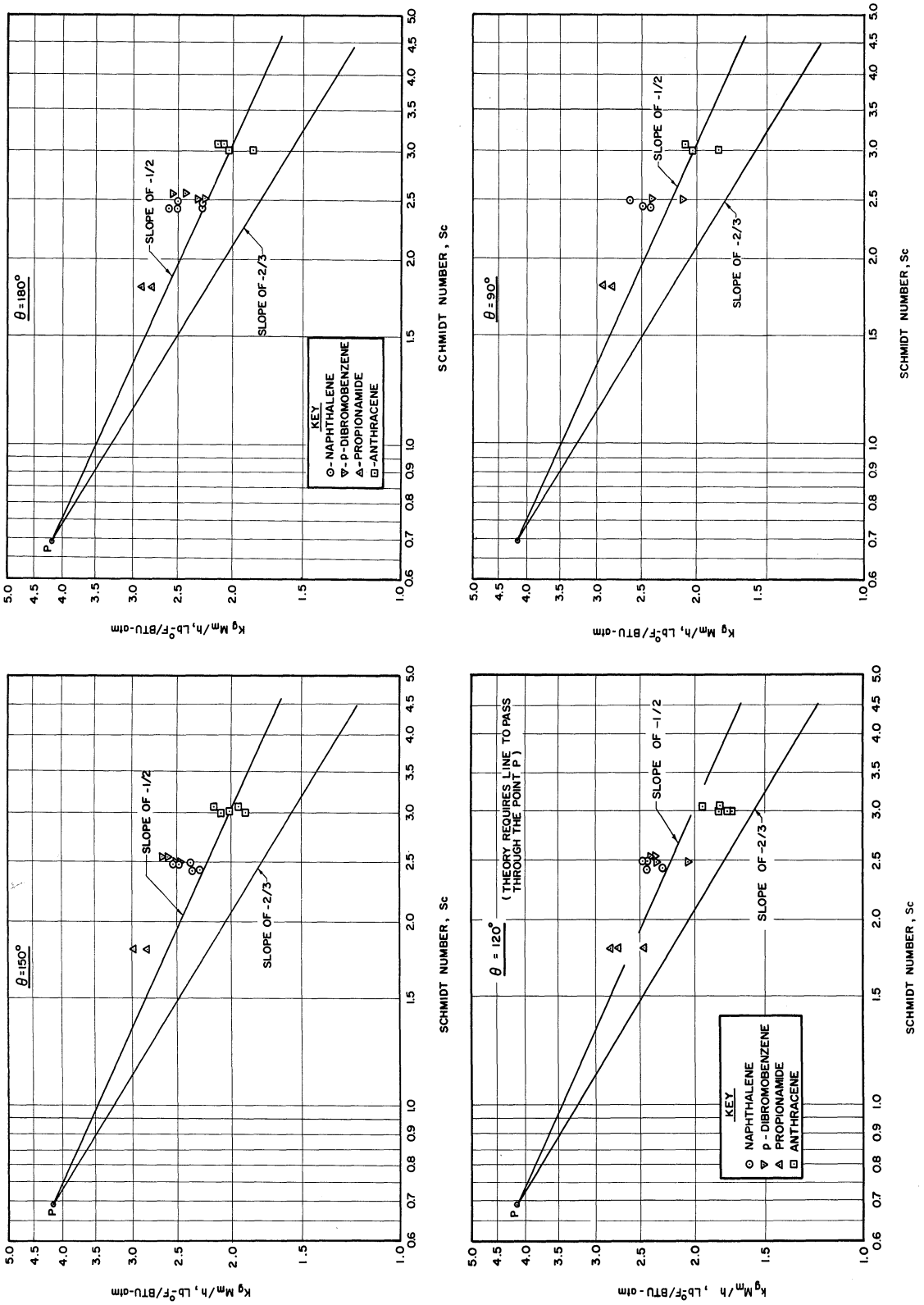

Figure 10a. $(k_g M_m/h)$ as a Function of Schmidt Number for $\theta = 180°, 150°, 120°, 90°$ at Re = 2000

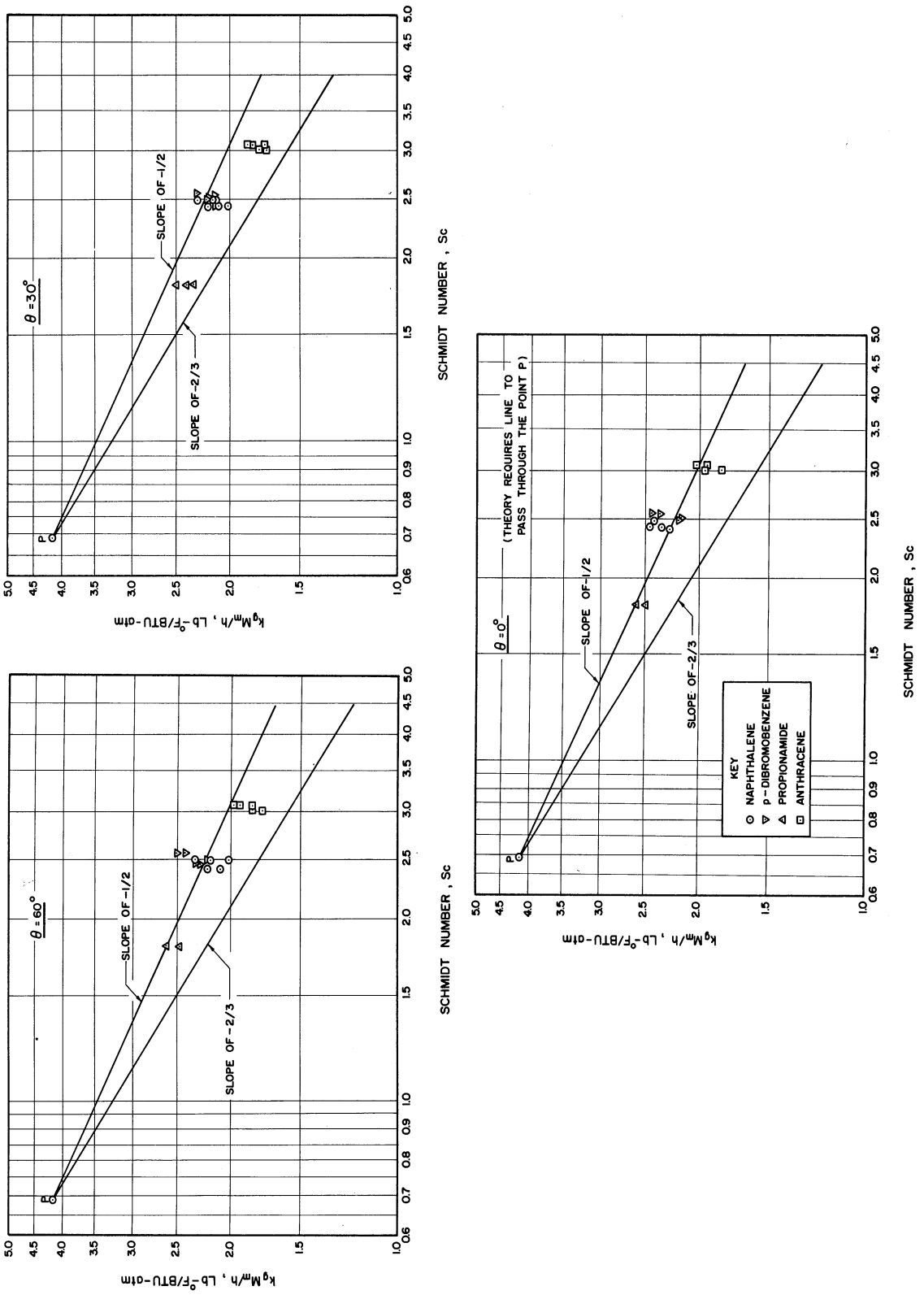

Figure 10b. $(k_g M_m/h)$ as a Function of Schmidt Number for $\theta = 60°, 30°, 0°$ at Re = 2000

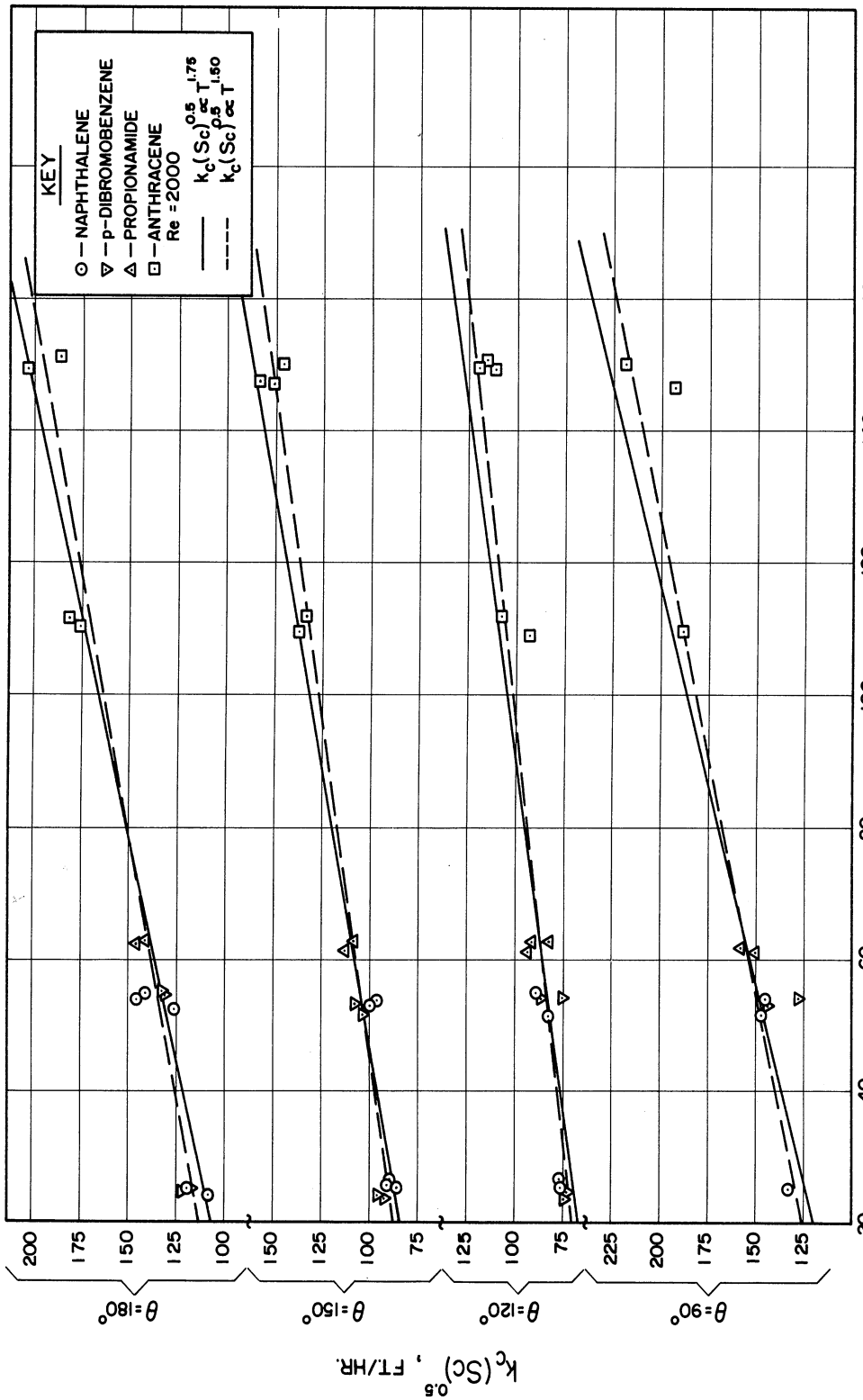

Figure 11a. Temperature Variations of $k_c(Sc)^{0.5}$ for θ = 180°, 150°, 120°, 90° at Re = 2000.

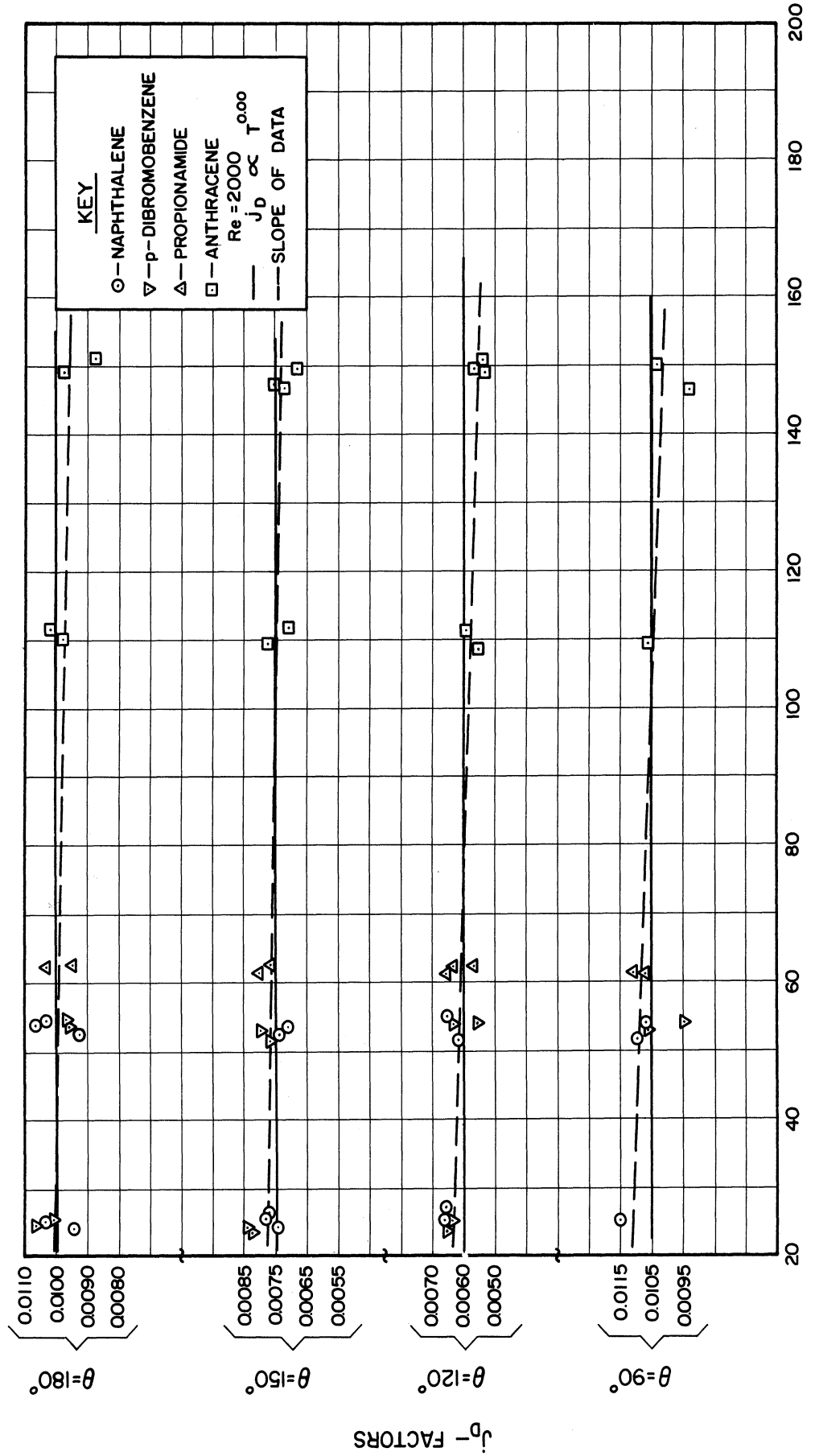

Figure 12a. Temperature Variations of the Mass-Transfer j_D-Factors for $\theta = 180°$, 150°, 120°, 90° at Re = 2000.

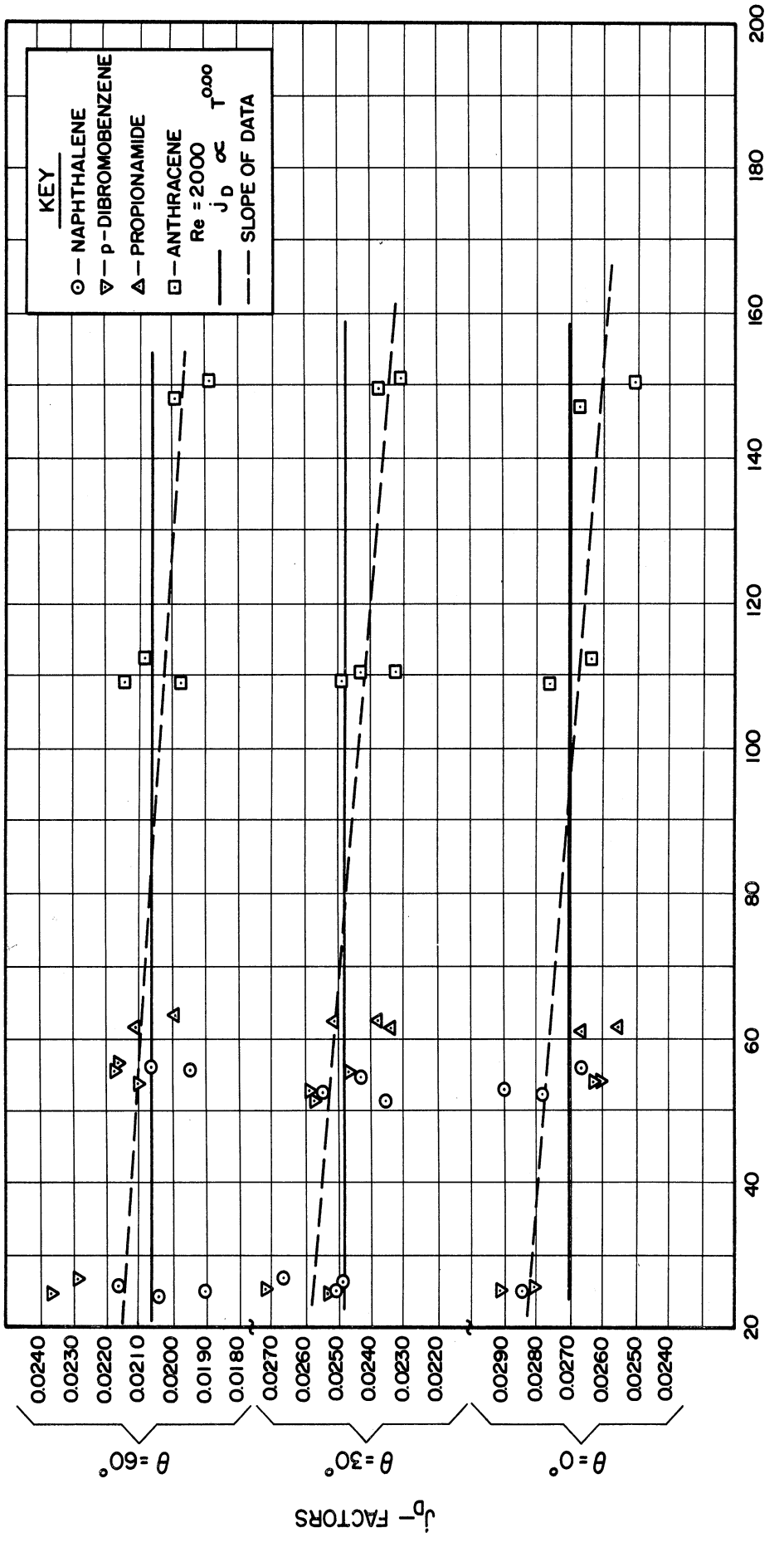

Figure 12b. Temperature Variations of the Mass-Transfer j_D-Factors for $\theta = 60°$, 30°, 0° at Re = 2000.

V DISCUSSION OF RESULTS

1. Evaluation of Results

The results correlate well with the heat transfer data of Churchill using an exponent of 1/2 on both the Schmidt and Prandtl numbers. The agreement of the heat and mass j-factors is significant in view of the differences in methods and mechanisms.

Employing hot wire anemometer explorations, Churchill confirmed the presence of uniform turbulence in the vicinity of the test object. Maisel and Sherwood[77] found no variation in the mass transfer rates below a turbulence of 12% for Re = 1000; while at Re = 5000, no effect was noticed below 4%. The work of Baines and Peterson[2] relating turbulence levels to screen dimensions indicates a turbulence of less than 2% in the present work.

Figures 5 through 8 show the agreement of the local heat and mass transfer j-factors. High values are observed in the impact region, somewhat lower at the back, and minima at about 120°-150° from the stagnation point. At Re = 400, the minima occurs at 150° which decreases to 120° for Re = 4000. Similar distributions of skin friction coefficients have been found[26, 37].

From Figures 10a and 10b, it is evident that the 2/3 power of the Schmidt number is too large while 1/2 is more representative. An accurate value for the Pr exponent cannot be obtained from heat transfer to gases because the Prandtl number varies little. In the Bedingfield and Drew[4] investigations of mass transfer from cylindrical surfaces, an exponent of 0.56 is obtained. The data of Gilliland and

Sherwood[38] support this value. In these studies, the Schmidt number is varied from 0.5 to 2.5. In packed beds, Gaffney and Drew[32] observed that the j-factor increased with the 0.58 power of the Schmidt number which varied from 150 to 13,000. However, in pipes the studies of Linton and Sherwood[72] for Schmidt numbers between 1000 to 3000 and Lin et al.[71] for the transfer from flowing electrolytes to the surface of an electrode where Sc varied from 325 to 3100 give a 2/3 exponent on the Schmidt number. Carberry[9] shows that a fixed exponent should not cover a large variation of the Schmidt number. Instead a variable exponent from 1/2 to 2/3 with increasing Schmidt number is proposed. A firm choice for a constant exponent cannot be made.

The surface temperature was taken as the gas temperature minus a small wet-bulb correction. This correction was calculated by the heat and mass transfer analogy. If the relation were in error, this would introduce only a slight error in the surface temperature which is used to obtain the vapor pressure and mass transfer coefficient. In the present investigation the heat transfer coefficient was not determined.

No direct comparison with other local measurements, except Churchill's, is possible since they were at other flow rates.

At a Reynolds number of 2000, sublimation rates were determined over a temperature range of 125°C. Since experiments evaluating the effect of temperature on mass transfer coefficients are limited, it must be approximated from available correlations. Gilliland and Sherwood[38] and others confirmed that the mass transfer coefficients can be described by the dimensionless equation,

$$k_c D/D_v = \text{const } (Re)^a (Sc)^b \qquad (41)$$

Equation (41) may be written as

$$\frac{k_c}{u}\left(\frac{Du\rho}{\mu}\right)\left(\frac{\mu}{D_v\rho}\right) = \frac{k_c}{u}\,(Re)\,(Sc) = \text{const}\,(Re)^a(Sc)^b \quad (42)$$

By definition,

$$j_D = \frac{k_c}{u}\,(Sc)^{0.5} = \text{const}\,(Re)^{a-1}\,(Sc)^{b-0.5} \quad (43)$$

For the conditions of this investigation where b = 0.5 and the Reynolds number is constant, the j_D - factor would be expected to be temperature independent.

The temperature dependencies of the physical properties involved in the above equations are

$\rho \alpha 1/T$ - for air

$D_v \alpha T^{1.95}$ - according to the Hirschfelder et al.[47] technique

$\mu \alpha T^{0.75}$ - for air

$G \alpha T^{0.75}$ - for constant Re where $G \alpha \mu \alpha T^{0.75}$

$u \alpha T^{1.75}$ - since $u = G/\rho \alpha (T^{0.75})(T^{1.0}) = T^{1.75}$

The effect of temperature on the Schmidt factor to the 0.5 power is then

$$(Sc)^{0.5} \alpha (T^{-0.20})^{0.5} = T^{-0.10}$$

At a constant Reynolds number, there then results from Equation (41)

$k_c \alpha T^{1.95} \times T^{-0.10} = T^{1.85}$ or $k_c(Sc)^{0.5} \alpha T^{1.85} \times T^{-0.10} = T^{1.75}$

Similarly, from Equation (43)

$$j_D \alpha T^{0.00}$$

Temperature variations of $k_c(Sc)^{0.5}$ for given angular positions are shown in Figures 11a and 11b. The dashed lines with the predicted

variation of $T^{1.75}$ are included and within experimental limitations give a fair representation of the data. A slope with $T^{1.50}$ is far more in accord with the data. A closer study of these data indicates considerable scatter with a slight increasing variation of k_g with increasing temperature for each of the organic solids.

Figures 12a and 12b show that j_D decreases less than 10% over the 125°C temperature range for any position and may be taken as constant.

2. Comparison of Local Distributions with Other Investigations

Only a few studies of local measurements of heat transfer and none of mass transfer are reported for Reynolds numbers of the present investigation. In Table II are references to other local transfer studies together with their ranges and methods.

The distributions can be classified into the pre-critical, critical and the post-critical Reynolds number. In the pre-critical region, all j-factor distribution curves have maximums at the stagnation point, $\theta = 0$, and decrease to minimuma at approximately 90°-120° nearly coinciding with the point of separation of the laminar boundary layer from the surface. The curves continue to gradually increase to a second maximum at the rear stagnation point, $\theta = 180°$. For large Reynolds numbers, the rear stagnation maximum is the greater due to the eddy motion of fluid behind the body. In the critical and post-critical regions, the distribution in the forward region, $\theta < 90°$ is similar to that for pre-critical flow. However, the first minimum occurs between 80° and 95° and is attributed to a transition from laminar to a turbulent boundary layer. The sharp maximum between 100° to 120°, is apparently

due to increasing turbulence in the boundary layer and vorticity sheet. The second minimum, at about 140° coincides with the separation point of the boundary layer from the surface. The distribution curves increase gradually from here to a maximum at the rear stagnation point. This is ascribed to a circular motion of fluid going from the joining point (where the two branches of fluid join behind the cylinder) towards the separation point of the boundary layer. Increasing turbulence causes a decrease in the critical Reynolds number.

Distributions obtained in this study and other investigations are given in Figures 13a to 13g. From the published data, heat and mass transfer j-factors were calculated in 30° increments. Most of the pre-critical data give linear plots of log j versus log Re with slopes varying with angular position. For the studies spanning the critical range, linearity is apparent for the front of the cylinder while the data in the rear often are scattered. For these plots, straight lines are drawn by sight. Unfortunately the 30° segmental average transfer distributions particularly in the rear half at the higher Reynolds numbers do not indicate the lobes of the distribution curve. In view of the meagerness of data points, nearly all j-factor distributions are calculated from the graphical results which in certain instances could only be approximately determined. This is true particularly for the study of Krujilin and Schwab[67] who presented smooth distributions for Reynolds numbers of 1000, 2000, and 4000 in small graphs.

In Figures 13a through 13d, studies including the present agree on the impact half, while on the rear discrepencies are appreciable. As an example, the plots for the data of Eckert and Soehngen[27] at low Reynolds numbers from 23 to 597 agree satisfactorily with the present study

Table II

Comparison of Previous Local Heat and Mass-Transfer Studies

No.	Study	Reynolds Number & Turbulence Level	Cylindrical Diameters	Methods and Comments	Constant	Constants (B & n) for j-Factor Equation, $j = B(Re)^{-n}$, for Various Angular Positions 0°	30°	60°	90°	120°	150°	180°
1	This study	400 < Re < 4000 Turb. < 2% (est.)	1.00",1.25"	Sublimation of organic solids from 30° cylindrical segments.	B	0.817	0.860	0.899	1.330	0.685	0.0829	0.0204
					n	0.451	0.466	0.496	0.635	0.624	0.279	0.101
2	Churchill,S.W. & J.C. Brier, CEP Sym.Ser.No.17,51,57 (1955)	300 < Re < 2300 Turb. < 2% (est.)	1.00"	Heat transfer from radial temperature profile through 30° sector of tube wall	B	0.847	0.947	0.842	1.602	0.715	0.0644	0.0224
					n	0.456	0.477	0.486	0.671	0.592	0.293	0.117
3	Drew,T.B. & W.P.Ryan, Trans.AIChE,26,118(1948)	Report Distribution at Re=39,000.	1.49"	Measured steam condensation over 30° segments. Data only given for Re=39.000.								
4	Eckert,E.R.G. & E.Soehngen, Trans.ASME,74,343(1952)	23 < Re < 597 Turb. not reported	0.5",1", 1.5"	Employed interferometer to determine radial temperature field around cylinder.	B	1.182	1.124	0.954	1.289	0.498	0.396	0.430
					n	0.516	0.518	0.527	0.656	0.614	0.549	0.510
5	Fage,A. & V.M.Falkner, Gr. Brit.Aero.Res.Com.Rept. & Memo.No.1408(1931)		5.89"	Heat transfer rates measured from electrical input to a nickel strip substending 2°. (Linearity not apparent.)								
6	Giedt,W.H.,Trans.ASME,71, 375(1949);J.Aeronat.Sci., 18,725(1951)	70,800 < Re < 219,000 Turb.approx. 2.25% and < 1%.	4"	Measured temperature variation around heated cylinder by heating ribbon wrapped helically around surface. (4% Turb. not included.)	B	0.171	0.168	0.0977	0.00551	1.048×10^{-4}	0.00341	0.00566
					n	0.330	0.331	0.297	0.067	-0.290	0.014	0.046
7	Klein,V.,Arch.Warmewirstch. u.Dampkessekw.,15,150(1934)	8,000 < Re < 75,000 Turb. not reported		Measured change in dimensions of subliming ice cylinders.	B	2.687	2.330	1.753	0.0788	0.01524	0.0473	0.0671
					n	0.582	0.573	0.568	0.338	0.180	0.243	0.261
8	Krujilin,G. & B.Schwab, Tech.Physics USSR,2,312 (1935)	20,000 < Re < 75,000 Turb. not reported	4.4cm	Thermocouples inserted in surface grooves of steam heated tube.	B	1.776	1.761	2.178	1.473	0.921	0.638	0.574
					n	0.538	0.545	0.578	0.592	0.511	0.452	0.427
8a		1060,2080, & 4020 Turb. not reported			B	3.389	3.598	2.575	1.141	0.562	1.171	0.676
					n	0.539	0.655	0.628	0.649	0.518	0.571	0.479
8b	Krujilin,G.,Tech.Physics USSR,5,289(1938)	6,000 < Re < 425,000 Turb. not reported			B	0.497	0.439	0.239	0.0416	0.0553	0.505	1.374
					n	0.408	0.407	0.382	0.260	0.243	0.407	0.478
					B				Re > 130,000		0.108	0.138
					n						0.277	0.281
9	Lohrisch,W.,Forsch.Gebiete Ingenieuw.,No.322,45(1929)	5,000 < Re < 25,000 Turb. not reported	5cm	Air-Ammonia stream absorbed on 12 longitudinal strips of blotting paper saturated with phosphoric acid.	B	0.758	0.679	0.581	0.273	0.0274	0.00769	0.0222
					n	0.454	0.450	0.456	0.459	0.238	0.016	0.099
10	Powell,R.W. & E.Griffiths, Trans.Inst.Chem.Engrs., London,13,175(1935)			Relative rates of evaporation from nonagonal prism approximating a cylinder were measured. No quantitative data appear in the article.								
11	Robinson,W. & L.S.Han, Proc.Midwest Conf. Fluid Mech.(2nd Conf.), 349, (1952)	Report distribution at 21,300	1.5"	Heat transfer distributions in ducts determined from radial temperature differenials. Results for single cylinder similar to (12).								
12	Schmidt,E. & K. Wenner, NACA TM 1050,1943	8,290 < Re < 426,000 Turb. not reported	5cm,10cm, 25cm	Measurements of heat transfer distribution from steam heated tube presented in 10° intervals.	B	1.132	1.076	0.765	0.01434	0.00970	0.0348	0.0700
					n	0.494	0.479	0.484	0.194	0.097	0.204	0.247
					B				Re > 120,000			1.516
					n							0.514
13	Seban,R.A.,Trans.ASME, Series C, 82,101(1960)	50,000 < Re < 300,000 Turb. from 1-3%	1.25"1.87"	Bakelite cylinders with Nichrome heating ribbons wrapped on their surfaces. Influence of turbulence intensity on local heat transfer studied.								
14	Small,J., London Phil Mag.,19,251(1935)	22,400 < Re < 84,100 Turb. not reported	4.5"	Thermopile embedded in steam heated tube used to measure the distribution.	B	1.131	1.177	0.876	0.00446	0.0384	0.1968	0.272
					n	0.459	0.471	0.467	0.026	0.183	0.313	0.324
15	Winding,C.C. & A.J. Cheney,Jr., IEC,40, 1087(1948)	10,600 < Re < 32,000 Turb. not reported	1.49"	Measured change in dimensions of subliming naphthalene cylinders.	B	1.910	1.801	1.068	1.360	0.1219	0.1086	0.1761
					n	0.543	0.544	0.516	0.611	0.330	0.282	0.303

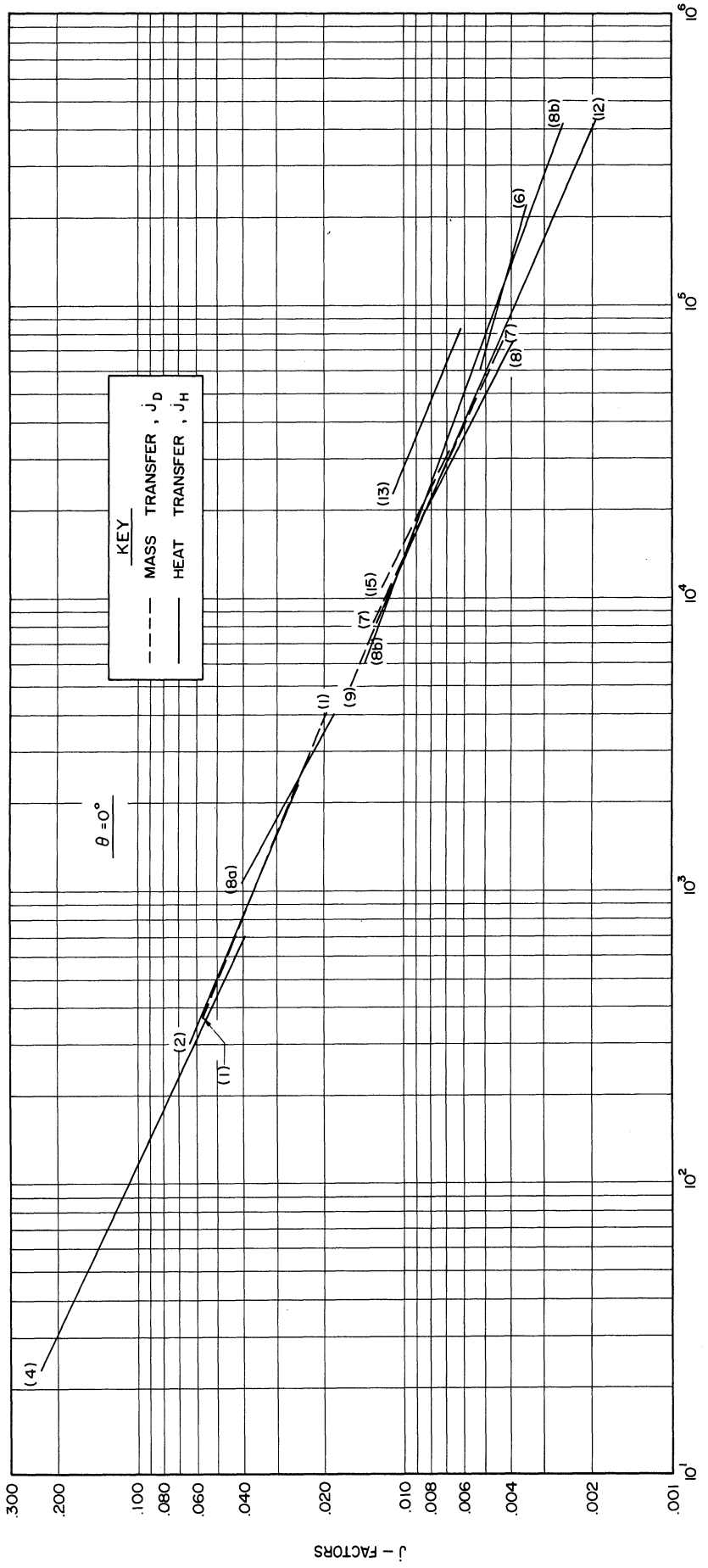

Figure 13a. Comparison of Previous Local Heat and Mass-Transfer Investigations for $\theta = 0°$. See Table II for explanation of numbering system.

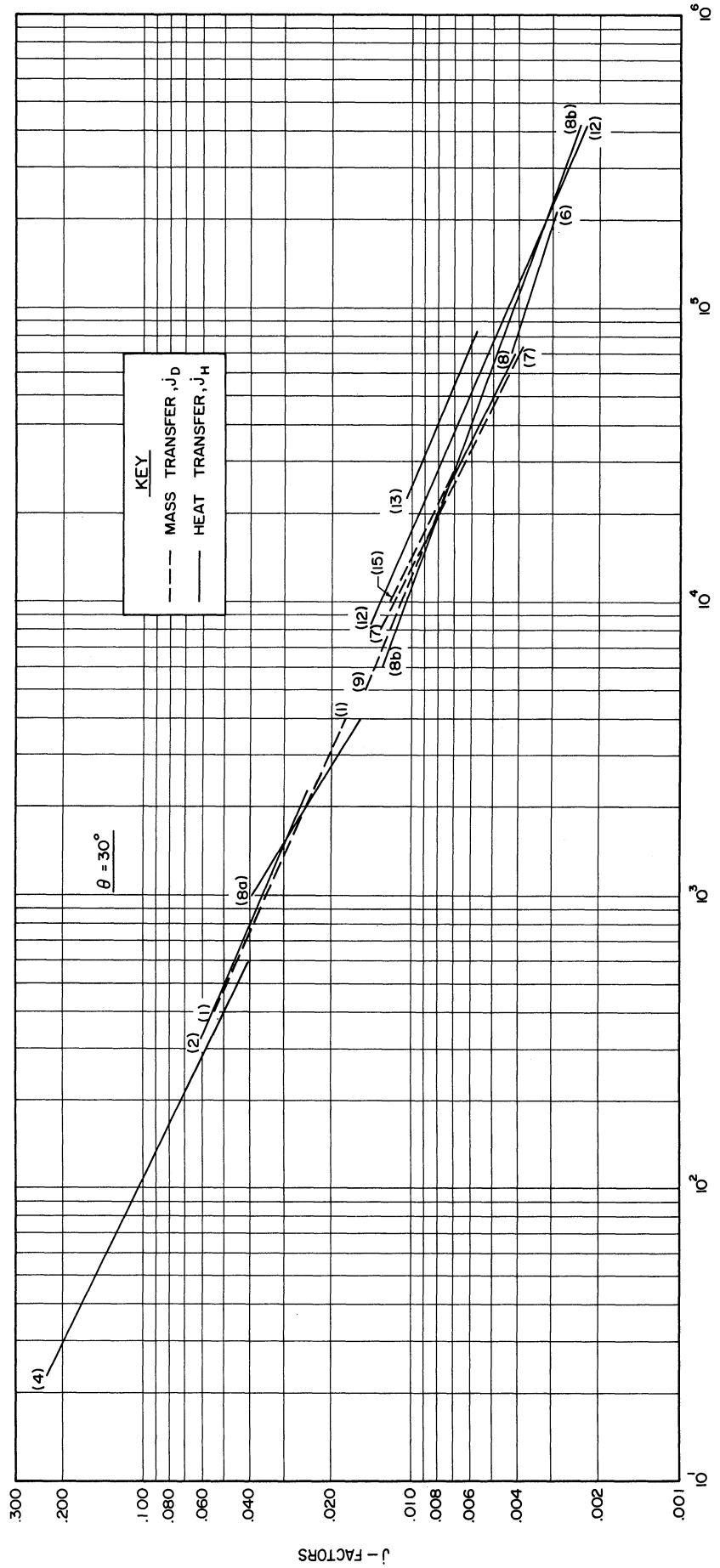

Figure 13b. Comparison of Previous Local Heat and Mass-Transfer Investigations for θ = 30°. See Table II for explanation of numbering system.

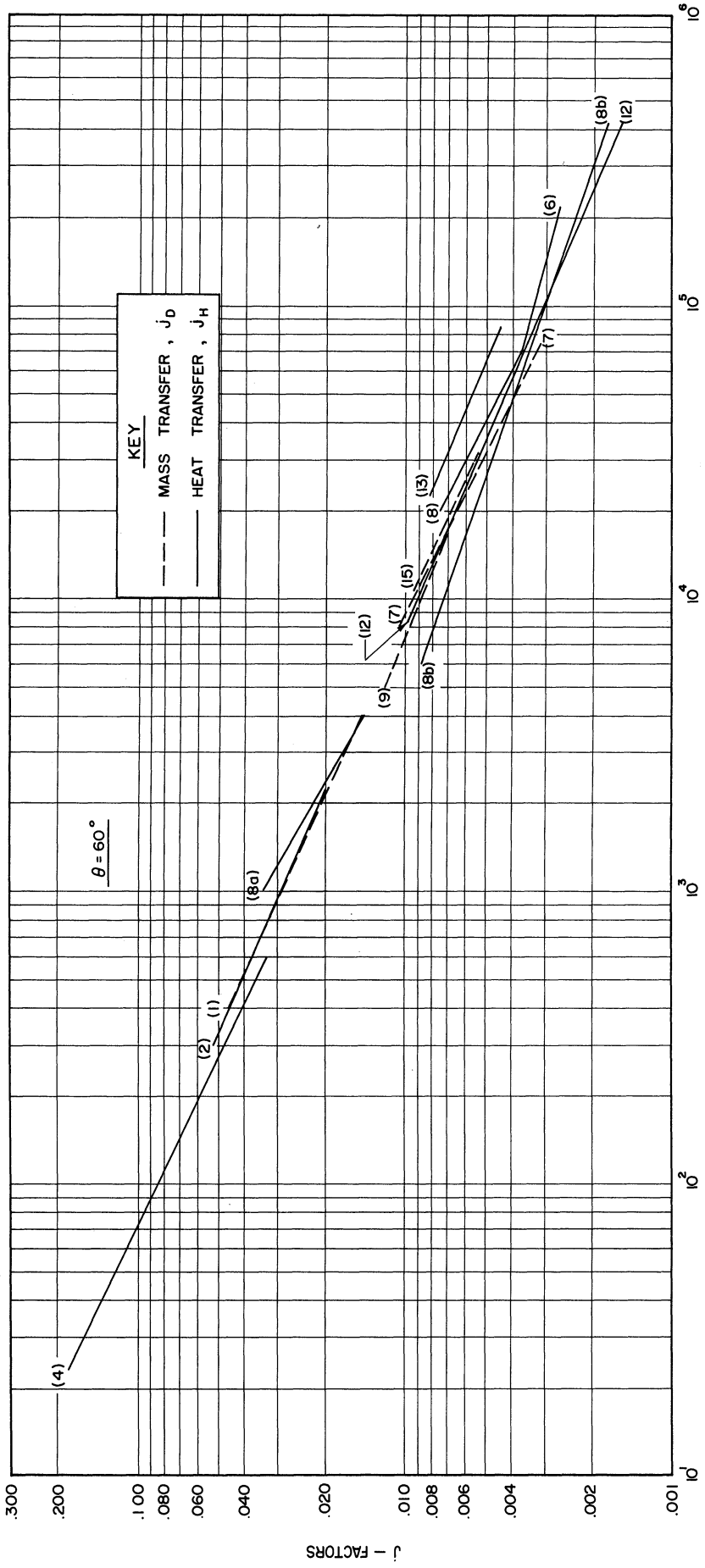

Figure 13c. Comparison of Previous Local Heat and Mass-Transfer Investigations for θ = 60°. See Table II for explanation of numbering system.

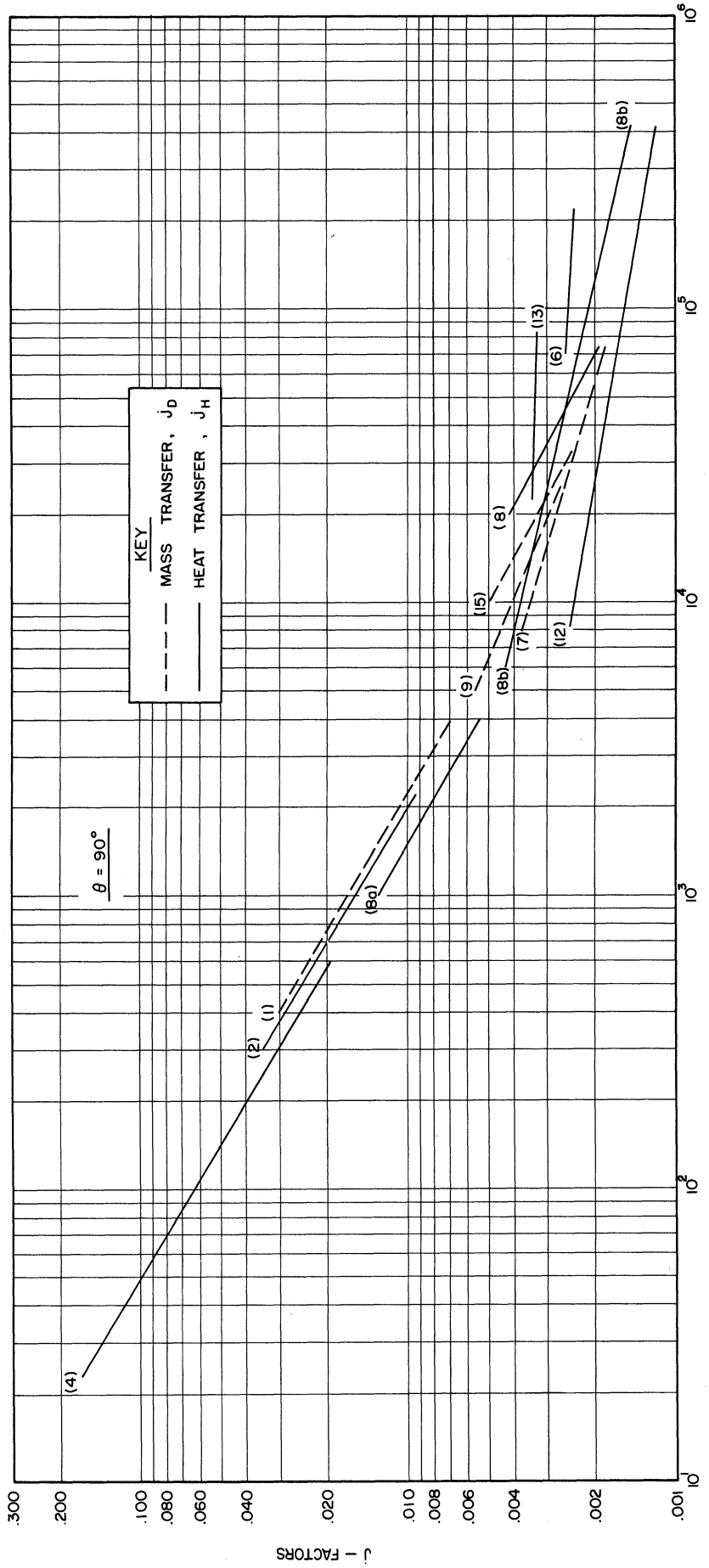

Figure 13d. Comparison of Previous Local Heat and Mass-Transfer Investigations for θ = 90°. See Table II for explanation of numbering system.

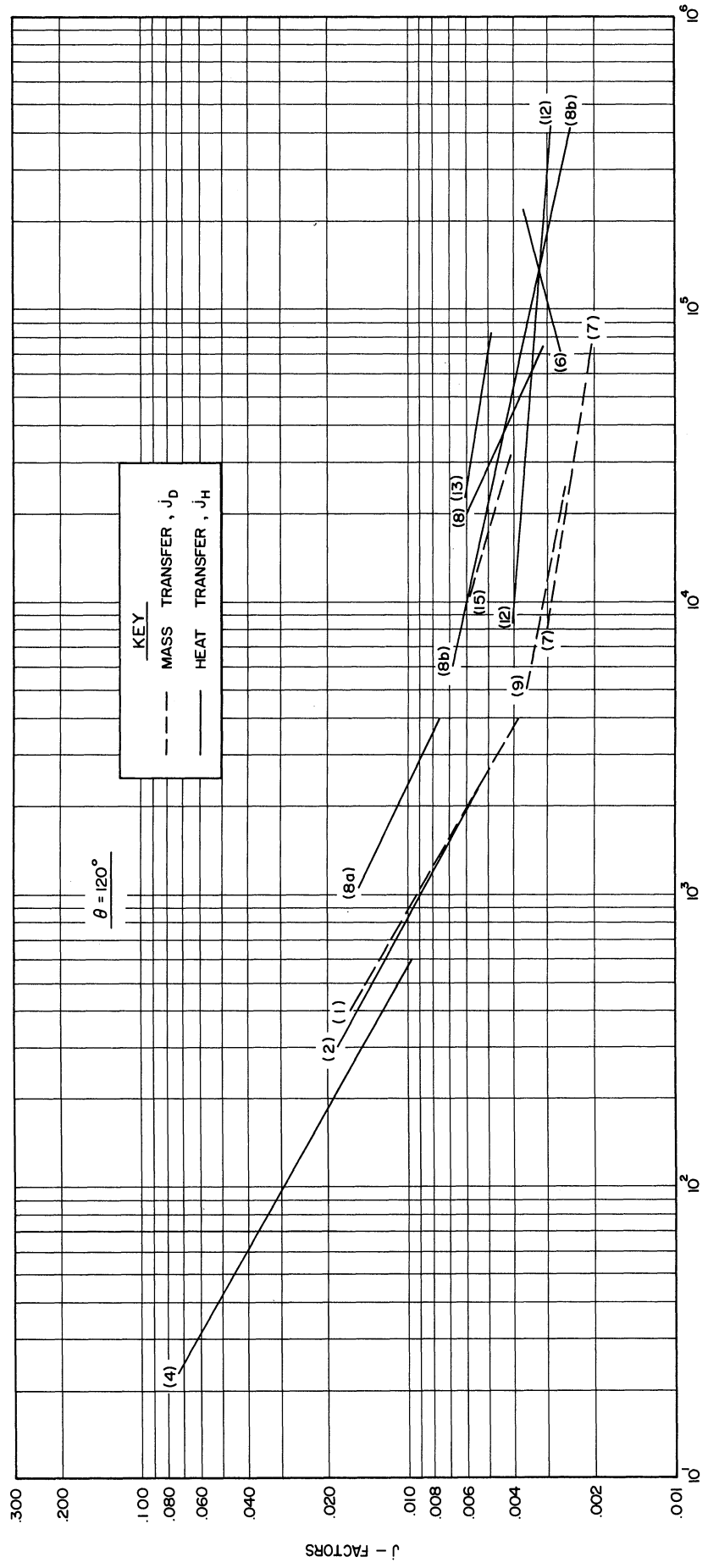

Figure 13e. Comparison of Previous Local Heat and Mass-Transfer Investigations for $\theta = 120°$. See Table II for explanation of numbering system.

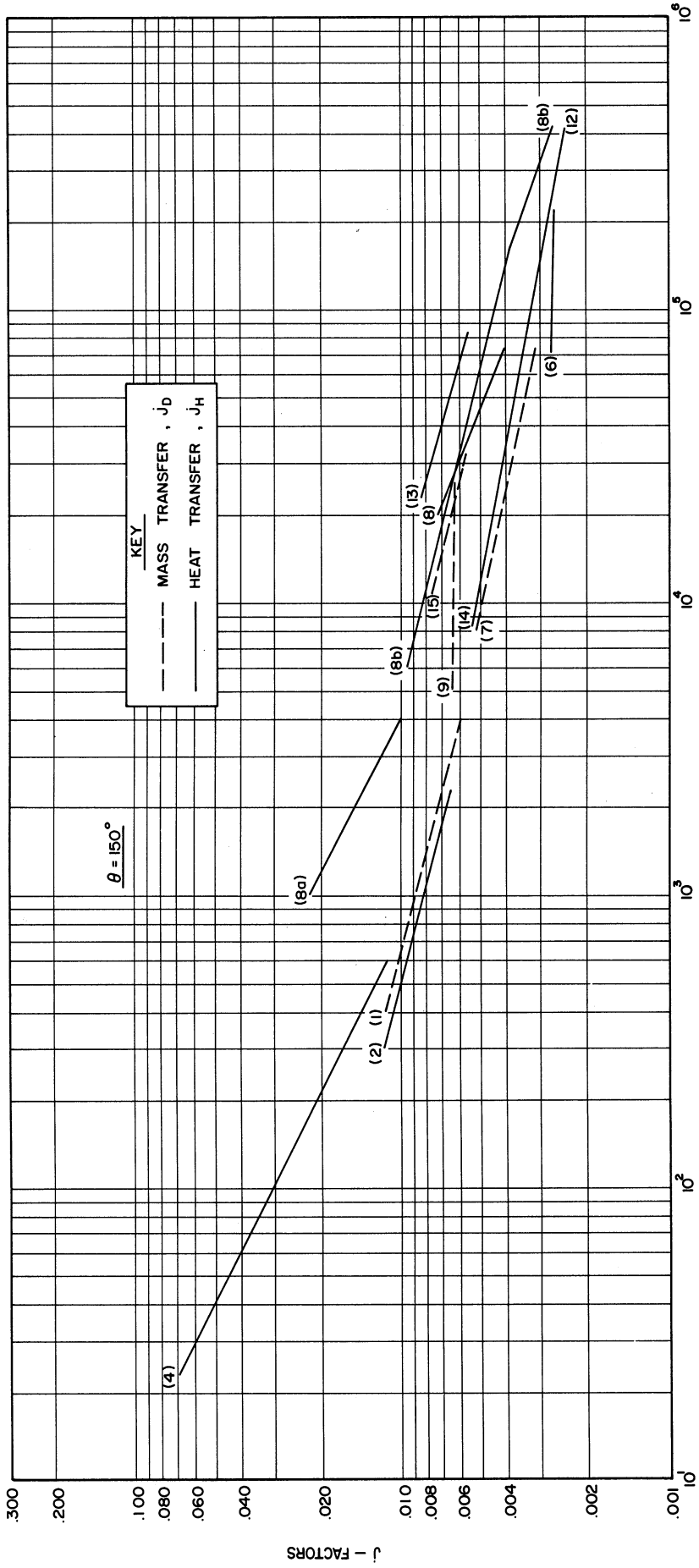

Figure 13f. Comparison of Previous Local Heat and Mass-Transfer Investigations for $\theta = 150°$. See Table II for explanation of numbering system.

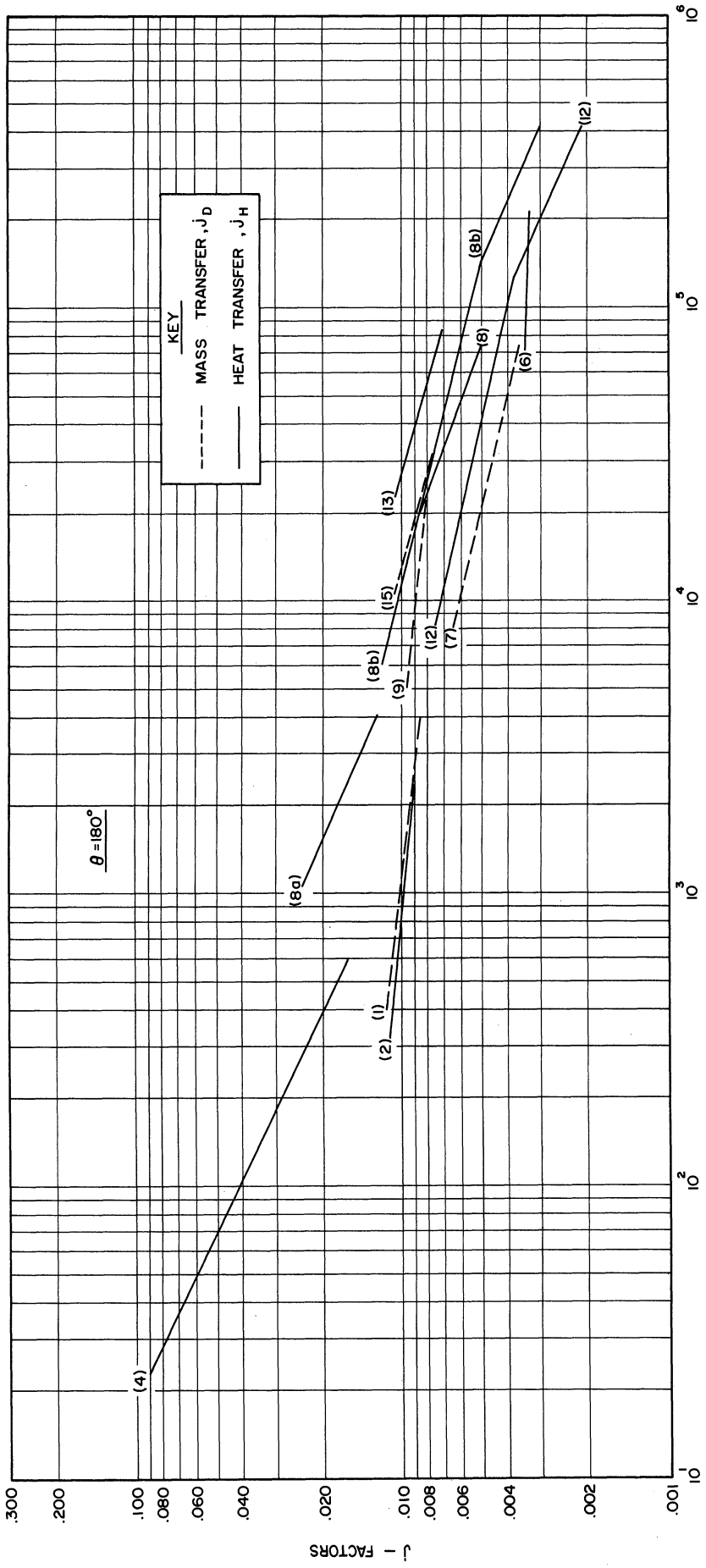

Figure 13g. Comparison of Previous Local Heat and Mass-Transfer Investigations for θ = 180°. See Table II for explanation of numbering system.

for 0° to 135° with increasing disagreement for 135° to 180°. Evidently the rear of the cylinder is more sensitive than the front half to the process conditions.

The agreement of various studies is good in light of dissimilar techniques used including sublimation, absorption, and heat transfer.

3. Comparison of j-Factors with Other Investigations

The assumption of the equality of j_H and j_D has been used to predict mass transfer from heat transfer data and vice versa. The validity of this assumption has not been adequately proved. A verification would be helpful in interpreting data such as from heterogeneous catalysis, absorbers, packed and fluidized beds.

Table III contains references to studies of the heat-mass analogy together with comments and suggested ratios of (j_H/j_D). The table indicates the equivalence of the j-factors for flow past objects including cylinders, spheres, disks, and flat surfaces. The studies of Ranz and Marshall[85], Sogin[99] Furber,[31] and Jakob et al.,[54] contribute convincing support to the approximate equality of the heat and mass transfer j-factors averaged for the whole surface area.

For wetted-wall columns, the (j_H/j_D) ratios differ. Sherwood's[95] comparisons indicates that the ratio may vary from 0.62-1. Opposed to Sherwood's results are those of Barnett and Kobe [3] which indicate that the heat transfer data without simultaneous mass transfer are 24% greater than the mass transfer data. Cairns and Roper[8] indicate the equivalence of the j-factors at low humidities for the flow of air and water within a wetted-wall column. Overall evaluation of the transfer processes within

the wetted-wall columns indicates a (j_H/j_D) ratio less than one for laminar Reynolds numbers and approaching unity with increasing Reynolds numbers.

For wall to fluid transfer within packed beds, the equivalence of j_H and j_D for turbulent flow was verified by Yagi and Wakao[116]. For transfer between the packing and fluid within packed beds, the j_H-factor is greater than j_D. The recent study of DeAcetis and Thodos[19] indicates, contrary to previous assumptions, that the temperature of the packing surface is not the same as the adiabatic saturation temperature of the incoming air for the evaporation of water in air. For the case where the adiabatic saturation temperature is assumed, a value of (j_H/j_D) equal to 1.08 is obtained. The independent heat and mass measurements of DeAcetis and Thodos give values of (j_H/j_D) from 1.17 to 3.06 with an average of 1.51. A decreasing ratio was noted with increasing Reynolds numbers. The authors note that the wet-bulb temperature is reached at the higher intersticial velocities, thus it may be inferred that (j_H/j_D) would approach 1.08 at the high velocities. In the Wilke and Hougen[114] fixed bed experiments, it was observed that the solid particles rapidly reached the adiabatic saturation temperature so that it was necessary to limit the bed height to a few particle diameters to prevent the outlet gas from becoming saturated. Surface temperatures higher than the adiabatic case (from 0.8 to 10.2°F for DeAcetis and Thedos) have a marked increased effect on (j_H/j_D) in that j_H increases while j_D decreases. Additional support that the (j_H/j_D) ratio is greater than unity for packed beds is supplied by the chemical reaction experiments of Satterfield and Resnick[91]. A ratio of 1.37 is reported for packed beds while 1.09 is observed for reaction in a cylindrical tube

fabricated from the same catalytic metal as the bed packing. Gordon[40] compares the data of many investigators relating independently obtained j_H and j_D- factors to Reynolds numbers for fixed beds of spheres. The plotted data points, covering wide ranges of variables, indicate that j_H is consistently greater than j_D. The ratio (j_H/j_D) may be approximated by 1.5.

Independent measures of heat and mass transfer in the same fluidized column are reported by Kettering et al.[60] The results were calculated on the basis of many questionable assumptions. Wamsley and Johanson[110] discuss weaknesses inherent in the Kettering et al. investigation. Recalculation of the heat transfer coefficients by using the adiabatic saturation temperature of inlet air as the fluidized bed temperature gives an average (j_H/j_D) ratio of 1.09. Since the magnitude of the heat transfer coefficient and the transfer mechanism is not established with certainty[111], the (j_H/j_D) ratio for fluidized beds remains in doubt.

Satterfield et al.[90] attribute the heat and mass j-factor differences from their tube studies to: (1) a temperature gradient and simultaneous heat and mass transfer, (2) the effect of counter and bulk diffusion, (3) thermal diffusion, or (4) and effects. These four conditions may possibly account for discrepencies noted in other investigations.

Nusselt as noted in Eckert[26] indicates that if heat and mass transfer occur separately in geometrically similar fields with the same boundary conditions for each case, the principle of similarity may be applied to predict the transfer of one from measurements of the other. Equations for heat and mass transfer occurring separately and simultaneously have been derived by Nusselt. For low solute concentrations, the simpler equations for separate fields is usually applied. It is possible

Table III

Representative Studies Concerned with the Heat-Mass Analogy

Type Study	Study	Comments	j_H/j_D	j_H/j_D Limits
Cylinders (normal flow)	*This study	Local mass transfer measurements for 30° segments compared with analogous heat transfer results of Churchill and Brier.(15) The j_H and j_D distributions nearly coincide for the chosen experimental conditions.	≈1.0	0.84 - 1.18 (3)
	Dobry,R. & R.K.Finn, IEC, 48, 1540(1956)	Mass transfer to a cylinder at low Re(≤ 10) agree with the heat transfer measurements of Davis.(18)	≈1.0	-
	*Comings,E.W.,J.T.Clapp, & J.F.Taylor,IEC,40,1076(1948)	Studied effects of air turbulence for heat and mass transfer from cylinders. Even though results are widely scattered, it is evident that the heat transfer data are consistent with the mass transfer results.	1.0	-
	Sherwood,T.K.,IEC,42,2077 (1950)	Compares literature values with McAdams' generalization for flow transverse to a cylinder.	≈1.0	0.85 - 1.30 (3)
Spheres	*Ranz,W.E. & W.R.Marshall, CEP,48,141 and 173 (1952)	Correlations of heat and mass transfer obtained from drop temperatures and evaporation rates. Data obtained from Re = 0 - 200.	1.0	0.8 - 1.2 (1)
	Sherwood, T.K.,IEC,42,2077 (1950)	Comparison of Maisel's data (j_D) with McAdams' (j_H) shows that the j_H line is slightly higher than j_D by approximately 10%.	≈1.10	0.95 - 1.35 (3)
	Linton,M. & K.L.Sutherland, Chem.Eng.Sci.,12,214(1960)	This paper compares the transfer predicted from theory of a laminar boundary layer with experimental results for heat and mass transfer. Agreement noted between j_H and j_D.	≈1.0	-
	*Hsu,N.T. & B.H.Sage,AIChE Journ.,3,405(1957)	Agreement indicated between thermal and material transfer in turbulent gas streams (Re from 1530 to 4200).	≈1.0	-
	Garner,F.H. & R.D.Suckling, AIChE Journ.,4,114(1958)	Comparison of j_D values obtained with j_H from McAdams suggest that the analogy is applicable. Values of j_D are approximately 15% higher.	≈1.15	-
Disks	*Sogin,H.H.,Trans.ASME,80, 61 (1958)	Sogin shows that his mass transfer results coincide with the data for heat transfer by convection in an identical configuration.	1.0	-
Flat Surfaces	*Heertjes,P.M. & W.P.Ringens, Chem.Eng.Sci.,5,226(1956)	Heat and mass transfer data obtained for the evaporation of four liquids in air.	≈1.0	0.81 - 1.32 (2)
	*Furber, B.N.,Proc.Inst.Mech. Engrs.(London),168,847(1954)	Presents heat and mass transfer data on humid air flowing over a plane containing an isolated cooled region.	1.0	0.55 - 1.55 (2)
	*Jakob,M.,R.L.Rose, & M. Spielman,Trans.ASME,72,859 (1950)	Heat and mass transfer results obtained by discharging hot air from a continuous slot parallel to a plane surface.	1.0	0.75 - 1.20 (4)
	Sherwood, T.K.,IEC,42,2077 (1950)	Compares mass transfer data with McAdams' representation for flow over flat plates. Agreement is satisfactory.	≈1.0	0.80 - 1.35 (3)
Wetted-Wall Columns	*Barnett,W.I. & A.Kobe,IEC, 33,436(1941)	Heat and mass transfer data obtained. Results show that j_H/j_D = 1.24. Their mass transfer data are 13% less than Gilliland and Sherwood's (38). An equivalent basis for H_2O vaporization with (38) give j_H/j_D = 1.10.	1.24	0.90 - 1.60 (4)
	*Cairns,R.C. & G.H.Roper, Chem.Eng.Sci.,4,97(1954)	Simultaneous heat and mass transfer data obtained with flow of air and water. For low humidities $j_H = j_D$.	≈1.0	0.77 - 1.37 (2)
	Sherwood,T.K.,IEC,42,2077 (1950)	Compares many sets of mass transfer data with McAdams' heat transfer correlation for flow of gases through pipes. All data lie from 0 - 60% above the McAdams' line.	≈1	0.60 - 1.00 (3)
(diffusion controlled chemical reaction in tube)	*Satterfield,C.N.,H.Resnick, & R.L.Wentworth,CEP,50,460 (1954)	The rates of simultaneous heat and mass transfer in a gas-solid diffusion controlled chemical reaction (decomposition of H_2O_2) were measured with the flow of H_2O_2 vapor through a cylindrical tube.	1.09	0.94 - 1.24 (1)

Table III (Cont'd)

Representative Studies Concerned with the Heat-Mass Analogy

Type Study	Study	Comments	j_H/j_D	j_H/j_D Limits
Container (liquid-solid agitation systems)	*Hixson,A.W. & S.J.Baum, IEC,33,1433(1941)	Equations correlating heat transfer data for several liquids in a series of geometrically similar agitators is similar in form to the expression correlating mass transfer data in the same equipment.	1.29	1.06 - 1.58 (1)
Packed Beds	Gamson,B.W.,G.Thodos,O.A. Hougen,Trans.AIChE,39,1 (1943) Wilke,C.R. & O.A.Hougen, Trans.AIChE,41,445(1945) Taecker,R.G. & O.A.Hougen, CEP,45,188(1949)	Present data on drying of wet cylinders and spheres randomly packed with through air circulation. It is shown that j_H/j_D = 1.08. However, since the surface temperature is assumed equal to the wet-bulb temperature of the entering air, the j_H's given are not based on independent measurements. Sherwood(94) shows that j_H can be calculated from j_D.	1.08	-
	*DeAcetis,J. & G.Thodos, IEC,52,1007(1960)	The temperature of water evaporating from spherical catalyst carriers has been measured directly, and it was found that the surface temperature is the same as the wet-bulb temperature only at the high air velocities.	1.51	1.17 - 3.06 (2)
(diffusion controlled chemical reaction)	*Satterfield,C.N. & H. Resnick,CEP,50,504(1954)	The reaction mentioned above was observed in a bed packed with spheres of the same catalytic metal.	1.37	1.29 - 1.45 (1)
	Gordon,K.F., Paper presented at Chem.Eng.meeting, Washington,D.C.,1960	For fixed beds of spheres, the data of many investigators relating to j_H and j_D factors are presented. Approximately 1000 data points from 20 investigations indicate that $j_H/j_D \approx 1.5$.	$\approx$1.5	-
(wall to fluid in a packed bed)	*Yagi,S. & W.Wakao,AIChE Journ.,5,79(1959)	Heat and mass transfer from tube wall to fluids flowing through packed beds were determined separately. It was found that $j_H = j_D$ in the turbulent region.	1.0	0.75 - 1.50 (4)
Fluidized Beds	*Kettering,K.N.,E.L. Manderfield, & J.M.Smith, CEP,46,139(1950)	Heat and mass transfer between solid particles and the gas stream were measured for desorption of water from silica-gel and activated alumina fluidized in air. Irregularly shaped particles were assumed to be equivalent spheres. Temperatures of the gas were determined by bare thermocouples immersed in the bed. The solid temperature was assumed constant and equal to the equilibrium temperature of the gas leaving the fluidized column. (Temps. 10-20°F higher than the adiabatic saturation temps. were recorded.)	11.68	10.94 - 12.42 (1) (see comments of Wamsley et al. next ref.)
	Wamsley,W.W. & L.N.Johanson, CEP,50,347(1954)	Recalculated heat transfer coefficients of Kettering et al. by assuming the adiabatic saturation of the inlet air as the temperature of the fluidized bed. The j_H-factors decreased from the original values by factors from 4.83 to 24.6 increasing with increasing Re and decreasing particle size. The average decrease of this ratio being 10.65. Thus the recalculated j_H/j_D ratio becomes 11.68/10.65 = 1.09.	1.09	-

Footnotes

* indicates independently measured heat and mass transfer data
(1) calculated from average deviations of j_H and j_D
(2) calculated from maximum and minimum j_H's and j_D's
(3) ratio of j_D extremes to j_H from specified source
(4) calculated from j_D and j_H extremes of correlating line

that differences between j_H and j_D may be caused by lack of field similarity.

No other explanations for the disparity between the j_H and j_D factors, particularly for packed beds, can be advanced. Further studies in which heat and mass transfer data are obtained under similar physical circumstances in packed beds (fixed and fluidized) are needed to determine the limitations of the (j_H/j_D) ratio. Particular attention should be devoted to ascertaining the surface temperature of the packings.

PART II

DETERMINATION OF VAPOR PRESSURES FOR NAPHTHALENE p-DIBROMOBENZENE, PROPIONAMIDE, AND ANTHRACENE

VI INTRODUCTION

Unsatisfactory literature values for vapor pressures, disagreeing in some cases by a factor of two, necessitated measuring the vapor pressures of

Naphthalene,	(crystal reagent, Baker and Adamson)
p-Dibromobenzene,	(practical grade, Eastman)
Propionamide,	(highest purity, Fischer Scientific)
Anthracene	(highest purity, Fischer Scientific)

They were determined by the air saturation method where a measured volume of air is saturated by passing through a bed of the solid at a definite temperature. The amount sublimed is determined by the weight loss. The vapor pressure is then calculated from the gas laws.

The heat of sublimation is obtained from the Clausius-Clapeyron equation,

$$\lambda = -Rd(\ln p)/d(1/T) \qquad (44)$$

VII EXPERIMENTAL EQUIPMENT

The equipment, shown in Figure 14, consists of: a) a silica gel bed for drying the air; b) an air flow control and measuring system; c) a constant temperature bath; d) a U-tube holding a bed or the organic solid; e) instruments to measure pressure, temperature, and cumulative air flow.

The air feed system contains a cut-off valve, pressure regulator, thermometer, Bourdon pressure gauge, rotameter, and needle control valve.

A nest of three stirred baths maintained the U-tube to $\pm$0.1°C. The outermost, made by Precision Scientific, has three independently controlled 1 KW heaters. The middle bath is a battery jar whose temperature is maintained by a 1/4 KW heater controlled by a mercury thermostat. The unheated inner bath is a 3 liter stainless steel beaker.

The air flows through copper tubing submerged in each bath. The U-tube bed, 5/8" I.D. and 10" long, is in the stainless steel beaker. A manometer gives the outlet bed pressure. The air from the bed goes to a series of three bubblers prior to a wet test meter.

Temperatures are determined by calibrated porcelain-jacketed thermocouples.

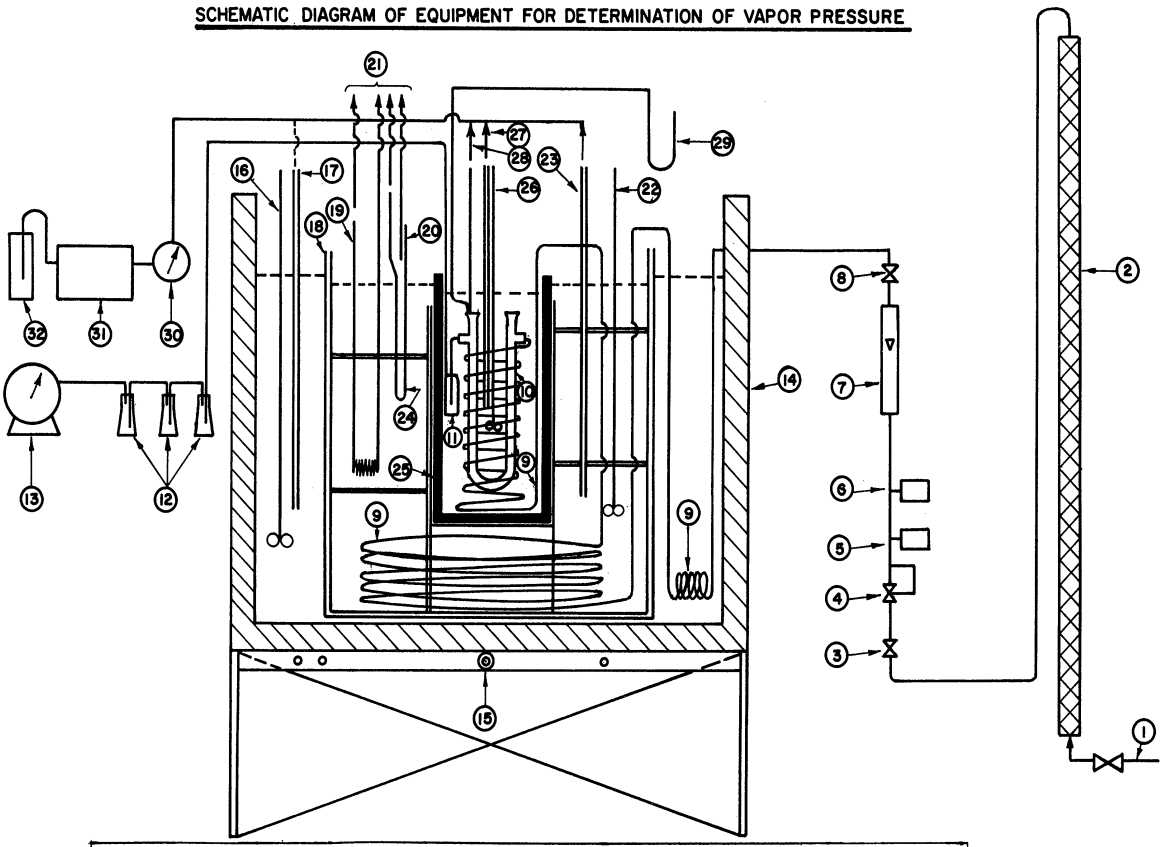

Key to Figure 14

1. Air supply (90 psig)
2. Silica-gel bed
3. Cut-off valve
4. Pressure regulator
5. Bimetallic thermometer
6. Pressure gauge
7. Rotameter
8. Needle valve
9. Air heating coil
10. U-tube bed
11. Holdup tube
12. Air-water saturator
13. Wet test meter
14. Outer bath
15. Outer bath temperature controller
16. Outer bath stirrer
17. Outer bath thermocouple
18. Glass jar
19. Knife heater
20. Mercury contactor
21. Leads to relay controller
22. Glass jar stirrer
23. Glass jar thermocouple
24. Stainless steel container
25. S.S. container support
26. S.S. container stirrer
27. S.S. container thermocouple
28. Bed outlet thermocouple
29. Open end manometer to bed outlet
30. Thermocouple selector switch
31. Precise potentiometer
32. Ice bath

Figure 14. Schematic Diagram of Vapor Pressure Equipment.

VIII EXPERIMENTAL PROCEDURE

The solids were pressed into 1/8", 1/4", and 1/2" spheres by punches and dies (F. J. Stokes Co.).

The temperature of the middle bath was maintained slightly above those of the other baths for improved steady state conditions. The temperature fluctuations decreased from the outermost to the inner bath.

After the packed U-tube was weighed and inserted in the inner bath, it equilibrated with the bath for approximately 15 min. before passage of air. In all runs, the air through the bed was less than 1 ft^3/hr. The air pressure was reduced from 90 to 30 psig prior to the rotameter. Constant flow was maintained.

The U-tube was stoppered to reduce loss prior to post-weighing. Preliminary tests indicated that the weight loss of the bed while exposed to the atmosphere during the loading and recovery operations was insignificant.

Approximately ten experimental runs at different temperatures were made for each of the organic solids. The runs were from 5 to 15 hours. Operating temperatures, bed and atmospheric pressures, and air flow rates were periodically recorded. A sample data sheet is shown in Figure 15.

DATA SHEET FOR VAPOR PRESSURE DETERMINATIONS

MATERIAL *p-Dibromobenzene* DATE - *Feb. 28, '60*

RUN No. *2*

TIME	(Hours)	0	1	3	5				
TEMPERATURES									
BED OUTLET	(mv)	2.540	2.545	2.540	2.535				
	(°C)	62.2	62.3	62.2	62.1				
S.S. BEAKER	(mv)	2.545	2.555	2.540	2.540				
	(°C)	62.3	62.5	62.4	62.2				
GLASS JAR	(mv)	2.558	2.555	2.555	2.550				
	(°C)	62.6	62.5	62.5	62.4				
OUTER BATH	(mv)	2.550	2.545	2.540	2.545				
	(°C)	62.4	62.3	62.2	62.3				
PRESSURES									
BED OUTLET	(mm H$_2$O)	70	72	72	72				
	(mm Hg)	5	5	5	5				
ATMOSPHERIC	(mm Hg)	741	741	740	739				
AIR FLOW									
ROTAMETER UNITS		8.0	8.0	8.0	8.0				
PRESSURE	(psig)	30	30	30	30				
W.T. VOLUME	(cu ft)	0.00	0.79	2.46	4.16				
TEMP.	(°F)	75	75	75	76				
PRESS.	(mm Hg)	atm.	atm	atm	atm				
WT. LOSS OF BED									
INITIAL WT.	(gms)								112.7820
FINAL WT.	(gms)								110.7033
WT. LOSS	(gms)								2.0787

REMARKS

RUN STARTED @ 0712
GAS FLOW @ 0730
RUN ENDED @ 1230

Figure 15 Data Sheet for Vapor Pressure Studies

IX RESULTS

The original and processed data are summarized in Table V.

The data are correlated by plots of log p versus 1/T shown in Figures 16a and 16b. The following represent the least-square lines.

1) Naphthalene	$\log p = 11.61705 - 3786.64/T$
2) p-Dibromobenzene	$\log p = 11.73772 - 3885.20/T$
3) Propionamide	$\log p = 10.45681 - 3543.20/T$
4) Anthracene	$\log p = 9.07248 - 3827.42/T$

The respective average deviations are 0.64%, 2.40%, 0.36%, and 2.16%.

Heats of sublimation calculated by the Clausius-Claperyon equation are

MATERIAL	$\lambda_{ave.}$ (BTU/lb-mole)
1) Naphthalene	31,112
2) p-Dibromobenzene	32,044
3) Propionamide	28.417
4) Anthracene	30,132

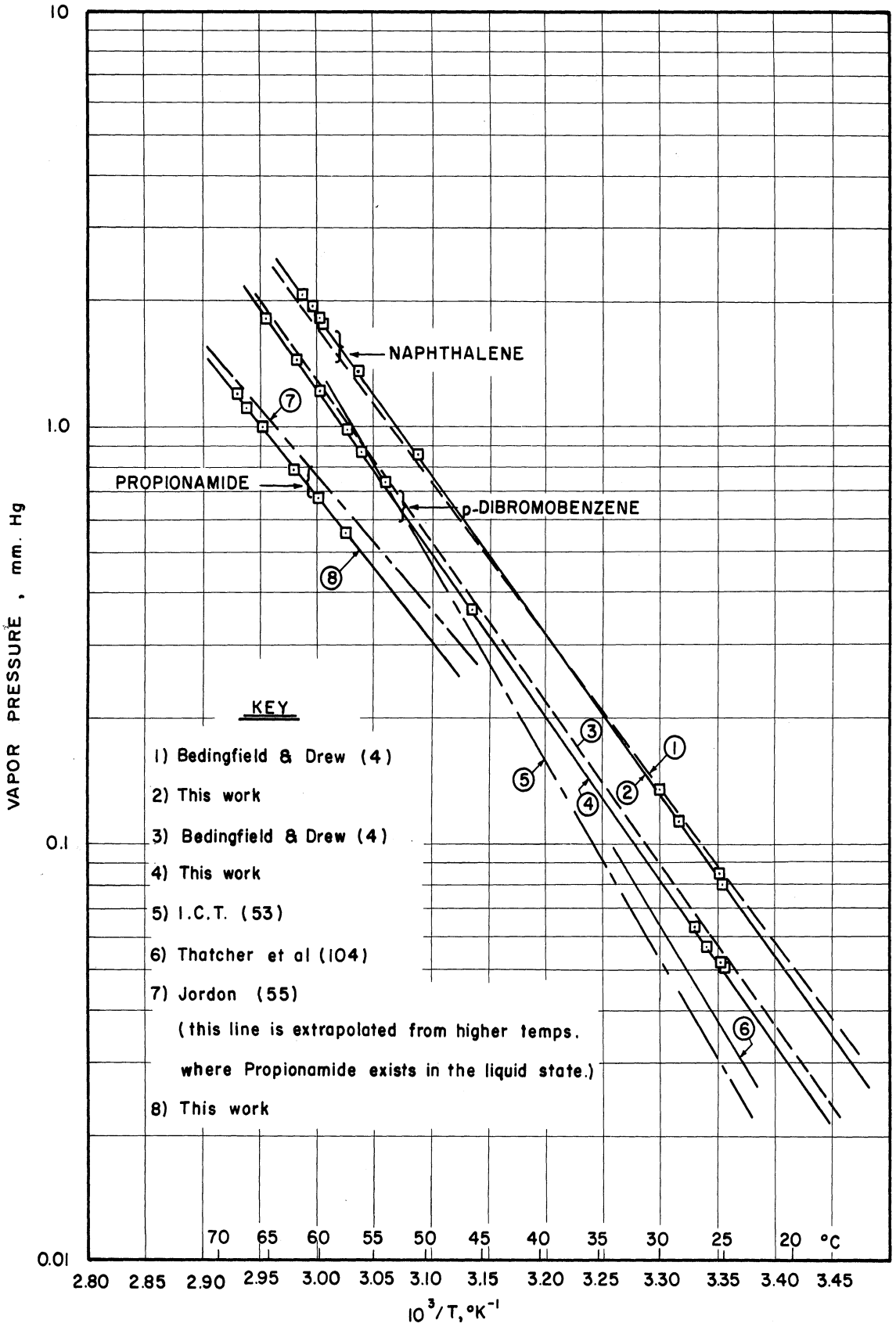

Figure 16a. Correlation of Vapor-Pressure Data for Naphthalene, p-Dibromobenzene, and Propionamide.

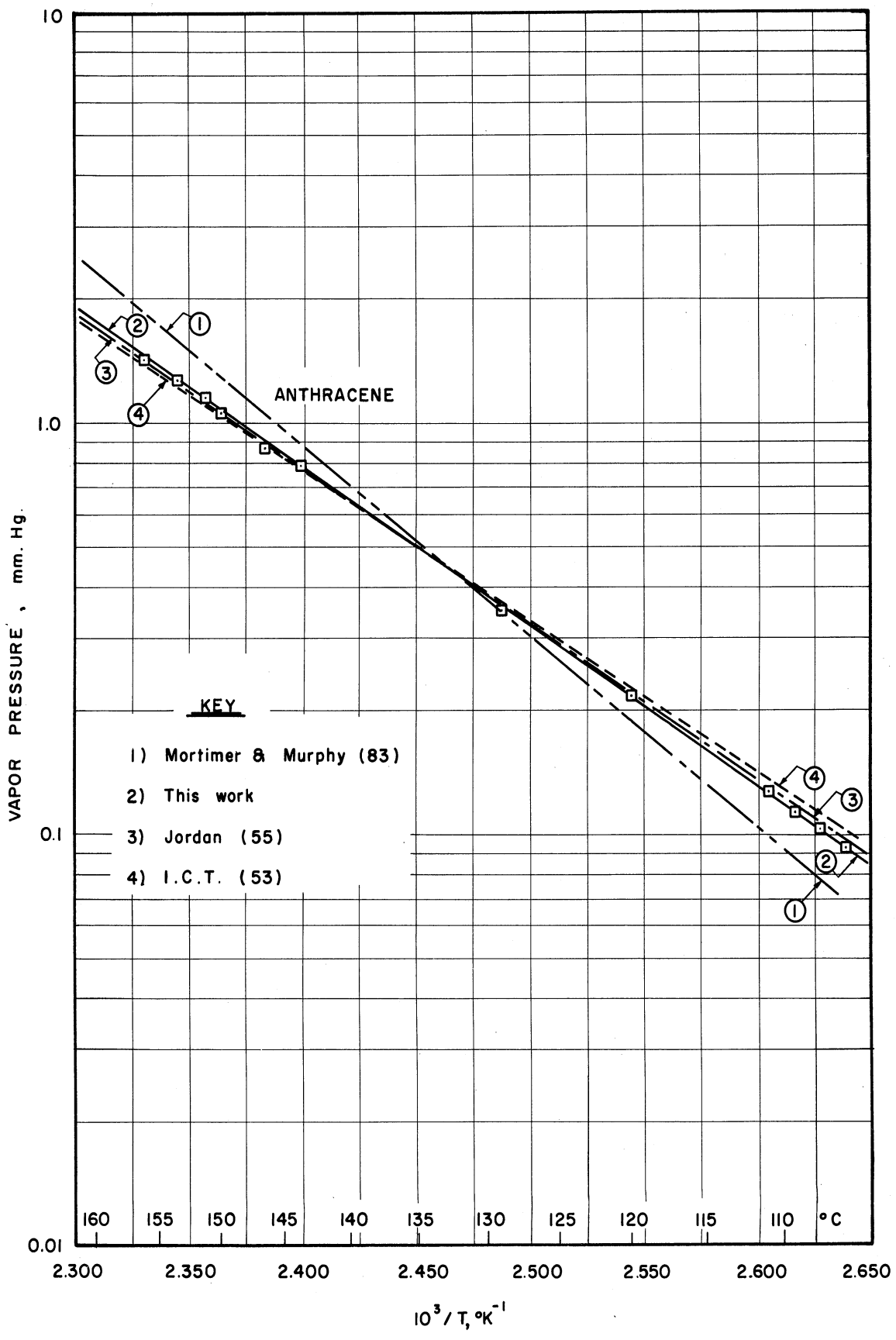

Figure 16b. Correlation of Vapor-Pressure Data for Anthracene.

X DISCUSSION OF RESULTS

The accuracy of the temperature is probably not better than $\pm$0.1°C at 100°C, and the error is less at the lower temperatures. The sublimed weight was determined to the nearest 0.1 mg and pressures (atmospheric and bed outlet) to the nearest 1 mm Hg.

According to the j_D correlation[40], the 10" bed is estimated to achieve saturation to within 10^{-5}% for all vapor pressure runs.

Except for naphthalene, there is disagreement with some of the results of other investigators as shown in Figures 16a and 16b. For p-dibromobenzene, the results are in agreement with those of Bedingfield and Drew but not those in the International Critical Tables. It should be noted that Bedingfield and Drew used the air saturation technique for both p-dibromobenzene and naphthalene.

No experimental vapor pressures at the temperatures of interest were found in the literature for propionamide. The straight line shown in Figure 16a is extrapolated from higher temperatures where propionamide exists as a liquid. Since the log p vs 1/T plot increases slope when going from liquid to solid, it is expected that the experimental line would lie below the line extrapolated from the liquid, as was found.

XI SUMMARY

1. By simulating the heat transfer arrangement of Churchill with one for mass transfer, it was possible to compare local mass transfer by convection with heat transfer under similar conditions.

The apparatus included an air flow system; a furnace for heating the air; an adiabatic tube for measuring the air temperature and developing uniform and low turbulence; and a test piece surrounded by a heating shield.

The organic solids were cast and a smooth surface obtained by shaving the curing. Local mass transfer from 30° cylindrical segments were measured from sublimation losses. Tests were made with naphthalene, p-dibromobenzene, propionamide, and anthracene; Reynolds numbers from 400 to 4000; surface temperatures from about 25-150°C; diameters of 1" and 1.25"; and an estimated turbulence of less than 2%.

The local mass transfer results were correlated by $j_D = B(Re)^{-n}$, where the values of B and n vary with angular position but are independent of diameter and air flow rate. Most local j_D-factors are within 15% of Churchill's j_H-factors, confirming the analogy between heat and mass transfer. The standard deviations of the j_D's are 6.2% from the j_D correlating lines and 7.8% from Churchill's j_H correlations.

From $4x10^2 \leq Re \leq 4x10^3$, the average j_D-factors are expressed by

$$j_D = 0.64\ (Re)^{-0.5}$$

The average j_D-factors are greater than the average j_H-factors of Churchill, $j_H = 0.63(Re)^{-0.5}$ and McAdams but agree within 15%.

At a Reynolds number of 2000, sublimation rates of the four organics were measured over a temperature range of 125°C. The j_D-factor which decreased less than 10% with increasing temperature for all angles may be taken as constant.

The Schmidt numbers of the four organic solids ranged from 1.79 to 3.05. The results indicate that 1/2, rather than 2/3, is a more representative value of the Schmidt number exponent in the j-factor equations.

2. Appreciable disagreement in literature values for vapor pressures required that the vapor pressure of the solids used in the mass transfer studies be determined. Vapor pressures were obtained by an air-saturation method. A measured volume of air was saturated by passing through a U-tube bed, 5/8" O.D. and 10" long, of solid spheres situated within a constant temperature bath maintaining the bed to ±0.1°C. The amount sublimed was determined by weighing. The vapor pressures were then calculated from the gas laws.

Approximately 10 runs, 5 to 15 hours long, were made at different temperatures for each solid. For all runs, the air rate through the bed was less than 1 ft^3/hr.

The vapor pressures were correlated by equations of the form, $\log p = B - C/T$. The least-square values of B and C are:

MATERIAL	B	C
Naphthalene	11.61705	3786.64
p-Dibromobenzene	11.73772	3885.20
Propionamide	10.45681	3543.20
Anthracene	9.07248	3827.42

Heats of sublimation were obtained from the Clausius-Clapeyron equation.

XII CONCLUSIONS

Local mass transfer rates from 30° segments of a cylindrical surface were determined from the weight loss of naphthalene, p-dibromobenzene, propionamide, and anthracene. Tests were made with cylindrical diameters of 1" and 1.25"; Reynolds numbers from 400 to 4000; surface temperatures from about 25 - 150°C; and an estimated turbulence of less than 2%. The following conclusions were reached:

1. Most measured j_D - factors agree within 15% of the independent j_H correlations determined by Churchill and Brier. The standard deviations of the j_D's for all positions from the determined j_D and Churchill and Brier's j_H correlating lines are 6.2% and 7.8% respectively. This confirms the heat and mass transfer analogy for the laminar and eddy flow regions of a cylinder. The local mass transfer were correlated by $j_D = B(Re)^{-n}$, where B and n are independent of the Reynolds number.
2. The area average rates can be expressed by $j_D = 0.64(Re)^{-0.5}$ which may be compared with $j_H = 0.63(Re)^{-0.5}$ as found by Churchill and Brier for small temperature potentials. This shows agreement to within 2%.
3. An exponent of 1/2 for the Schmidt number in the j-factor is more representative of the data than 2/3.
4. At a Reynolds number of 2000, no appreciable variation of local j_D - factors for a temperature range of 125°C is apparent.

5. The vapor pressures for naphthalene, p-dibromobenzene, propionamide, and anthracene were determined and satisfactorily correlated by, $\log p = B - C/T$.

XIII APPENDICES

1. Details of Apparatus

a. Air supply system

Parallel silica gel units consisted of two vertical pipes 3" I.D. by 6' high dehumidified the air stream. During a run, air flows through one of the two beds. The other bed may be dried or replaced without interrupting the air flow. Each of the tubes is externally wrapped with an insulated chromel resistance heating wire and asbestos insulation. The water absorbed by the gel is removed by slowly passing a stream of air through a hot bed heated by surrounding heating wire.

The center and right panels shown in Figure 3a contained three sets of regulating and indicating components. Each set contained a cut-off valve, a pressure regulator of the bleeding type (Nulmatic 40E50), a bimetallic-element thermometer (Weston 228-C), a Bourdon type pressure gauge (Duragauge 4-1/2"), rotameter (Fischer Porter B-5N25, B-4A25, B2-26-250), and needle valve for controlling the flow.

The rotameter fluctuated little, if at all, during a run. Rotameter calibrations for air at 70°F and 45 psia are presented in Figures 18a-c. Since the air regulator reduced the pressure from 100 psi to 45 psia in all mass transfer runs, the calibration curves were used directly with a small correction applied for deviations from 70°F.

b. Air heating unit

As shown in Figure 1, the air heating unit consists of a high temperature tube furnace containing a 2" I.D. and 3" O.D. by 36" silicon carbide Globar element with water cooled contact plates, temperature controller, and transformer unit.

Two 6 KVA transformers operating on 220 volt, 2 phase 60 cycle power supply voltage from 20 to 100 volts. An ammeter indicates the current to the primary power transformer. The terminals of the heating element are water cooled.

A spring loaded plate holds the electrical contact plate, the carbon block, and Globar element in place and allowing thermal expansion. The Globar is surrounded by refractory brick insulation which is surrounded by 4" of rockwool in a cabinet.

The furnace temperature is maintained by an electronic controller (Whelco 292). The thermocouple of 24 gauge platinum and 10% rhodium-90% platinum wire is 1/8" outside and 12" below the top of the Globar.

After the metering system, the air passes through a tube of three sections. The first or heat transfer section, at the bottom of the furnace, is 38" in length, 1-3/4" O.D. by 1-5/8" I.D.; the middle or throat section is 6" in length, 11/16" O.D. by 1/2" I.D.; the third or adiabatic tube section, projecting above the furnace, is 6" long with a square cross section 2" O.D. by 1-3/4" I.D. The throat section is surrounded by a cast refractory inside a split zircotube of the same O.D. as the heat transfer tube.

The whole assembly, containing the three sections, is set within the Globar element, being maintained in place by the projecting corners of the square adiabatic section resting upon transite sheets which lie on the spring loaded plate.

The adiabatic tube section is surrounded with 1" of high temperature insulation and 2" of low temperature insulation.

The heat transfer section is packed with 1/4" alumina spheres. A manometer determines the pressure drop across the furnace. To prevent

bed movement of the alumina spheres, the tightly packed bed is held by a retaining screen located immediately below the throat tube section.

The adiabatic section establishes the gas temperature, a uniform velocity and a low turbulence level for the air flowing past the test piece. It is filled with 1/4" alumina spheres held in place by screens. The combination of two 52 mesh platinum screens mounted on the outlet of the adiabatic section and separated by 1/4" furnished a uniform velocity profile and low turbulence level, about 2%. The air temperature is determined by a 24 gauge butt-welded chromel-alumel thermocouple with the junction located 1/4" below the center surface of the lower platinum screen. Within the adiabatic tube, the bare thermocouple wire is inserted in a 0.9 mm I.D. by 1.5 mm O.D. porcelain tube. This section is surrounded by insulation. The top layer of alumina spheres contacting the lower platinum screen are covered with platinum foil thereby minimizing radiation losses. Because of the negligible heat losses, the temperature of the packing 1/4" below the level of the lower screen is assumed equal to the exit air stream. The upper layers of the alumina spheres are arranged to provide a nearly flat velocity profile.

c. The mass transfer test unit

The Inconel test piece is shown in Figures 1 and 2. The cylindrical portion is 3-1/2" in length by 1-1/4" in diameter. The test piece was machined from 2" inconel bar stock then cut longitudinally in half for inserting thermocouples within the test unit and for ease in constructing a niche to contain the boat. Two set screws on each end extension hold the test piece together. The organic material in the boat subtends 30° and is

1-1/4" long. Removal of the boat is facilitated by winged screws inserted in two holes on each end of the 1/16" thick boat. A longitudinal set screw through the cylinder holds the boat in position. Along the flat interior faces are five parallel grooves for the 40 gauge chromel-alumel thermocouples. The junctions of the thermocouples are all located in the same cross-sectional plane as shown in Figure 2. The thermocouples are butt-welded and coated with an electrical insulating enamel.

The thermocouple leads from the test piece are insulated with asbestos braided tubing. The potentiometer (Leeds and Northrup, Model 8662) is read to within 2 microvolts, corresponding to 0.1°C. The thermocouples were calibrated against N.B.S. thermometers.

An electrically heated shield, 12" long by 12" in diameter, reduces radiation losses by maintaining its surface at approximately the temperature of the test piece. The shield bottom contains a 2-1/2" square hole in its center to allow the air from the square adiabatic tube to flow past the test piece. Bolted to the base of the shield are a pair of 1" right angled steel brackets to support the test piece.

A truncated conical heated shield, above the cylindrical heated shield, has an altitude of 10" and diameters of 12" and 1-1/2". To reduce radiation losses, the exit air leaves the conical shield through three parallel disoriented screens, 1/2" apart, then passes to a vent blower.

Both shield temperatures are regulated independently by Variacs. A probing thermocouple indicated the shield's temperatures which are regulated to the test piece temperature.

2. Table IV

Summary of Original and Processed Data for Local Mass Transfer Rates

for Re = 400, 2000, 4000 (cylindrical diameter = 1")

No.	Material	θ	Re	ΔW (mg)	t (min)	T_g (°C)	T_i (°C)	T_s (°C)	p_s (mm Hg)	k_g lb-moles / hr-ft-2-atm	$(Sc)^{1/2}$	G_m lb-moles / hr-ft^{-2}	j_D
1	Naphthalene	180	400	6.0	420	26.3	26.2	26.1	0.09084	0.0542	1.57	7.40	0.0115
2	"	180	"	5.4	420	25.8	25.8	25.6	0.08697	0.0510	1.57	7.40	0.0108
3	"	0	"	6.5	100	25.7	25.5	25.5	0.08590	0.261	1.57	7.40	0.0554
4	"	0	"	6.4	100	26.0	25.9	25.8	0.08850	0.249	1.57	7.40	0.0529
5	"	180	2000	5.9	120	23.5	23.5	23.4	0.06994	0.242	1.57	36.8	0.01033
6	"	180	"	6.6	120	23.9	23.9	23.8	0.07242	0.262	1.57	36.8	0.01117
7	"	0	"	7.5	60	24.3	24.2	24.2	0.07565	0.570	1.57	36.8	0.00243
8	"	0	"	6.8	60	24.2	24.0	24.1	0.07470	0.524	1.57	36.8	0.00224
9	"	180	4000	9.3	100	25.3	25.2	25.2	0.08326	0.384	1.57	74.0	0.00815
10	"	180	"	9.0	100	25.4	25.4	25.3	0.08404	0.370	1.57	74.0	0.00785
11	"	0	"	6.4	30	25.6	25.6	25.4	0.08453	0.870	1.57	74.0	0.0185
12	"	0	"	7.0	30	25.7	25.6	25.5	0.08590	0.936	1.57	74.0	0.0199

Summary of Original and Processed Data for Local Mass Transfer Rates

for Re = 400 (cylindrical diameter = 1.25")

No.	Material	θ	ΔW (mg)	t (min)	T_g (°C)	T_i (°C)	T_s (°C)	p_s (mm Hg)	k_g lb-moles / hr-ft-2-atm	$(Sc)^{1/2}$	G lb-moles / hr-ft^{-2}	j_D
13	Naphthalene	180	4.0	420	23.6	23.6	23.5	0.07055	0.0372	1.57	5.88	0.00993
14	"	"	3.7	360	23.7	23.6	23.6	0.07177	0.0399	1.57	5.88	0.01064
15	"	"	4.0	360	24.2	24.2	24.1	0.07470	0.0410	1.57	5.88	0.01095
16	p-Dibromobenzene	"	4.0	360	23.7	23.6	23.6	0.04373	0.0380	1.59	5.88	0.01027
17	"	"	4.4	360	24.0	24.0	23.9	0.04491	0.0407	1.59	5.88	0.01100
18	Naphthalene	150	4.2	300	26.5	26.4	26.3	0.09245	0.0418	1.57	5.92	0.01108
19	"	"	4.4	300	26.5	26.5	26.3	0.09245	0.0453	1.57	5.92	0.01201
20	p-Dibromobenzene	"	5.0	400	23.9	23.8	23.8	0.04451	0.0420	1.59	5.88	0.01134
21	"	"	5.0	350	24.3	24.2	24.2	0.04655	0.0459	1.59	5.88	0.01241
22	Naphthalene	120	5.1	240	26.2	26.2	26.0	0.09005	0.0651	1.57	5.92	0.01726
23	"	"	5.0	240	26.5	26.4	26.3	0.09245	0.0620	1.57	5.92	0.01644
24	p-Dibromobenzene	"	6.1	265	26.2	26.2	26.1	0.05620	0.0612	1.59	5.92	0.0164
25	"	"	6.3	265	25.9	25.8	25.8	0.05468	0.0650	1.59	5.92	0.0175
26	Naphthalene	90	4.5	170	23.7	23.6	23.6	0.07117	0.1025	1.57	5.88	0.0274
27	"	"	5.0	180	23.8	23.8	23.7	0.07177	0.1078	1.57	5.88	0.0288
28	"	"	5.0	170	23.8	23.8	23.7	0.07177	0.1130	1.57	5.88	0.0302
29	p-Dibromobenzene	"	6.1	145	26.4	26.4	26.3	0.05720	0.1100	1.59	5.92	0.0295
30	"	"	8.6	200	26.0	26.0	25.9	0.05518	0.1165	1.59	5.92	0.0313
31	"	"	5.7	145	25.8	25.7	25.7	0.05420	0.1085	1.59	5.92	0.0291
32	Naphthalene	60	6.3	120	25.5	25.5	25.3	0.08404	0.1725	1.57	5.92	0.0458
33	"	"	7.0	120	25.8	25.7	25.6	0.08697	0.1851	1.57	5.92	0.0492
34	p-Dibromobenzene	"	6.8	120	24.8	24.8	24.7	0.04890	0.1732	1.59	5.90	0.0466
35	"	"	7.1	120	25.2	25.2	25.1	0.05088	0.1736	1.59	5.90	0.0468

Table IV (Cont'd)

Summary of Original and Processed Data for Local Mass Transfer Rates

for Re = 400 (cylindrical diameter = 1.25")
(continued)

No.	Material	θ	ΔW (mg)	t (min)	T_g (°C)	T_i (°C)	T_s (°C)	p_s (mm Hg)	k_g lb-moles / hr-ft^{-2}-atm	$(Sc)^{1/2}$	G_m lb-moles / hr-ft^{-2}	j_D
36	Naphthalene	30	6.3	100	25.2	25.2	25.1	0.08245	0.211	1.57	5.90	0.0561
37	"	"	5.6	100	25.0	25.0	24.9	0.08110	0.1908	1.57	5.90	0.0508
38	p-Dibromobenzene	"	6.8	120	23.8	23.6	23.7	0.04410	0.1920	1.59	5.88	0.0519
39	"	"	7.8	120	24.3	24.2	24.2	0.04655	0.209	1.59	5.88	0.0565
40	Naphthalene	0	8.8	120	26.3	26.1	26.1	0.09084	0.223	1.57	5.92	0.0591
41	"	"	6.3	100	25.9	25.8	25.7	0.08775	0.198	1.57	5.92	0.0525
42	"	"	6.6	100	25.8	25.8	25.6	0.08697	0.209	1.57	5.92	0.0554
43	p-Dibromobenzene	"	9.0	140	23.8	23.8	23.7	0.04410	0.218	1.59	5.88	0.0589
44	"	"	8.5	140	24.1	24.0	24.0	0.04532	0.201	1.59	5.88	0.0510
45	"	"	8.6	140	24.0	24.0	23.9	0.04491	0.204	1.59	5.88	0.0551

Summary of Original and Processed Data for Local Mass Transfer Rates

for Re = 1000 (cylindrical diameter = 1")

No.	Material	θ	ΔW (mg)	t (min)	T_g (°C)	T_i (°C)	T_s (°C)	p_s (mm Hg)	k_g lb-moles / hr-ft^{-2}-atm	$(Sc)^{1/2}$	G_m lb-moles / hr-ft^2	j_D
46	Naphthalene	180	8.1	300	25.5	25.5	25.3	0.08404	0.1110	1.57	18.4	0.00948
47	"	"	8.0	300	24.8	24.7	24.7	0.07930	0.1160	1.57	18.4	0.00991
48	"	"	7.5	260	25.2	25.2	25.1	0.08425	0.1205	1.57	18.4	0.0103
49	p-Dibromobenzene	"	6.6	200	25.7	25.6	25.6	0.05371	0.1149	1.59	18.4	0.00995
50	"	"	7.3	200	25.5	25.5	25.4	0.05229	0.1307	1.59	18.4	0.0113
51	"	"	7.3	200	25.9	25.9	25.8	0.05468	0.1248	1.59	18.4	0.0108

Summary of Original and Processed Data for Local Mass Transfer Rates

for Re = 1000 (cylindrical diameter = 1")

No.	Material	θ	ΔW (mg)	t (min)	T_g (°C)	T_i (°C)	T_s (°C)	p_s (mm Hg)	k_g lb-moles / hr-ft^{-2}-atm	$(Sc)^{1/2}$	G_m lb-moles / hr-ft^{-2}	j_D
52	Naphthalene	150	5.8	260	23.8	23.8	23.7	0.07177	0.1072	1.57	18.4	0.00915
53	"	"	5.7	260	24.0	23.9	23.9	0.07305	0.1035	1.57	18.4	0.00883
54	p-Dibromobenzene	"	6.2	240	24.2	24.0	24.1	0.04590	0.1050	1.59	18.4	0.00908
55	"	"	6.8	240	24.2	24.2	24.1	0.04590	0.1153	1.59	18.4	0.00996
56	Naphthalene	120	6.6	260	25.4	25.2	25.2	0.08326	0.1052	1.57	18.4	0.00898
57	"	"	6.5	260	25.6	26.6	25.4	0.08473	0.1018	1.57	18.4	0.00868
58	"	"	6.9	260	25.5	25.5	25.3	0.08404	0.1086	1.57	18.4	0.00927
59	p-Dibromobenzene	"	5.9	240	24.1	23.9	24.0	0.04532	0.1015	1.59	18.4	0.00877
60	"	"	6.4	240	24.2	24.2	24.1	0.04590	0.1085	1.59	18.4	0.00937
61	Naphthalene	90	7.6	180	24.5	24.3	24.4	0.07698	0.189	1.57	18.4	0.0161
62	"	"	6.8	155	24.4	24.3	24.3	0.07630	0.199	1.57	18.4	0.0170
63	"	"	7.4	155	24.8	24.8	24.7	0.07930	0.208	1.57	18.4	0.0178
64	p-Dibromobenzene	"	8.1	135	25.7	25.6	25.6	0.05371	0.209	1.59	18.4	0.0180
65	"	"	8.4	160	25.6	25.4	25.5	0.05300	0.185	1.59	18.4	0.0160
66	Naphthalene	60	8.0	100	26.5	26.4	26.3	0.09245	0.298	1.57	18.4	0.0254
67	"	"	8.8	100	26.4	26.2	26.2	0.09165	0.331	1.57	18.4	0.0283
68	p-Dibromobenzene	"	8.4	85	25.5	25.5	25.4	0.05229	0.354	1.59	18.4	0.0306
69	"	"	7.6	85	25.3	25.3	25.2	0.05136	0.326	1.59	18.4	0.0282
70	Naphthalene	30	8.2	100	24.2	24.2	24.1	0.07470	0.378	1.57	18.4	0.0322
71	"	"	8.7	100	24.2	24.2	24.1	0.07470	0.402	1.57	18.4	0.0343
72	p-Dibromobenzene	"	11.2	85	26.3	26.2	26.2	0.05667	0.436	1.59	18.4	0.0377
73	"	"	9.8	85	25.7	25.7	25.6	0.05371	0.402	1.59	18.4	0.0347
74	Naphthalene	0	8.9	100	23.7	23.5	23.6	0.07177	0.428	1.57	18.4	0.0365
75	"	"	9.1	100	24.0	24.0	23.9	0.07370	0.426	1.57	18.4	0.0364
76	"	"	8.0	100	24.1	24.0	24.0	0.07370	0.375	1.57	18.4	0.0319
77	p-Dibromobenzene	"	8.3	85	24.1	23.9	24.0	0.04532	0.403	1.59	18.4	0.0348
78	"	"	9.5	85	24.1	24.1	24.0	0.04532	0.462	1.59	18.4	0.0399
79	"	"	9.0	85	24.1	24.1	24.0	0.04532	0.438	1.59	18.4	0.0378

Table IV (Cont'd)

Summary of Original and Processed Data for Local Mass Transfer Rates

for Re = 2000 (cylindrical diameter = 1.25")

No.	Material	θ	ΔW_t (mg)	W_c (mg)	t (min)	T_g (°C)	T_f (°C)	T_s (°C)	p_s (mm Hg)	k_g lb-moles/hr-ft^{-2}-atm	k_c ft/hr	$(Sc)^{1/2}$	$k_g(Sc)^{1/2}$	$k_c(Sc)^{1/2}$	G_m lb moles/hr-ft^2	J_D	$\frac{k_g M_m}{h}$ lb-°F/Btu-atm
80	Naphthalene	180	6.4	0.0	135	24.2	24.2	24.1	0.07470	0.1763	68.6	1.57	0.277	107.7	29.4	0.00942	2.352
81	"	"	7.8	0.0	135	25.2	25.1	25.1	0.08245	0.193	75.4	1.57	0.304	118.4	29.5	0.0103	2.565
82	"	"	8.0	0.9	11	54.2	54.0	52.3	0.9480	0.188	80.1	1.56	0.292	125.0	31.7	0.00920	2.326
83	"	"	9.7	1.0	11	56.8	56.5	54.4	1.128	0.211	90.5	1.55	0.327	140.3	31.8	0.0103	2.602
84	"	"	9.4	1.0	11	55.8	55.5	53.7	1.062	0.218	93.3	1.55	0.338	144.6	31.8	0.0106	2.688
85	p-Dibromobenzene	"	9.0	0.0	140	25.3	25.2	25.2	0.05136	0.187	73.1	1.59	0.298	116.2	29.5	0.0101	2.486
86	"	"	9.0	0.0	140	24.8	24.8	24.7	0.04890	0.196	76.5	1.59	0.312	121.6	29.5	0.0106	2.601
87	"	"	7.8	0.8	7	56.3	56.2	54.8	0.7724	0.194	83.3	1.58	0.306	131.6	31.8	0.00962	2.392
88	"	"	7.3	0.8	7	55.7	55.7	54.2	0.7320	0.190	81.5	1.58	0.300	128.8	31.8	0.00943	2.343
89	Propionamide	"	8.4	0.6	20	63.5	63.3	62.0	0.7592	0.248	108.9	1.34	0.333	145.9	32.3	0.0103	3.011
90	"	"	8.2	0.7	20	64.3	64.2	62.7	0.7968	0.238	104.7	1.34	0.305	140.3	32.4	0.00941	2.881
91	Anthracene	"	5.5	0.1	40	111.6	111.5	111.4	0.1306	0.205	103.3	1.75	0.359	180.8	35.6	0.0101	2.258
92	"	"	4.9	0.1	40	110.2	110.0	110.0	0.1201	0.198	99.4	1.75	0.347	174.0	35.6	0.00975	2.181
93	"	"	8.7	1.2	7	150.5	150.3	149.0	1.007	0.212	117.2	1.73	0.367	202.8	38.1	0.00964	2.182
94	"	"	8.9	1.4	7	152.5	152.2	150.8	1.100	0.193	107.2	1.73	0.334	185.5	38.3	0.00873	1.976
95	Naphthalene	150	4.6	0.0	110	25.3	25.3	25.2	0.08326	0.1385	54.1	1.57	0.218	84.9	29.5	0.00738	2.343
96	"	"	6.0	0.0	120	26.7	26.5	26.5	0.09490	0.1453	57.0	1.57	0.228	89.5	29.6	0.00772	2.450
97	"	"	8.0	0.0	180	25.5	25.5	25.4	0.08473	0.1460	57.1	1.57	0.229	89.6	29.5	0.00777	2.470
98	"	"	12.3	0.8	22	54.5	54.3	52.6	0.9734	0.148	63.2	1.56	0.231	98.6	31.7	0.00730	2.331
99	"	"	10.1	0.9	17	55.5	55.2	53.4	1.034	0.144	61.6	1.56	0.225	96.1	31.7	0.00710	2.267
100	p-Dibromobenzene	"	3.7	0.0	80	24.0	24.0	23.9	0.04491	0.1540	59.9	1.59	0.245	95.2	29.4	0.00833	2.615
101	"	"	4.4	0.0	100	23.7	23.6	23.6	0.04373	0.1504	58.5	1.59	0.239	93.0	29.4	0.00824	2.554
102	"	"	6.8	0.9	10	52.5	52.5	51.4	0.5752	0.1533	65.2	1.58	0.242	103.0	31.6	0.00767	2.422
103	"	"	8.0	1.0	10	54.3	54.2	53.0	0.6614	0.1582	67.6	1.58	0.250	106.8	31.7	0.00790	2.491
104	Propionamide	"	12.7	0.7	40	64.2	64.0	62.6	0.7908	0.184	80.9	1.34	0.246	108.4	32.4	0.00760	2.835
105	"	"	7.6	0.5	25	62.6	62.5	61.1	0.7104	0.193	84.5	1.34	0.259	113.2	32.2	0.00805	2.992
106	Anthracene	"	5.5	0.1	60	109.4	109.3	109.2	0.1144	0.156	78.1	1.75	0.273	136.7	35.4	0.0077	2.199
107	"	"	5.8	0.1	60	111.9	111.7	111.7	0.1329	0.142	75.8	1.75	0.249	132.7	35.6	0.0070	1.991
108	"	"	10.5	1.0	12	151.2	151.0	149.6	1.037	0.151	83.6	1.73	0.261	144.6	38.2	0.0068	1.973
109	"	"	9.4	0.8	12	148.0	147.8	146.7	0.8977	0.158	86.9	1.73	0.273	150.3	38.0	0.0072	2.076
110	"	"	9.9	0.8	12	148.4	148.2	147.0	0.9116	0.165	90.8	1.73	0.285	157.1	38.0	0.0075	2.168

No.	Material	θ	ΔW_t (mg)	ΔW_c (mg)	t (min)	T_g (°C)	T_f (°C)	T_s (°C)	p_s (mm Hg)	k_g lb-moles/hr-ft^{-2}-atm	k_c ft/hr	$(Sc)^{1/2}$	$k_g(Sc)^{1/2}$	$k_c(Sc)^{1/2}$	G_m lb-moles/hr ft^2	J_D	$\frac{k_g M_m}{h}$ lb-°F/Btu-atm
111	Naphthalene	120	6.1	0.0	165	25.2	25.0	25.1	0.08245	0.1240	48.4	1.57	0.195	76.0	29.5	0.00661	2.430
112	"	"	7.2	0.0	165	27.0	26.9	26.8	0.09741	0.1235	48.5	1.57	0.194	76.1	29.6	0.00656	2.412
113	"	"	10.0	0.9	16	57.3	57.0	54.9	1.180	0.133	57.2	1.55	0.206	88.7	31.9	0.00646	2.410
114	"	"	8.5	0.7	20	53.0	52.8	51.3	0.8725	0.123	52.2	1.56	0.192	81.4	31.6	0.00609	2.250
115	p-Dibromobenzene	"	5.2	0.0	150	23.6	23.6	23.5	0.04335	0.1193	46.3	1.59	0.1900	73.6	29.4	0.00646	2.346
116	"	"	3.9	0.0	100	24.9	24.7	24.8	0.04956	0.1175	45.8	1.59	0.1870	72.8	29.5	0.00635	2.302
117	"	"	6.2	0.9	10	55.3	55.2	53.9	0.7130	0.1111	47.6	1.58	0.1757	75.2	31.7	0.00555	2.026
118	"	"	6.8	0.8	10	55.2	55.0	53.8	0.7063	0.1270	54.4	1.58	0.201	86.0	31.7	0.00634	2.315
119	Propionamide	"	9.6	0.4	40	62.5	62.3	61.1	0.7104	0.157	68.7	1.34	0.210	92.1	32.2	0.00652	2.818
120	"	"	7.4	0.6	30	64.2	63.9	62.6	0.7908	0.138	60.7	1.34	0.186	81.3	32.3	0.00575	2.470
121	"	"	10.4	0.6	40	63.9	63.7	62.3	0.7747	0.153	67.2	1.34	0.205	90.0	32.3	0.00635	2.738
122	Anthracene	"	6.4	0.1	100	108.9	108.8	108.7	0.1109	0.112	56.0	1.75	0.196	98.4	35.4	0.00554	1.829
123	"	"	8.1	0.1	100	111.7	111.5	111.5	0.1313	0.121	61.0	1.75	0.212	106.8	35.6	0.00596	1.965
124	"	"	7.7	0.7	12	150.4	150.1	148.9	1.002	0.116	64.1	1.73	0.201	110.9	38.1	0.00528	1.760
125	"	"	7.3	0.8	10	152.0	151.7	150.4	1.079	0.119	66.0	1.73	0.206	114.2	38.2	0.00540	1.801
126	"	"	7.1	0.7	10	150.8	150.6	149.3	1.022	0.124	68.6	1.73	0.215	118.7	38.2	0.00563	2.028
127	Naphthalene	90	4.5	0.0	70	25.1	25.0	25.0	0.08182	0.217	84.7	1.57	0.340	133.0	29.5	0.0115	2.591
128	"	"	9.5	1.0	10	56.1	55.8	53.9	1.080	0.217	93.0	1.55	0.336	144.2	31.8	0.0106	2.404
129	"	"	8.0	0.9	10	53.2	53.0	51.5	0.8855	0.221	94.0	1.56	0.343	146.6	31.6	0.0109	2.463
130	p-Dibromobenzene	"	7.1	0.8	7	55.3	55.2	53.9	0.7130	0.189	81.0	1.58	0.298	128.0	31.7	0.00941	2.101
131	"	"	7.8	0.8	7	55.1	54.9	53.7	0.7000	0.214	91.6	1.58	0.338	144.7	31.7	0.0106	2.379
132	Propionamide	"	8.9	0.7	20	63.2	63.0	61.7	0.7420	0.267	117.1	1.34	0.358	156.9	32.3	0.0111	2.912
133	"	"	8.2	0.6	20	62.7	62.5	61.2	0.7155	0.257	112.5	1.34	0.344	150.8	32.2	0.0107	2.812
134	Anthracene	"	5.1	0.1	40	109.6	109.4	109.4	0.1158	0.214	107.2	1.75	0.374	187.6	35.4	0.0106	2.130
135	"	"	7.4	1.0	7	147.6	147.5	146.3	0.8806	0.202	110.0	1.73	0.350	192.0	37.9	0.00925	1.878
136	"	"	9.9	1.4	7	151.5	151.2	149.9	1.053	0.228	126.3	1.73	0.395	218.5	38.2	0.0103	2.103

Table IV (Cont'd)

Summary of Original and Processed Data for Local Mass Transfer Rates

for Re = 2000 (cylindrical diameter = 1.25")

No.	Material	θ	ΔW_t (mg)	ΔW_c (mg)	t (min)	T_g (°C)	T_i (°C)	T_s (°C)	p_s (mm Hg)	k_g lb-moles/hr-ft²-atm	k_c ft/hr	$(Sc)^{1/2}$	$k_g(Sc)^{1/2}$	$k_c(Sc)^{1/2}$	G_m lb-moles/hr-ft²	J_D	$\frac{k_g M_m}{h}$ lb-°F/Btu-atm
137	Naphthalene	60	7.3	0.0	70	25.0	25.0	24.9	0.08110	0.355	138.6	1.57	0.557	217.6	29.5	0.0189	1.984
138	"	"	7.1	0.0	55	25.9	25.8	25.7	0.08775	0.406	158.9	1.57	0.637	249.5	29.5	0.0216	2.269
139	"	"	10.3	0.0	100	24.2	24.2	24.1	0.07470	0.380	147.9	1.57	0.597	232.2	29.4	0.0203	2.131
140	"	"	10.4	1.4	5	58.2	57.9	55.6	1.243	0.400	172.2	1.55	0.620	266.9	31.9	0.0194	2.068
141	"	"	11.2	1.5	5	58.5	58.1	55.8	1.264	0.423	182.3	1.55	0.656	282.6	31.9	0.0206	2.186
142	p-Dibromobenzene	"	10.0	0.0	60	26.6	26.5	26.5	0.05874	0.424	166.4	1.59	0.675	264.6	29.5	0.0228	2.370
143	"	"	8.6	0.0	60	24.8	24.8	24.7	0.04890	0.438	170.9	1.59	0.696	271.7	29.5	0.0236	2.448
144	"	"	13.3	1.5	6	55.1	55.0	53.7	0.7000	0.421	180.2	1.58	0.665	284.7	31.7	0.0210	2.190
145	"	"	12.3	1.8	4	58.4	58.2	56.6	0.8933	0.440	190.0	1.57	0.690	298.3	31.9	0.0216	2.274
146	"	"	13.7	1.7	5	57.1	56.9	55.5	0.8150	0.440	189.4	1.57	0.691	297.4	31.8	0.0217	2.281
147	Propionamide	"	10.1	1.1	12	62.7	62.5	61.2	0.7155	0.507	222.0	1.34	0.680	297.5	32.2	0.0211	2.596
148	"	"	9.5	1.4	10	64.7	64.4	63.0	0.8140	0.482	212.2	1.34	0.645	284.3	32.4	0.0199	2.453
149	Anthracene	"	11.8	0.2	40	112.3	112.2	112.1	0.1361	0.422	212.9	1.75	0.739	372.6	35.6	0.0208	1.955
150	"	"	9.2	0.2	40	109.0	108.8	108.8	0.1117	0.399	199.6	1.75	0.698	349.3	35.4	0.0197	1.858
151	"	"	10.0	0.2	40	109.1	109.0	108.9	0.1124	0.432	216.2	1.75	0.756	378.4	35.4	0.0214	2.012
152	"	"	11.8	1.3	5	149.4	449.3	147.9	0.9529	0.436	232.2	1.73	0.755	401.7	38.0	0.0199	1.892
153	"	"	12.9	1.4	5	152.3	152.0	150.6	1.089	0.418	232.0	1.73	0.723	401.4	38.2	0.0189	1.804
154	Naphthalene	30	9.9	0.0	70	25.2	25.2	25.1	0.08326	0.469	183.2	1.57	0.737	287.6	29.5	0.0250	2.109
155	"	"	10.6	0.0	60	27.0	26.9	26.8	0.09741	0.502	197.2	1.57	0.788	309.6	29.6	0.0266	2.249
156	"	"	9.3	0.0	60	26.4	26.3	26.2	0.09165	0.467	183.1	1.57	0.734	287.5	29.6	0.0248	2.093
157	"	"	8.9	1.2	5	53.4	53.2	51.6	0.8921	0.476	202.5	1.56	0.743	315.9	31.6	0.0235	1.998
158	"	"	13.3	1.6	5.5	57.3	57.0	54.9	1.180	0.498	214.0	1.55	0.772	331.7	31.8	0.0242	2.077
159	"	"	11.4	1.3	5.5	54.7	54.5	52.7	0.9824	0.516	220.2	1.56	0.805	343.5	31.7	0.0254	2.159
160	p-Dibromobenzene	"	6.9	0.0	45	24.8	24.8	24.7	0.04890	0.468	182.6	1.59	0.745	290.3	29.5	0.0252	2.104
161	"	"	6.9	0.0	40	25.3	25.2	25.2	0.05136	0.503	196.6	1.59	0.800	312.6	29.5	0.0271	2.262
162	"	"	12.4	1.8	4	56.8	56.7	55.2	0.7934	0.500	215.1	1.57	0.785	337.7	31.8	0.0246	2.085
163	"	"	12.7	1.5	5	54.0	54.0	52.7	0.8460	0.519	221.5	1.58	0.820	350.0	31.7	0.0258	2.171
164	"	"	13.1	1.3	6	52.5	52.5	51.4	0.5752	0.511	217.2	1.58	0.809	343.2	31.6	0.0256	2.145

No.	Material	θ	ΔW_t (mg)	ΔW_c (mg)	t (min)	T_g (°C)	T_i (°C)	T_s (°C)	p_s (mm Hg)	k_g lb-moles/hr-ft²-atm	k_c ft/hr	$(Sc)^{1/2}$	$k_g(Sc)^{1/2}$	$k_c(Sc)^{1/2}$	G_m lb-moles/hr-ft²	J_D	$\frac{k_g M_m}{h}$ lb-°F/Btu-atm
165	Propionamide	30	10.9	1.4	10	64.3	64.0	62.7	0.7968	0.577	253.8	1.34	0.773	340.0	32.4	0.0238	2.362
166	"	"	11.0	1.3	10	63.9	63.7	62.3	0.7747	0.606	266.3	1.34	0.814	356.8	32.3	0.0251	2.488
167	"	"	11.2	1.2	12	62.7	62.5	61.2	0.7155	0.562	246.0	1.34	0.753	329.6	32.2	0.0234	2.315
168	Anthracene	"	11.7	0.2	40	109.2	109.2	109.0	0.1130	0.504	252.3	1.75	0.882	441.5	35.4	0.0249	1.888
169	"	"	12.4	0.2	40	110.5	110.3	110.3	0.1223	0.494	248.1	1.75	0.864	434.2	35.5	0.0243	1.846
170	"	"	12.0	0.2	40	110.7	110.5	110.5	0.1237	0.473	237.7	1.75	0.827	416.0	35.6	0.0232	1.762
171	"	"	12.5	1.5	4	151.2	150.8	149.6	1.037	0.527	291.8	1.73	0.910	504.8	38.2	0.0238	1.830
172	"	"	13.2	1.7	4	152.8	152.5	151.1	1.116	0.511	284.0	1.73	0.884	491.3	38.3	0.0231	1.770
173	Naphthalene	0	9.5	0.0	60	25.1	25.0	25.0	0.08182	0.535	209.0	1.57	0.840	328.1	29.5	0.0284	2.370
174	"	"	11.3	1.6	4.5	55.2	55.0	53.1	1.010	0.587	250.8	1.56	0.916	391.2	31.7	0.0289	2.419
175	"	"	10.2	1.5	4.5	54.2	54.0	52.3	0.9480	0.563	240.0	1.56	0.879	374.4	31.6	0.0278	2.328
176	"	"	13.2	1.9	4.5	58.4	58.1	55.8	1.264	0.548	236.1	1.55	0.850	366.0	31.9	0.0266	2.245
177	p-Dibromobenzene	"	6.6	0.0	36	25.2	25.2	25.1	0.05088	0.539	210.5	1.59	0.857	334.7	29.5	0.0290	2.387
178	"	"	6.0	0.0	33	25.5	25.5	25.4	0.05229	0.520	203.3	1.59	0.827	323.2	29.5	0.0280	2.303
179	"	"	11.9	1.7	4	55.5	55.3	54.1	0.7255	0.526	225.4	1.58	0.831	356.1	31.7	0.0262	2.168
180	"	"	12.5	1.8	4	56.2	56.0	54.7	0.7655	0.522	224.1	1.58	0.825	354.1	31.8	0.0260	2.145
181	Propionamide	"	10.6	1.4	10	62.9	62.7	61.4	0.7258	0.613	268.6	1.34	0.821	359.9	32.2	0.0255	2.487
182	"	"	10.6	1.3	10	62.5	62.3	61.0	0.7054	0.638	279.3	1.34	0.855	374.3	32.2	0.0266	2.589
183	Anthracene	"	7.6	0.2	20	112.4	112.2	112.2	0.1369	0.535	270.0	1.75	0.937	472.5	35.6	0.0263	1.964
184	"	"	6.6	0.2	20	109.3	109.3	109.1	0.1137	0.558	279.4	1.75	0.976	489.0	35.4	0.0276	2.060
185	"	"	12.4	1.6	4	148.4	148.2	147.0	0.9116	0.586	322.5	1.73	1.015	557.9	38.0	0.0267	2.015
186	"	"	13.8	1.8	4	152.0	151.7	150.4	1.079	0.551	305.7	1.73	0.953	528.9	38.2	0.0250	1.885

Table IV (Cont'd)

Summary of Original and Processed Data for Local Mass Transfer Rates

for Re = 4000 (cylindrical diameter = 1.25")

No.	Material	θ	△W (mg)	t (min)	T_g (°C)	T_i (°C)	T_s (°C)	p_s (mm Hg)	k_g $\frac{\text{lb-moles}}{\text{hr-ft}^{-2}\text{-atm}}$	$(Sc)^{1/2}$	G_m $\frac{\text{lb-moles}}{\text{hr-ft}^{-2}}$	j_D
187	Naphthalene	180	9.0	120	23.8	23.7	23.7	0.07177	0.288	1.57	58.8	0.00769
188	"	"	9.0	120	23.5	23.5	23.4	0.06994	0.296	1.57	58.8	0.00791
189	p-Dibromobenzene	"	10.2	100	24.2	24.2	24.1	0.04590	0.332	1.59	58.8	0.00898
190	"	"	9.4	100	24.2	24.2	24.1	0.04590	0.306	1.59	58.8	0.00827
191	Naphthalene	150	5.9	100	24.1	24.0	24.0	0.07370	0.221	1.57	58.8	0.00590
192	"	"	6.1	100	24.0	24.0	23.9	0.07305	0.230	1.57	58.8	0.00614
193	p-Dibromobenzene	"	8.6	130	23.8	23.7	23.7	0.04410	0.225	1.59	58.8	0.00608
194	"	"	9.0	130	23.6	23.5	23.6	0.04373	0.236	1.59	58.8	0.00638
195	Naphthalene	120	7.2	200	24.5	24.4	24.4	0.07698	0.129	1.57	59.0	0.00344
196	"	"	7.8	200	24.7	24.6	24.6	0.07832	0.138	1.57	59.0	0.00368
197	p-Dibromobenzene	"	6.4	130	24.6	24.6	24.5	0.04785	0.154	1.59	59.0	0.00415
198	"	"	6.7	130	24.8	24.8	24.7	0.04890	0.158	1.59	59.0	0.00423
199	Naphthalene	90	9.0	130	24.7	24.5	24.6	0.07832	0.244	1.57	59.0	0.00649
200	"	"	7.3	100	24.5	24.5	24.4	0.07698	0.262	1.57	59.0	0.00697
201	"	"	9.3	130	24.4	24.3	24.3	0.07630	0.259	1.57	59.0	0.00690
202	p-Dibromobenzene	"	12.6	130	25.2	25.0	25.1	0.05088	0.288	1.59	59.0	0.00776
203	"	"	10.5	130	25.1	25.0	25.0	0.05038	0.240	1.59	59.0	0.00648
204	Naphthalene	60	9.7	60	25.3	25.3	25.2	0.08326	0.538	1.57	59.0	0.0143
205	"	"	10.3	60	25.0	24.9	24.9	0.08110	0.585	1.57	59.0	0.0156
206	p-Dibromobenzene	"	10.3	45	26.4	26.3	26.3	0.05720	0.599	1.59	59.2	0.0161
207	"	"	9.7	45	26.1	26.1	26.0	0.05567	0.580	1.59	59.2	0.0156
208	Naphthalene	30	9.9	50	25.5	25.5	25.3	0.08404	0.648	1.57	59.0	0.0172
209	"	"	10.8	50	25.5	25.5	25.3	0.08404	0.709	1.57	59.0	0.0189
210	p-Dibromobenzene	"	8.7	33	25.9	25.8	25.8	0.05468	0.722	1.59	59.2	0.0194
211	"	"	9.1	33	25.8	25.8	25.7	0.05420	0.762	1.59	59.2	0.0205
212	Naphthalene	0	6.8	33	24.9	24.8	24.8	0.08401	0.707	1.57	59.0	0.0188
213	"	"	6.9	33	25.4	25.2	25.2	0.08326	0.690	1.57	59.0	0.0184
214	"	"	7.7	33	24.9	24.8	24.8	0.08401	0.800	1.57	59.0	0.0213
215	p-Dibromobenzene	"	7.8	33	24.3	24.3	24.2	0.04655	0.758	1.59	59.0	0.0204
216	"	"	8.3	39	24.7	24.5	24.6	0.04824	0.660	1.59	59.0	0.0178
217	"	"	8.1	33	24.5	24.5	24.4	0.04739	0.776	1.59	59.0	0.0209

3. Table V

Summary of Original and Processed Data for Determination of Vapor Pressures

No.	Material	t_b (°F)	p_a (mm Hg)	p_b	V_t (cu ft)	V_d	T_m (°F)	p_m (mm Hg)	V_c (scf)	n_c (gr-mol)	W (gr)	p_s (mm Hg)
1	p-Dibromobenzene	65.5	741	746	4.14	4.03	74	741	3.62	4.56	2.6627	1.847
2	"	62.2	740	745	4.16	4.04	75	740	3.62	4.56	2.0787	1.439
3	"	60.0	741	747	4.13	4.02	75	741	3.60	4.54	1.7235	1.200
4	"	58.6	738	743	4.12	4.01	73	738	3.59	4.52	1.4112	0.982
5	"	56.8	739	744	4.18	4.05	76	739	3.62	4.56	1.2659	0.875
6	"	54.0	740	745	4.14	4.02	75	740	3.60	4.54	1.0561	0.734
7	"	45.9	741	746	5.00	4.85	75	741	4.35	5.48	0.6365	0.368
8	"	27.3	736	742	12.65	12.25	77	736	10.87	13.70	0.2751	0.0632
9	"	26.5	749	744	13.58	13.10	75	749	11.88	14.97	0.2694	0.0575
10	"	25.3	745	750	13.46	13.06	75	745	11.78	14.84	0.2465	0.0528
11	"	24.8	747	752	18.90	18.40	73	747	16.69	21.03	0.3325	0.0503
12	Naphthalene	62.0	736	741	4.09	3.98	73	736	3.64	4.59	1.6265	2.049
13	"	61.3	739	744	4.13	4.01	75	739	3.61	4.55	1.5101	1.931
14	"	59.8	737	742	4.17	4.05	75	737	3.64	4.59	1.4184	1.790
15	"	59.5	743	749	4.18	4.06	74	743	3.68	4.64	1.3602	1.718
16	"	56.7	744	750	4.16	4.04	75	744	3.67	4.62	1.0650	1.362
17	"	51.2	746	751	4.60	4.46	77	746	4.03	5.08	0.7537	0.870
18	"	30.1	745	751	13.19	12.78	77	745	11.55	14.55	0.3426	0.1380
19	"	28.5	746	752	14.74	14.32	75	746	13.03	16.42	0.3219	0.1151
20	"	25.6	747	753	14.68	14.25	75	747	12.98	16.35	0.2397	0.0862
21	"	25.2	746	752	14.53	14.09	76	746	12.80	16.13	0.2280	0.0830

No.	Material	t_b (°F)	p_a (mm Hg)	p_b	V_t (cu ft)	V_d	T_m (°F)	p_m (mm Hg)	V_c (scf)	n_c (gr-mol)	W (gr)	p_s (mm Hg)
22	Propionamide	68.3	744	750	4.34	4.21	76	744	3.78	4.76	0.5582	1.203
23	"	67.4	738	744	4.40	4.26	76	738	3.80	4.79	0.5227	1.110
24	"	65.8	745	751	4.08	3.97	73	745	3.59	4.52	0.4364	0.992
25	"	62.4	745	751	4.28	4.15	75	745	3.74	4.71	0.3603	0.786
26	"	60.5	742	748	4.01	3.89	75	742	3.49	4.40	0.2916	0.678
27	"	57.6	743	748	4.84	4.69	75	743	4.22	5.32	0.2873	0.552
28	Anthracene	156.1	731	731	3.56	3.44	77	731	3.03	3.83	1.3135	1.421
29	"	153.4	732	732	3.50	3.38	78	732	2.98	3.77	1.1673	1.284
30	"	151.2	731	731	3.67	3.55	78	731	3.12	3.94	1.1067	1.163
31	"	149.8	729	729	3.87	3.74	77	729	3.29	4.16	1.0622	1.055
32	"	148.2	730	730	3.87	3.72	76	730	3.28	4.14	0.8786	0.878
33	"	143.7	728	728	3.92	3.80	75	728	3.35	4.23	0.8073	0.787
34	"	128.9	730	730	8.58	8.32	75	730	7.35	9.29	0.7913	0.352
35	"	119.8	735	735	7.78	7.53	77	735	6.67	8.43	0.4420	0.218
36	"	110.9	737	737	8.78	8.48	78	737	7.53	9.51	0.2891	0.1270
37	"	109.2	736	736	8.32	8.05	77	736	7.14	9.02	0.2452	0.1132
38	"	107.4	735	735	10.14	9.83	76	735	8.74	11.04	0.2725	0.1027
39	"	105.9	740	740	10.58	10.26	76	740	9.17	11.59	0.2556	0.0924

4. Sample Calculations

The original data sheet is reproduced in Figure 4.

a. Calculation of mass transfer coefficients

The mass transfer coefficient k_g is

$$k_g = \Delta W/A\ (p_s - p_o)\ t \qquad (45)$$

The rate, $\Delta W/t$, is calculated for the weight-loss data. The final weight subtracted from the initial weight gives the weight-loss for the "test run proper." The "preliminary run" mainly accounts for the sublimation loss during the unsteady state periods between the two weighings. This loss is negligible for both p-dibromobenzene and naphthalene with the temperature in the 25°C range.

$$\Delta W_t = \text{initial wt.} - \text{final wt.} = 15.3562 - 15.3459$$

$$= 0.0103 \text{ gm}$$

$$\Delta W = \Delta W_t - \Delta W_c = 10.3 - 0.0 = 10.3 \text{ mg}$$

where

ΔW_c = "preliminary run" sublimation loss

The rate, $\Delta W/t$, is $10.3/45 = 0.229$ mg/min

The surface temperature is necessary to determine p_s. Plots of the surface temperature versus the air temperature are given in Figures 17a and 17b. The temperatures are recorded on the data sheets. The averaged air temperature, T_a, is 26.4°C. Referring to Figure 17a, the "wet-bulb depression," $(T_a - T_s)$, is 0.1°C for $T_a = 26.4$. The surface temperature is $(26.4 - 0.1) = 26.3$°C. At 26.3°C, the vapor pressure, p_s, is 0.05720 (Figure 16a).

Compared to p_s, p_b is negligible and is neglected.

The surface area is

$$\pi DxL/12 = \pi(1.25in)(1.25in)/12(144\ \frac{in^2}{ft^2}) = 2.84 \times 10^{-3}\ ft^2$$

Substituting into Equation (45),

$$k_g=(2.29x10^{-4}\ \frac{gr}{min})(60\ \frac{min}{hr})(\frac{1}{453.6}\ \frac{lb}{gr})(\frac{1}{235.9}\ \frac{mole}{lb})(\frac{1}{2.84x10^{-3}}\ \frac{1}{ft^2})$$

$$(\frac{1}{0.0572}\ \frac{1}{mm\ Hg})(760\ \frac{mm\ Hg}{atm})$$

$$k_g=0.599\ lb\text{-}mole/hr\text{-}ft^2\text{-}atm$$

$$k_c=k_gRT_s=(0.599\ \frac{lb\text{-}mole}{hr\text{-}ft\ \text{-}atm})(1.310\ \frac{ft^3\text{-}atm}{lb\text{-}mole\text{-}°K})(299.4°K) = 235.0\ \frac{ft}{hr}$$

b. Calculation of j_D-factors

The j_D-factor is defined by Equation (46),

$$j_D = (k_g M_m\ P_{bm}/G)(Sc)^{0.5} \tag{46}$$

The mass velocity is determined from the rotameter reading and corrections for pressure and temperature.

$$G_m = (\frac{\text{indicated SCFM}}{\text{SCF/lb-mole}})(\sqrt{\frac{(530)(P_r)}{(T)(45)}})(\frac{1}{\text{cross-sectional area}}) \tag{47}$$

The pressure at the rotameter, P_r, was 45 psia. The temperature, T, fluctuated slightly around 535°F. Thus the calibration correction term under the square root in Equation (47) is minute.

$$\text{indicated SCFM} = 8.10\ ft^3/min$$

$$P_r = 45\ psia$$

$$T = 536°R$$

$$\text{cross-sectional area} = 2.12 \times 10^{-2}\ ft^2$$

Substituting

$$G_m = (8.10/386)\left(\sqrt{(530)(45)/(536)(45)}\right)(1/2.12 \times 10^{-2})(60\ \tfrac{min}{hr})$$

$G_m = 59.2$ lb-mole/hr-ft^2 which gives Re = 4000.

For p-Dibromobenzene, $(Sc)^{0.5} = 1.59$ (Section d)

Then

$$j_D = (0.599)(1)(1.59)/(59.2) = 0.0161 \text{ dimensionless}$$

c. Calculation of surface temperatures

For steady state conditions, an energy balance is

$$\lambda_s k_g (p_s - p_b) = h(T_a - T_s) \tag{48}$$

Neglecting p_b and rearranging

$$T_s = T_a - p_s \lambda_s k_g / h \tag{49}$$

Assuming the identity of the heat and mass transfer j-factors,

$$j_D = (k_g M_m p_{bm}/G)(\rho/\mu D_v)^{0.5} = j_H = (h/c_p G)(c_p \mu/k)^{0.5} \tag{50}$$

Rearranging Equation (50),

$$k_g/h = (1/c_p M_m p_{bm})(\rho D_v/\mu)^{-0.5}(c_p\mu/k)^{0.5} = (1/c_p M_m p_{bm})(Sc)^{-0.5}(Pr)^{0.5} \tag{51}$$

For air at 70°F,

$c_p = 0.238$ BTU/lb-°F

$M_m = 28.85$ lb/lb-mole

$p_{bm} = 760$ mm Hg

$Pr = 0.69$ dimensionless

Substituting

$$k_g/h = \left(\frac{1}{(0.238)(28.85)(760)}\right)(0.69)^{0.5}(Sc)^{-0.5}\left(\frac{1}{1.8}\ \frac{°C}{°F}\right)$$

$$= (8.7661 \times 10^{-5})(Sc)^{-0.5}\ \frac{\text{mole-°C}}{\text{BTU-mm Hg}} \qquad (52)$$

The factors involved in calculating (k_g/h) are nearly independent of temperature variations over the experimental temperature limits. For this reason, (k_g/h) is taken to be a constant for each of the organic solids. In the case of p-dibromobenzene, $(Sc)^{0.5} = 1.58$; consequently,

$$k_g/h = (8.7661 \times 10^{-5})/(1.58) = 5.5483 \times 10^{-5}\ \frac{\text{mole-°C}}{\text{BTU-mm Hg}} \qquad (53)$$

Substituting into Equation (49),

$$T_a - T_s = (k_g/h)(p_s)(\lambda_s) = (5.5483 \times 10^{-5})(p_s)(\lambda_s)\ °C \qquad (54)$$

Similar results for naphthalene, propionamide, and anthracene are summarized in Table VI.

If the surface temperature of the subliming p-dibromobenzene surface is 25°C, the wet-bulb depression, $(T_a - T_s)$, is

at 25°C, $p_s = 0.05038$ mm Hg

$\lambda_s = 32{,}044$ BTU/lb-mole (from Clausius-Clapeyron equation)

Equation (54) becomes

$$T_a - T_s = (5.5483 \times 10^{-5})(0.05038)(32{,}044) = 0.090 = 0.1°C$$

The results of the wet-bulb depression calculation are presented in Figures 17a and 17b.

TABLE VI

PROPERTIES OF ORGANIC SOLIDS FOR DETERMINING WET-BULB DEPRESSION

Material	$(Sc)^{0.5}$	(k_g/h) mole-°F/BTU-mm Hg	$(T_a - T_s)$ °C
Naphthalene	1.56	5.6194×10^{-5}	$5.6194 \times 10^{-5} p_s \lambda_s$
p-Dibromobenzene	1.58	5.5483×10^{-5}	$5.5483 \times 10^{-5} p_s \lambda_s$
Propionamide	1.34	6.5422×10^{-5}	$6.5422 \times 10^{-5} p_s \lambda_s$
Anthracene	1.74	5.0383×10^{-5}	$5.0383 \times 10^{-5} p_s \lambda_s$

d. Calculation of diffusivities and Schmidt numbers

The diffusivity was calculated by the method of Hirschfelder et al.[47] For pairs of gases

$$D_V = ((1.492 \times 10^{-3})(T)^{3/2}/(P)(r_{AB})^2(\phi))(\sqrt{1/M_A + 1/M_B}) \quad (55)$$

The collision function, ϕ, is a function of k, T, and ϵ_{AB}. Hirschfelder et al. have tabulated ϕ for values of kT/ϵ_{AB}. The factors ϵ_{AB} and r_{AB} are calculated from values of the critical volumes and temperatures of the solids.

The critical constants are calculated by Equations (56) and (57) developed by Meissner.[81]

$$T_c = 20.2(T_B)^{0.60} - 143 - 1.2(P) + 10.4(R_D) + A \quad (56)$$

$$V_c = 0.55(1.5(P) + 9 - 4.34(R_D))^{1.155} \quad (57)$$

P = parachor term

R_D = molar refraction term

Using values of P and R_D tabulated by Meissner, T_c and V_c for p-dibromobenzene, $C_6H_4Br_2$, are calculated as follows:

Structual Components	Parachor (P)	Molar Refraction (R_D)
6 carbons	55.2	14.508
4 hydrogens to carbon	61.6	4.400
2 bromines	138.0	17.730
3 double bonds	57.0	5.166
1 six membered ring	0.8	0.000
Totals	314.2	41.804

For p-dibromobenzene, $T_B = 494°K$, $A = 10$, $P = 314.2$, $R_D = 41.804$. Substituting these values into Equations (56) and (57),

$$T_c = 757°K = 1363°R$$

$$V_c = 399 \text{ cc/g-mole} = 6.39 \text{ ft}^3\text{/lb-mole}$$

The radius of the p-dibromobenzene molecule and the factor ϵ/k are

$$\epsilon/k = 0.75T_c = 0.75(1361) = 1022°R \tag{58}$$

$$r = 3.30(V_c)^{1/3} = 3.30(6.39)^{1/3} = 6.13 \text{ A} \tag{59}$$

For air, $r = 3.63$ A, and $\epsilon/k = 179°R$

$$r_{AB} = 1/2(r_A + r_B) = 1/2(6.13 + 3.63) = 4.88 \text{ A} \tag{60}$$

$$\epsilon_{AB}/k = (1/k)(\sqrt{\epsilon_1 \times \epsilon_2}) = \sqrt{(1022)(179)} = 428°R \tag{61}$$

Substituting into Equation (55),

$$D_V = (1.492 \times 10^{-3}/1(4.88)^2)(\sqrt{(1/235.9) + (1/28.85)})((T)^{3/2}/(\phi))$$

$$D_V = (1.235 \times 10^{-5})(T)^{3/2}/(\phi) \text{ ft}^2/\text{hr}$$

For a given temperature the diffusivity of p-dibromobenzene through air at 1 atm is found by substitution in the above relationship. For p-dibromobenzene, $kT/\epsilon_{AB} = T/428$.

$$\text{At} \quad T = 528°R, \quad kT/\epsilon_{AB} = 1.233$$

$$\phi = 0.658$$

Therefore,

$$D_V = (1.235 \times 10^{-5})(528)^{3/2}/(0.658) = 0.228 \text{ ft}^2/\text{hr}$$

A summary of similar calculations appears in Table VIII. Tabulation of diffusivity values for the selected temperatures are presented in Table IX.

The dimensionless Schmidt group is defined by

$$Sc = \mu/\rho D_V \tag{62}$$

The values of the viscosity and density of the gaseous mixtures were taken to be those of air obtained from (56). Calculated Schmidt numbers are in Table IX. The Schmidt number was determined at a temperature intermediate between those of the surface and mainstream. Since the Schmidt number is almost independent of temperature, negligible numerical differences would result if the reference temperature were taken at the surface or mainstream value.

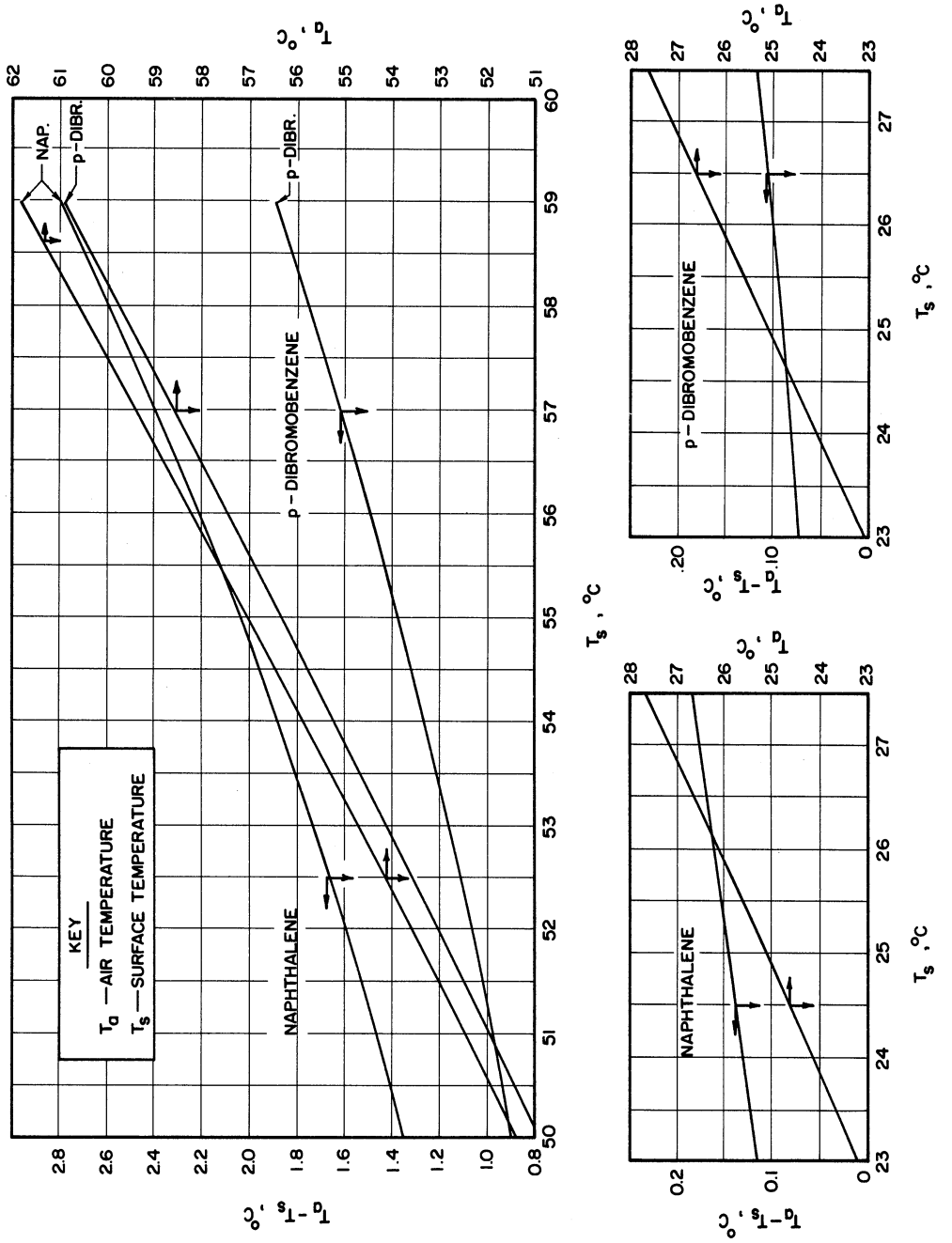

Figure 17a. Surface Temperature as a Function of Wet-Bulb Depression and Air Temperature for Naphthalene and p-Dibromobenzene.

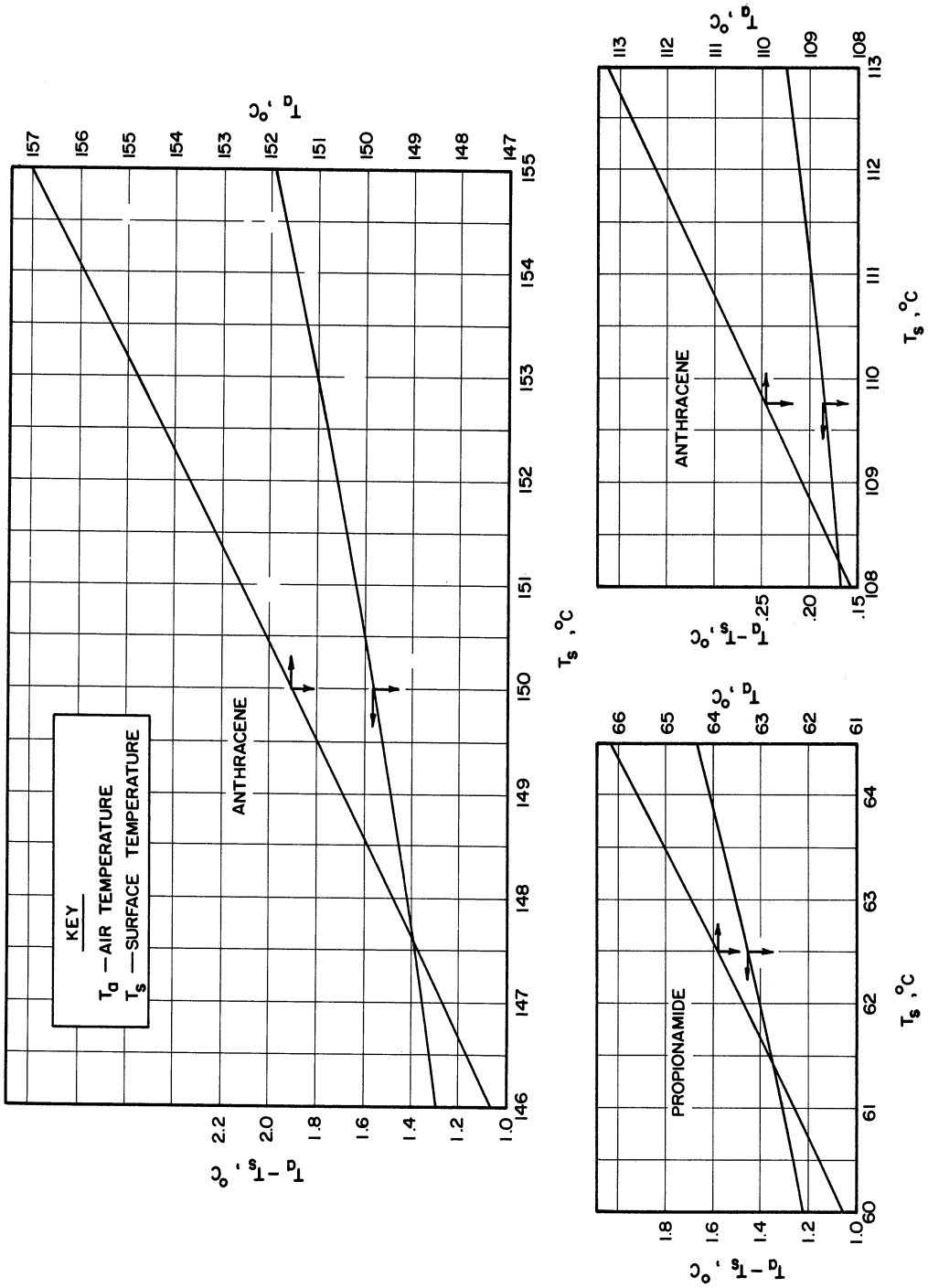

Figure 17b. Surface Temperature as a Function of Wet-Bulb Depression and Air Temperature for Propionamide and Anthracene.

Table VII

"Wet-Bulb Depression" for the Organic Solids

Material	T_s	T_a-T_s	T_a	Material	T_s	T_a-T_s	T_a	Material	T_s	T_a-T_s	T_a
Naphthalene	23.0	0.119	23.1	p-Dibromo-benzene	27.0	0.111	27.1	Anthracene	108.0	0.167	108.2
"	25.0	0.145	25.1	"	50.0	0.900	50.9	"	110.0	0.188	110.2
"	27.0	0.176	27.2	"	52.0	1.07	53.1	"	112.0	0.212	112.2
"	50.0	1.35	51.4	"	54.0	1.26	55.3	"	146.0	1.29	147.3
"	52.0	1.60	53.6	"	56.0	1.49	57.5	"	148.0	1.42	149.4
"	54.0	1.88	55.9	"	58.0	1.75	59.8	"	150.0	1.57	151.6
"	56.0	2.21	58.2	Propionamide	60.0	1.22	61.2	"	152.0	1.72	153.7
"	58.0	2.58	60.6	"	62.0	1.41	63.4	"	154.0	1.89	155.9
					64.0	1.62	65.6				
p-Dibromo-benzene	23.0	0.0742	23.1								
"	25.0	0.0909	25.1								

T_s = Surface Temperature (°C)

T_a = Air Temperature (°C)

Table VIII

Properties of Organic Solids for Determining Diffusivities

Material	T_B (°R)	T_C (°R)	$V_C\left(\frac{ft3}{mole}\right)$	$M\left(\frac{lb}{mole}\right)$	r_o (A)	ϵ/k (°R)	$D_v\left(\frac{ft^2}{hr}\right)$
Naphthalene	884	1351	6.56	128.16	6.17	1013	$1.265 \times 10^{-5} \times T^{3/2}/\phi$
p-Dibromobenzene	890	1363	6.39	235.92	6.13	1022	$1.235 \times 10^{-5} \times T^{3/2}/\phi$
Propionamide	875	1223	4.00	73.1	5.23	919	$1.678 \times 10^{-5} \times T^{3/2}/\phi$
Anthracene	1131	1657	9.14	178.22	7.21	1242	$1.017 \times 10^{-5} \times T^{3/2}/\phi$
Air		238.2	1.326	28.85	3.63	179	

Table IX

Schmidt Numbers and Diffusivities of the Organic Solids

Temp.(°C)	Material: Naphthalene D_v (ft^2/hr)	Sc	Material: p-Dibromobenzene D_v (ft^2/hr)	Sc	Material: Propionamide D_v (ft^2/hr)	Sc	Temp.(°C)	Material: Anthracene D_v (ft^2/hr)	Sc
20	0.234	2.50	0.228	2.56	0.319	1.83	100	0.289	3.08
30	0.252	2.46	0.244	2.54	0.341	1.82	110	0.304	3.07
40	0.268	2.44	0.262	2.50	0.364	1.80	120	0.320	3.05
50	0.284	2.44	0.277	2.50	0.386	1.80	130	0.384	3.05
60	0.306	2.42	0.298	2.45	0.414	1.79	140	0.352	3.02
70	0.320	2.41	0.312	2.45	0.432	1.79	150	0.368	3.00

5. Calibrations

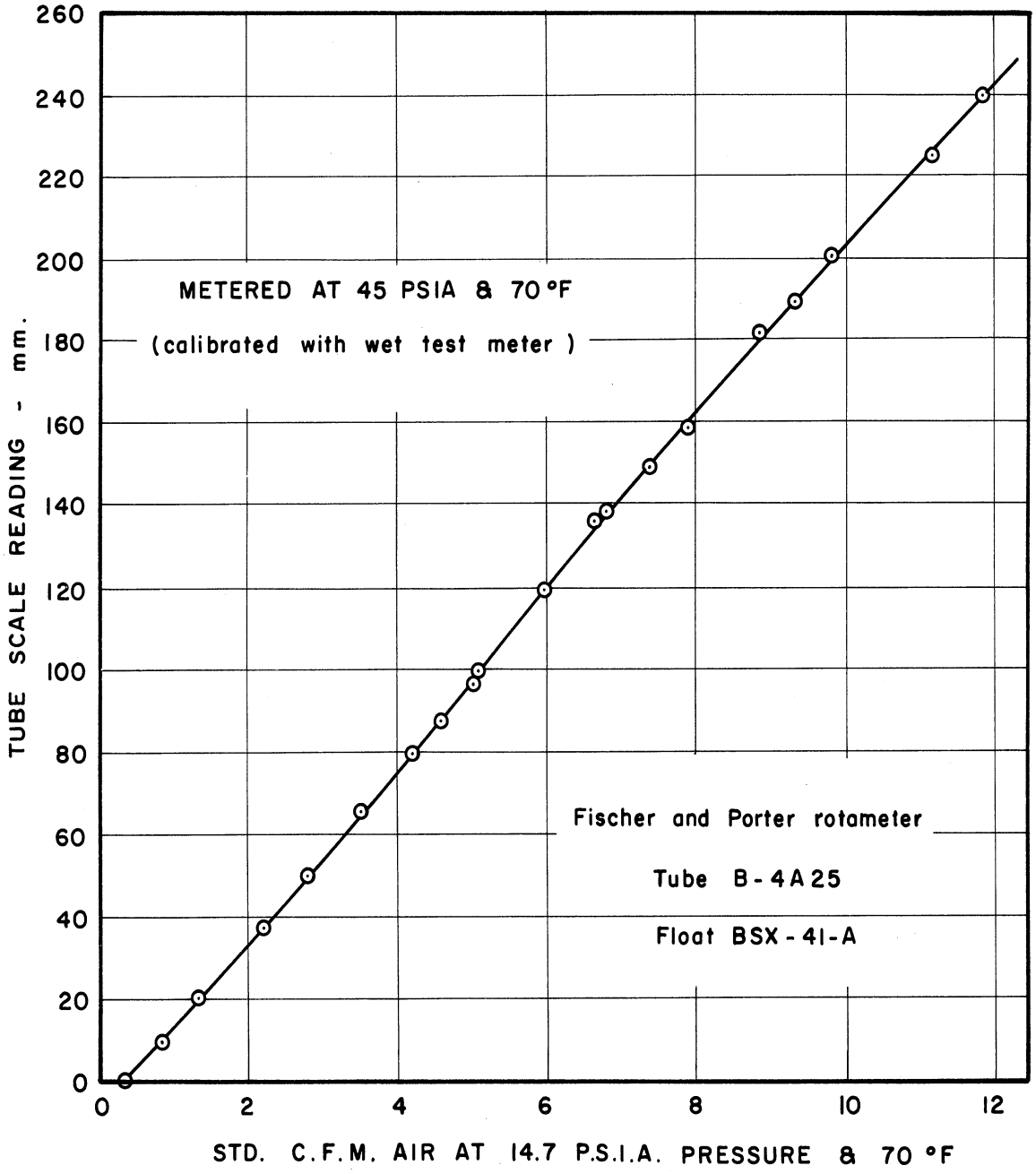

Figure 18a. Calibration Curves for Rotameter Number 1.

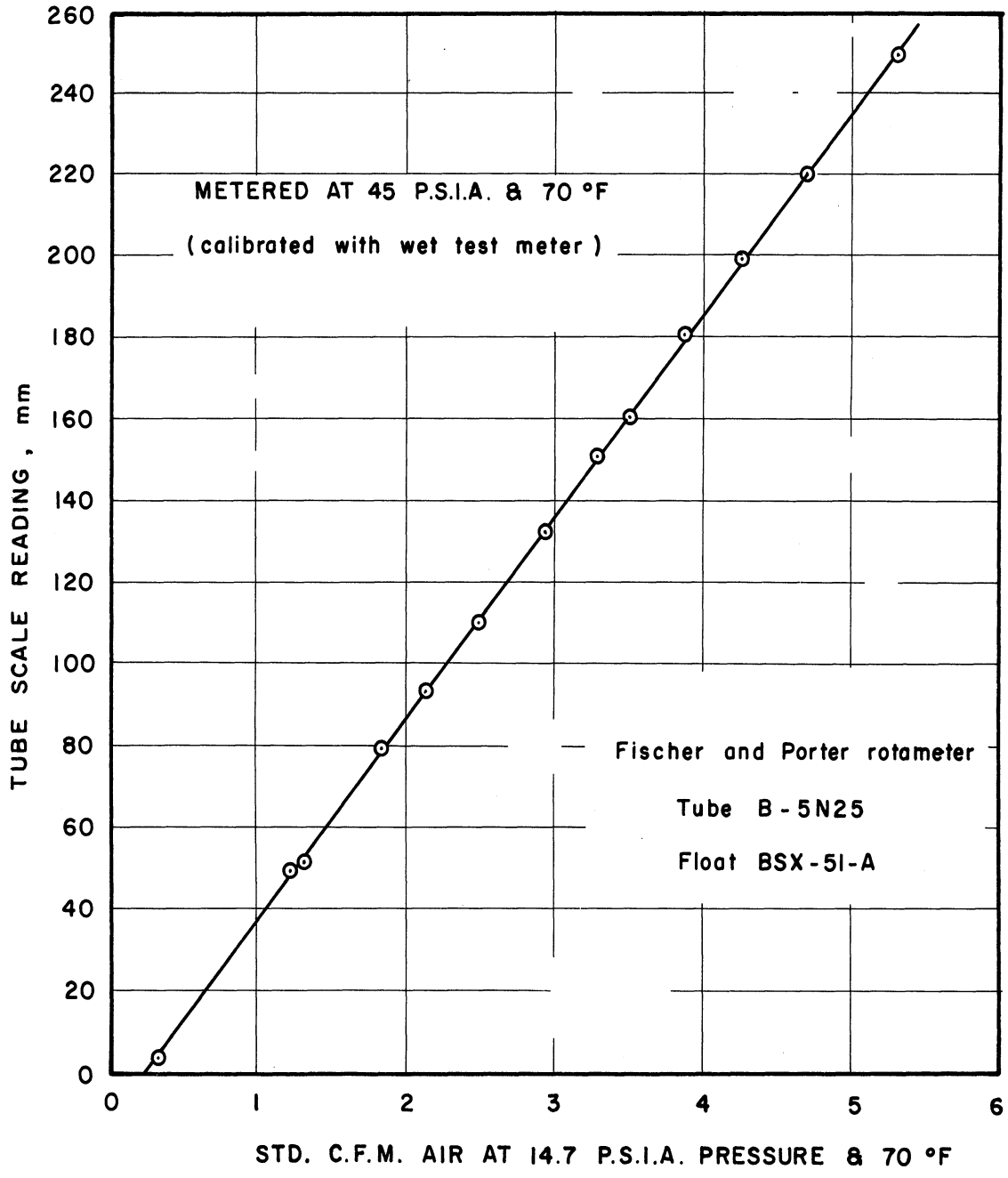

Figure 18b. Calibration Curves for Rotameter Number 2.

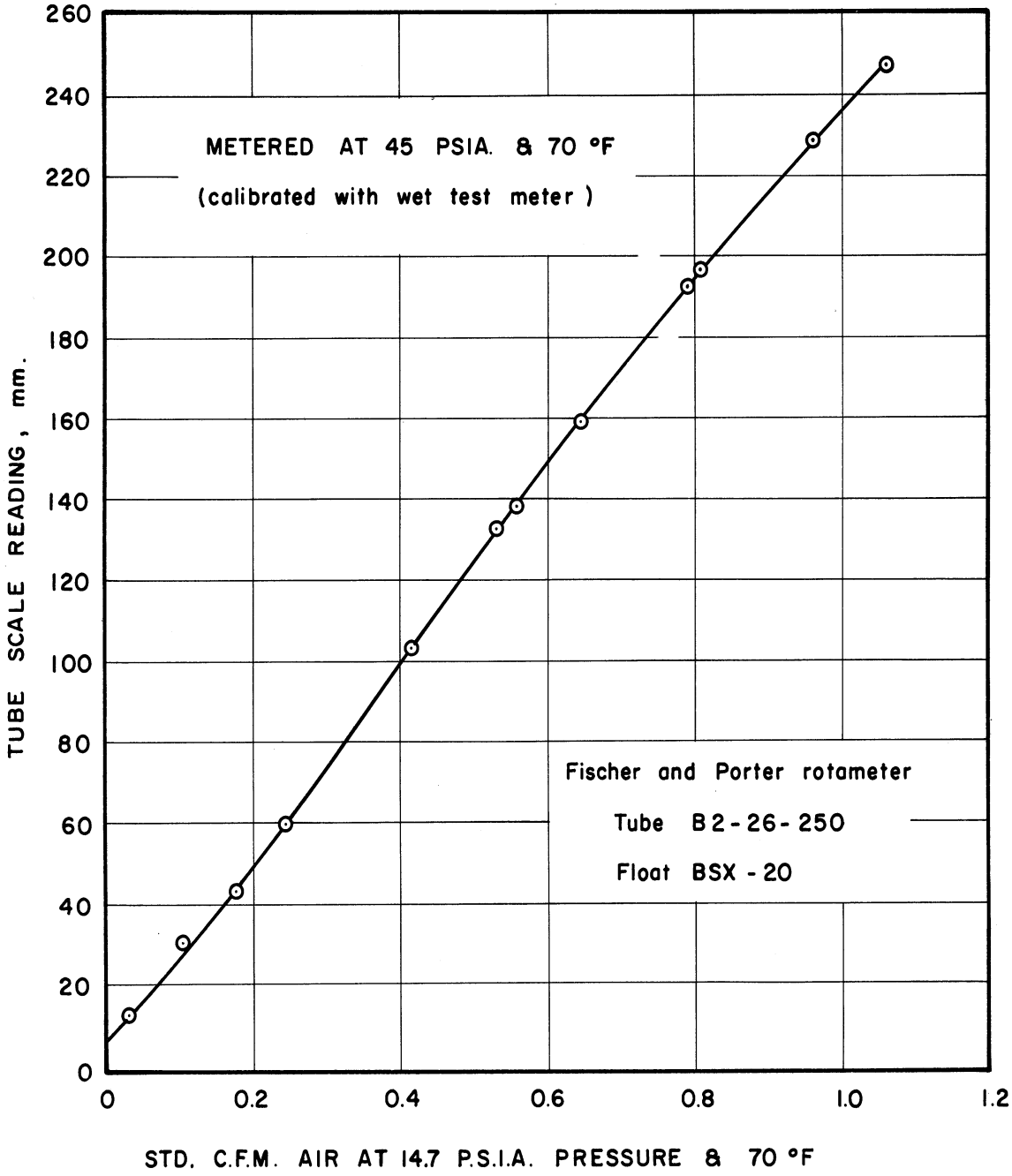

Figure 18c. Calibration Curves for Rotameter Number 3.

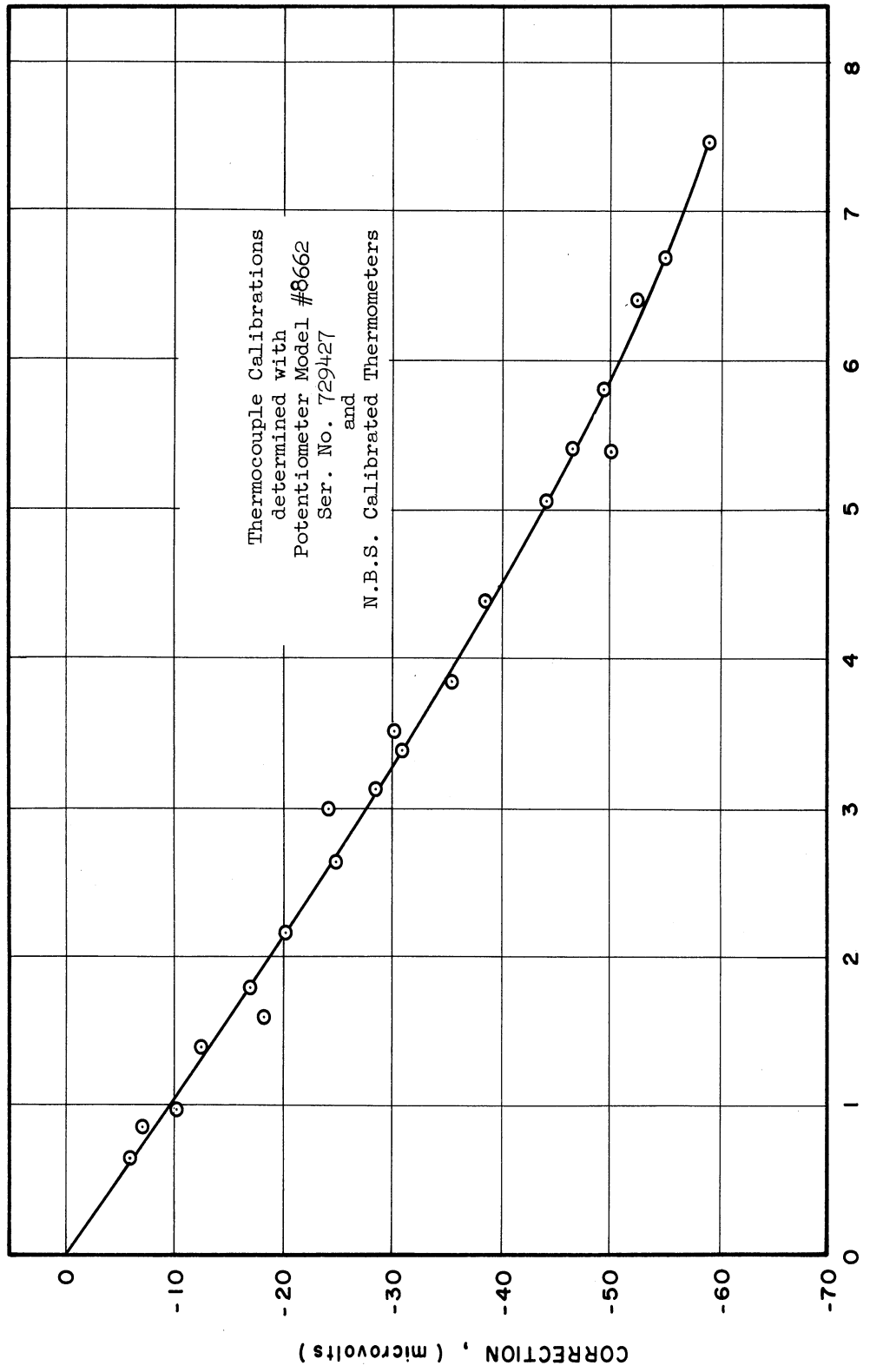

Figure 18d. Calibration Curves Chromel-Alumel Thermocouple.

NOMENCLATURE

a	area of interphase contact per unit volume, ft^{-1}
A	area, ft^2
B	constant
c_p	heat capacity at constant pressure, BTU/lb-°F
c_v	heat capacity at constant volume, BTU/lb-°F
C	constant
D	diameter, ft
D_v	molecular diffusivity, ft^2/hr
E	constant
f	friction factor, dimensionless
F	ratio of u_s/x, 1/hr
G	mass velocity, lbs/ft^2-hr
G_m	molar mass velocity, lb-moles/hr-ft^2
h	heat transfer coefficient, BTU/ft^2-hr-°F
j_D	$(k_g M_m p_{bm}/G)(Sc)^{0.5}$, dimensionless
j_H	$(St)(Pr)^{0.5}$, dimensionless
k	thermal conductivity, BTU/ft-hr-°F
k_c	mass transfer coefficient, ft/hr
k_g	mass transfer coefficient, lb-moles/hr-ft^2-atm
K_g	over-all mass transfer coefficient, lb-moles/hr-ft^2-atm
L	length, ft.
m	exponent
M	molecular weight, lbs/lb-mole
n	exponent
N	mass transfer rate, lbs/hr

Nu	Nusselt number, (hD_v/k), dimensionless
P	total pressure, mm Hg
p	partial pressure of one component in a gas mixture, mm Hg
Pr	Prandtl number, $(c_p\mu/k)$, dimensionless
r_{AB}	arithmetic average of radii of two molecules, Angstroms
R	gas-law constant, 0.728 ft^3-atm/lb-mole-^oR
Re	Reynolds number, (DG/μ), dimensionless
Sc	Schmidt number, (μ/ D_v), dimensionless
St	Stanton number, (h/c_pG), dimensionless
t	time, hr
T	absolute temperature, ^oR
u	linear velocity, ft/hr
V	gas volume, ft^3
W	weight loss, lb-moles
x	distance from stagnation point, ft

Greek

θ	angular position, degrees
λ	latent heat of sublimation, BTU/lb-mole
μ	viscosity, lbs_M/ft-hr
ρ	density, lb/ft^3
ϕ	collision function calculated by Hirschfelder et al (47)
ψ	function to be determined

Subscripts

a	air
ave	average
b	bulk
bm	inert component

c corrected

d dry

f film (arithmetic average)

i inconel surface

L liquid phase

m integrated mean

s surface

t total

Abbreviations

CFM cubic feet per minute

lb pound force

lb_M pound force

log common logarithm, base 10

ln natural logarithm, base e

N.B.S. National Bureau of Standards

SCFM standard cubic feet per minute at $70^{o}F$ and 14.7 psia

BIBLIOGRAPHY

1. Arnold, J.H., Physics, 4, 255, 334 (1934).

2. Baines, W.D., and E.G. Peterson, Trans. ASME, 73, 467 (1951).

3. Barnett, W.I., and A. Kobe, Ind. Eng. Chem., 33, 436 (1941).

4. Bedingfield, C.H., Jr., and T.B. Drew, Ind. Eng. Chem., 42, 1164 (1950).

5. Benke, R., Arch. Warmewirtsch, 19, 287 (1938).

6. Billman, G.W., D.M. Mason, and B.H. Sage, Chem. Eng. Prog., 46, 625 (1950).

7. Boussinesq, J., Comptes Rendus, 133, 257 (1905).

8. Cairns, R.C., and G.H. Roper, Chem. Eng. Sci., 4, 97 (1954).

9. Carberry, J.J., AIChE Journal, 6, 460 (1960).

10. Carpenter, R.C., "Heating and Ventilating Buildings," John Wiley and Sons, New York, 1911.

11. Chappell, E.L., and W.H. McAdams, Trans. ASME, 48, 1201 (1926).

12. Chilton, T.H., and A.P. Colburn, Ind. Eng. Chem., 26, 1164 (1934).

13. Chilton, T.H., and A.P. Colburn, Ind. Eng. Chem., 27, 253 (1935).

14. Churchill, S.W., Ph.D. thesis, Univ. Michigan, Ann Arbor (1952).

15. Churchill, S.W., and J.C. Brier, Chem. Eng. Prog. Symposium Series No. 17, 51, 57 (1955).

16. Colburn, A.P., Trans. AIChE, 29, 174 (1933).

17. Comings, E.W., J.T. Clapp, and J.F. Taylor, Ind. Eng. Chem., 40, 1076 (1948).

18. Davis, A.H., London Phil. Mag., 44, 940 (1922).

19. DeAcetis, J., and G. Thodos, Ind. Eng. Chem., 52, 1007 (1960).

20. Delany, K., and N.E. Sorenson, NACA TN 3038, 1953.

21. Dobry, R., R.K. Finn, Ind. Eng. Chem., 48, 1540 (1956).

22. Douglas, W.J.M., and S.W. Churchill, Chem. Eng. Prog. Symposium Series No. 18, 52, 23 (1956).

23. Drew, T.B., and W.P. Ryan, Trans. AIChE, 26, 118 (1931).

24. Dropkin, D., Cornell Univ. Eng. Expt. Sta., Bull. 23 (1936).

25. Dwyer, O.E., and B.F. Dodge, Ind. Eng. Chem., 33, 485 (1941).

26. Eckert, E.R.G., "Introduction to the Transfer of Heat and Mass," McGraw-Hill Book Co., Inc., New York, 1950.

27. Eckert, E.R.G., and E. Soehngen, Trans. ASME, 74, 343 (1952).

28. Fage, A., and V.M. Falkner, Gr. Brit. Aero. Res. Com. Rept. and Memo. No. 1408 (1931).

29. Fischenden, M., and O. Saunders, "The Calculation of Heat Transmission," His Majesty's Stationary Office, London, 1932.

30. Fischer, T.M., cited in reference # 112.

31. Furber, B.N., Proc. Inst. Mech. Engrs. (London). 168, 847 (1954).

32. Gaffney, B.J., and T.B. Drew, Ind. Eng. Chem., 42, 1120 (1950).

33. Gamson, B.W., G. Thodos, and O.A. Hougen, Trans. AIChE, 41, 1 (1943).

34. Garner, F.H., and R.D. Suckling, AIChE Journal, 4, 114 (1958).

35. Gibson, A.H., London Phil. Mag., 47, 324 (1924).

36. Giedt, W.H., Trans. ASME, 71, 375 (1949).

37. Giedt, W.H., J. Aeronat. Sci., 18, 725 (1951).

38. Gilliland, E.R., and T.K. Sherwood, Ind. Eng. Chem., 26, 516 (1934).

39. Goldstein, S., "Modern Developments in Fluid Dynamics," Vol. I and II, Oxford Univ. Press, London, 1938.

40. Gordon, K.F., Paper presented at the annual Chem. Eng. meeting, Washington, D.C., Dec., 1960.

41. Goukham, A., V. Joukovsky, and L. Loiziansky, Tech. Physics USSR, 1, 221 (1934).

42. Griffiths, E., and J.H. Awberry, Proc. Inst. Mech. Engrs., 125, 319 (1933).

43. Grimson, E.D., Trans. ASME, 59, 573 (1937).

44. Haslam, R.T., R.L. Hershey, and R.H. Kean, Ind. Eng. Chem., 16, 1224 (1924).

45. Heertjes, P.M., and W.P. Ringens, Chem. Eng. Sci., 5, 226 (1956).

46. Hilpert, R., Forsch. Gebiete Ingenieuw., 4, 215 (1933).

47. Hirschfelder, J.O., R.B. Bird, and E.L. Spotz, J. Chem. Phys., 16, 968 (1948).

48. Hirschfelder, J.O., R.B. Bird, and E.L. Spotz, Trans. ASME, 71, 921 (1949).

49. Hixson, A.W., and S.J. Baum, Ind. Eng. Chem., 33, 1433 (1941).

50. Hsu, N.T., and B.H. Sage, AIChE Journal, 3, 405 (1957).

51. Hughes, J.A., London Phil. Mag., 31, 118 (1916).

52. Hurt, D.M., Ind. Eng. Chem., 35, 522 (1943).

53. International Critical Tables, McGraw-Hill Book Co., Inc., New York, 1928.

54. Jakob, M., R.L. Rose, and M. Spielman, Trans. ASME, 72, 859 (1950).

55. Jordon, T.E., "Vapor Pressures of Organic Compounds," Interscience Publs., New York, 1954.

56. Keenan, J.H., and J. Kaye, "Thermodynamic Properties of Air," John Wiley and Sons, Inc., New York, 1945.

57. Keenan, J.H., and F.G. Keyes, "Thermodynamic Properties of Steam," John Wiley and Sons, Inc., New York, 1937.

58. Kennelly, A.E., C.A. Wright, and J.S. van Bylevelt, Trans. Am. Inst. Elect. Engrs., 28, 363 (1909).

59. Kestin, J., and P. Maeder, NACA TN 4018, 1957.

60. Kettering, K.N., E.L. Manderfield, and J.M. Smith, Chem. Eng. Prog., 46, 139 (1950).

61. King, L.V., Trans. Roy. Soc. (London), A214, 373 (1914).

62. Klein, V., Arch. Warmewirtsch. u. Dampfkessekw., 15, 150 (1934).

63. Knudson, J.G., and D.L. Katz, "Fluid Dynamics and Heat Transfer," McGraw-Hill Book Co., Inc., New York, 1958.

64. Kowalke, O.L., O.A. Hougen, and K.M. Watson, Chem.-Met. Eng., 32, 443 (1925).

65. Krujilin, G., Tech. Physics USSR, 3, 311 (1936).

66. Krujilin, G., Tech. Physics USSR, 5, 289 (1938).

67. Krujilin, G., and B. Schwab, Tech. Physics USSR, 2, 312 (1935).

68. Langmuir, I., Am. Inst. Elect. Engrs., 31, 1229 (1912).

69. Langmuir, I., Trans. Am. Elect. Chem. Soc., 23, 299 (1913).

70. Lemlich, R., Ind. Eng. Chem., 47, 1175 (1955).

71. Lin, C.S., E.B. Denton, H.S. Gaskill, and G.L. Putnam, Ind. Eng. Chem., 43, 2136 (1951).

72. Linton, W.H., and T.K. Sherwood, Chem. Eng. Prog., 46, 258 (1950).

73. Linton, M., and K.L. Sutherland, Chem. Eng. Sci., 12, 214 (1960).

74. Lohrisch, W., Forsch. Gebiete Ingenieuw.,No. 322, 45 (1929).

75. Loitsinsky, L.G., and B.A. Schwab, Central Aerod. Hydr. Inst. Moscow, Rep. 329, 1935.

76. London, A.L., H.B. Nottage, and L.M.K. Boelter, Ind. Eng. Chem., 33, 467 (1941).

77. Maisel, D.S., and T.K. Sherwood, Chem. Eng. Prog., 46, 172 (1950).

78. Mark, J.G., Trans. AIChE, 28, 107 (1932).

79. Martinelli, R.C., A.G. Guibert, E.H. Morrin, and L.M.K. Boelter, NACA W-14 (1943).

80. McAdams, W.H., "Heat Transmission," 3rd ed., McGraw-Hill Book Co., Inc., New York, 1954.

81. Meissner, H.P., Chem. Eng. Prog., 45, 149 (1949).

82. Molstad, M.C., J.F. McKinney and R.G. Abbey, Trans. AIChE, 39, 605 (1943).

83. Mortimer, F.S., and R.V. Murphy, Ind. Eng. Chem., 15, 1140 (1923).

84. Powell, R.W., and E. Griffiths, Trans. Inst. Chem. Engrs., London, 13, 175 (1935).

85. Ranz, W.E., and W.R. Marshall, Chem. Eng. Prog., 48, 141 and 173 (1952).

86. Reiher, H., Forsch, Gebiete Ingenieuw., No. 269, 1 (1925).

87. Rice, C.W., J. Am. Inst. Elect. Engrs., 42, 1288 (1923).

88. Robinson, W., and L.S. Han, Proc. Midwest Conf. Fluid Mechanics, 2nd Conf. Ohio State Univ., p. 349, 1952.

89. Russell, H., London Phil. Mag., 20, 591 (1910).

90. Satterfield, C.N., H. Resnick, and R.L. Wentworth, Chem. Eng. Prog., 50, 460 (1954).

91. Satterfield, C.N., and H. Resnick, Chem. Eng. Prog., 50, 504 (1954).

92. Schmidt, E., and K. Wenner, NACA TM 1050, 1943.

93. Seban, R.A., Trans. ASME, series C, J. Heat Transfer, 82, 101 (1960).

94. Sherwood, T.K., Trans. AIChE, 39, 583 (1943).

95. Sherwood, T.K., Ind. Eng. Chem., 42, 2077 (1950).

96. Sherwood, T.K. and F.A.L. Holloway, Trans. AIChE, 36, 39 (1940).

97. Sherwood, T.K., and R.L. Pigford, "Absorption and Extraction," McGraw-Hill Book Co., Inc., New York, 1952.

98. Small, J., London Phil. Mag., 19, 251 (1935).

99. Sogin, H.H., Trans. ASME, 80, 61 (1958).

100. Stanton, T.E., Tech. Report U.S. Advisory Comm. for Aero., p. 45, 1912-1913.

101. Stull, D.R., Ind. Eng. Chem., 39, 517 (1947).

102. Taecker, R.G., and O.A. Hougen, Chem. Eng. Prog., 45, 188 (1949).

103. Taylor, T.S., Trans. ASME, 42, 233 (1920).

104. Thatcher, C.M., Ph.D. thesis, Univ. of Mich., Ann Arbor (1954).

105. Thom, A., Proc. Roy. Soc., A141, 658 (1933).

106. Thoma, H., "Hochleistungskessel," Springer, Berlin, 1921.

107. Ulsamer, J., Forsch. Gebiete Ingenieuw., 3, 94 (1932).

108. van der Zijnen, B.G., Appl. Sci. Research, 7A, 205 (1958).

109. Vint, A.W., thesis in chem. eng., Mass. Inst. Tech., Cambridge, 1932.

110. Vornehem, L., cited in reference # 107.

111. Wamsley, W.W., and L.N. Johanson, Chem. Eng. Prog., 50, 347 (1954).

112. Wieselberger, C., Ergeb. Aerodyn. Versuchanstalt Gollingen, 2, 22 (1923).

113. Wilhelm, R.H., Chem. Eng., Prog., 45, 208 (1949).

114. Wilke, C.R., and O.A. Hougen, Trans. AIChE, 41, 445 (1945).

115. Winding, C.C., and A.J. Cheney, J., Ind. Eng. Chem., 40, 1087 (1948).

116. Yagi, S., and N. Wakao, AIChE Journal, 5, 79 (1959).